DOI: 10.2420/ACT-BOK-AF
ISSN: 2309-1940

Acta Futura

Issue 6

Bio-inspiration for future space systems

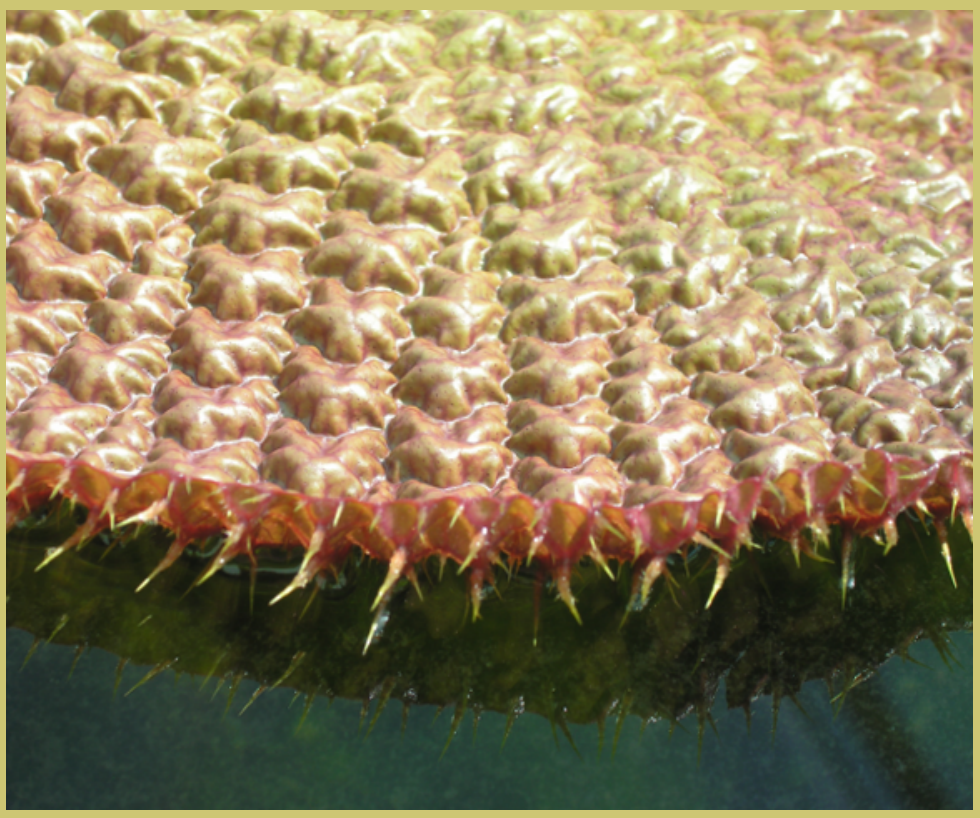

Advanced Concepts Team

http://www.esa.int/act

European Space Agency
Agence spatiale européenne

Publication: Acta Futura, Issue 6 (2013)

Editor-in-chief: Duncan James Barker

Associate editors: Dario Izzo
Jose M. Llorens Montolio
Pacôme Delva
Francesco Biscani
Camilla Pandolfi
Guido de Croon
Luís F. Simões

Published and distributed by: Advanced Concepts Team
ESTEC, PPC-PF
2201 AZ, Noordwijk
The Netherlands
`www.esa.int/gsp/ACT/publications/ActaFutura`
Fax: +31 71 565 8018

Cover image: Amazon Giant Waterlily, Botanic Gardens of Adelaide, Australia. Copyright ©2011 Camilla Pandolfi

ISSN: 2309-1940
D.O.I.:10.2420/ACT-BOK-AF

Typeset with XeTeX

Contents

Foreword

As we increase our knowledge of biological systems, we in turn become increasingly aware of the incredible set of engineering principles that natural systems employ. From mechanical to structural, from chemical to functional, all living organisms evolved a set of solutions that helped them survive during millions of years of evolution. This is becoming steadily more appreciated and the extraction of principles from biological systems is now a popular approach that is defined biomimetics, or biomimicry. The use of nature as source of inspiration for engineers and architects has a very long history and dates back to Leonardo da Vinci and his aviomorphic flying machines.

Nowadays, the incredible plethora of natural solutions are studied with the main goal to extract their working principles. The derived concepts are then translated into elegant and efficient solutions to unsolved challenges in science and engineerings. Biomimetic technologies from nano- to macro- scale are having a huge impact on our society, from sensors and actuators to active biomimetic materials, biohybrid brain-machine interfaces, artificial organs and intelligent prostheses. This special issue offers multiple perspectives on how biomimetic solutions can represent a source of inspiration for space exploration.

Exciting emerging topics within this field include: a bioinspired valveless pump inspired by the embryonic vertebrate heart; light-weight and flexible solar cells to optimize the future design of space solar power; brain-computer interface which can be employed to realise cyborgs, biology-technology hybrids; a review on the current knowledge on nacre, the iconic biomaterial with remarkable optical and mechanical properties; a review on the forisomes, plant proteins that can serve both as sensors and actuators; a programmable amorphous biological computer experimentally implemented in a slime mold, with an overview on the range of solvable tasks; an overview on soft robots to illustrate some advantages and constraints of their application in space; and finally a bioinspired air vehicles designed for Mars exploration.

The biomimetic principles and technologies of this issue were chosen to reflect promising topics from which space exploration may benefit in a very long time horizon. We invited all authors to write for us a review on the concept selected and to put it into a *space perspective*. In short, we are confident of the present and rising role of biomimetics as a new approach to boost new technologies for space science. We hope that this issue can be of great interest, use and benefit to readers.

Camilla Pandolfi
(Associate Editor)

Acta Futura 6 (2013) 9-16
DOI: 10.2420/AF06.2013.9

Acta Futura

A bioinspired pump for space applications

Derek Rinderknecht *, Mory Gharib
Option of Aeronautics, California Institute of Technology, 1200 E. California Blvd., Pasadena, CA. 91125, USA

Abstract. This paper discusses a valveless pumping mechanism, the impedance pump, inspired by the embryonic vertebrate heart in the context of fluid management aboard spacecraft. The impedance pump relies on a resonant wave mechanism to produce flow and can be highly efficient as well as robust to changes in material properties and size scale. Data is presented on the flow rate versus frequency response of the impedance pump demonstrating the basic characteristics of its output such as resonant flow peaks and flow reversals. The impedance pump is also examined for thermal management, a critical role for pumps aboard spacecraft, demonstrating its ability to provide flow in single-phase forced convection cooling loops for heat removal from electronics and thermal regulation of astronauts.

1 Introduction

Effective fluid handling is essential for long term space travel being fundamental to thermal management of electronics, supplying fuel to thrust generating systems and maintaining life support systems for manned space missions. Along with valves, and other fluidic components, pumps are critical to fluid management systems aboard spacecraft. Currently many different types of pumps have been implemented on spacecraft, the most frequently occurring types being passive pumps that operate by capillary forces such as, capillary pumped loops (CPLs) [9, 26] and heat pipes [6], or rotating vane turbo pumps to provide the high pressures required by fuel systems [13, 5]. Other pump systems, mainly being adapted from earth driven industrial based designs, have less of a history in mission based space flight. At present further development is needed as the current options for pumps do not provide a complete solution nor possess the flexibility in design to address all the needs of pumps aboard space missions.

More recently with the hope of reducing the cost and burden of long term missions, space programs have endeavored to move towards smaller spacecraft such as microsatellites and rovers, thereby prompting instruments and other components aboard the craft to proceed to smaller and smaller packages [2]. In this regard, pumps for space need to emphasize low power consumption, high efficiency and high reliability, in addition to meeting the pressure and flow requirements as well as payload and weight restrictions. Similar to consumer electronics, these constraints force more electronics into smaller areas resulting in drastically increased thermal heat fluxes. Extravehicular activity by astronauts is another circumstance requiring pumped fluid for thermal management. Current techniques employ either sublimation based systems or require the astronaut to be tethered to the craft through an umbilical cord which supplies coolant [11]. Sublimating systems require pressure to be relieved and umbilical cords are often difficult to manage creating a need for a self-contained circulating system with zero mass loss which can provide sustained

*Corresponding author. E-mail: rinderkn@caltech.edu

thermal regulation for astronauts.

Instrumentation and hardware for space applications, particularly with the drive to reduce the size and mass of spacecraft, have looked to microelectromechanical systems (MEMS) as a means to attain integrated sensing and diagnostic capabilities even micropropulsion, leveraging the low mass, low power consumption, small footprint and potential redundancy of these technologies [3]. Many of these MEMS technologies involve microfluidics. Microfluidic pumps have been tested in many different configurations to create thrusters for the next generation of microspacecraft [22]. There is also a growing need for MEMS pumps for nanosatellites or on rover missions to perform biological assays of planetary matter and to study the effects of microgravity and other environmental conditions found in space on biology. MEMS technologies also have a role in the medical well-being and performance enhancement of astronauts through their integrated drug delivery and diagnostic abilities. While there is much promise in MEMS for space technologies, the MEMS based pumps currently being utilized are for the most part miniaturizations of successful terrestrial designs, which commonly suffer due to reliability issues caused by wear on moving parts.

Although the environment of space varies quite a bit from that on the surface of the earth, engineers and scientists have benefitted greatly from understanding the methods by which nature solves problems. The idea of bioinspired design or learning from examples in nature, presents carefully crafted solutions to biochemical and physical sensing, actuation, and pumping. Organismal systems have the ability to perform multiple functions, self-sustain, adapt and evolve to maintain operation, concepts which are desirable for space based systems. To the aerospace and aeronautics community flight is an example which is close to heart. Observations of birds gave us the shape of the wing however, it was not until humans realized that a wing provides both lift and thrust that its functions were able to be separated and implemented for air travel. Nature has given us numerous mechanisms to move fluid whether for propulsion or pumping. One example is capillary action, utilized to draw water into plants, which involves similar physics to CPLs and many two-phase fluid systems currently utilized aboard spacecraft. Other examples are peristaltic action by the gut to move the contents of the stomach or valve-based positive displacement pumps who share an action similar to the heart. In this regard nature or biology has the potential to reveal many solutions applicable to long term space travel.

This paper will explore a bioinspired valveless pumping mechanism, the impedance pump, for its potential use in space applications first describing the mechanism and method of manufacturing, and then describing its potential use for space driven thermal management applications.

2 Background impedance pumps

Inspiration for the impedance pump mechanism came from a study of the developmental biology of the vertebrate heart [12]. The heart has the requirement of maintaining adequate cardiac output to supply nutrients and oxygen to the tissues and organs of the body. In its earliest stages, the vertebrate heart consists of a primitive tube that drives blood through a simple vascular network nourishing tissues and other developing organs. At this stage the embryonic heart does not possess valves and only has a simple band of active cardiomyoctes (the contractile cells in the heart), yet it demonstrates unidirectional blood flow. *In vivo* cell lineage tracking studies on the developmental biology of the primitive vertebrate embryonic heart revealed that early stage pumping relied on a wave based mechanism to produce a net mean flow. As a result of these wave based dynamics, the mechanism was named the impedance pump.

The impedance pump mechanism was first discovered in 1954 by Liebau who realized that periodic compression of a pliant tube at an asymmetric location relative to its ends could pump fluid against a pressure gradient [19]. In the late 1990s and beyond, a number of computational studies have appeared describing the pumps behavior [1, 4, 17, 21]. The first experimental parametric study of impedance pump behavior was conducted by Hickerson *et al.* while observations that the same mechanism was present in the embryonic zebrafish heart led to the first experimental investigation showing the ability of the impedance pump mechanism to function at the microscale [15, 24, 14]. Of late many papers on microimpedance pumps have appeared demonstrating the utility of the impedance pump mechanism for micro pumps [7, 18, 27].

In brief, the mechanism of pumping utilizes a mismatch in fluidic impedance to create constructive wave interactions which result in a time varying pressure gradient across the pump that generates a mean flow. The pump is simply formed requiring only a flexible medium on which wave interactions can occur, the pres-

 DOI: 10.2420/AF06.2013.9

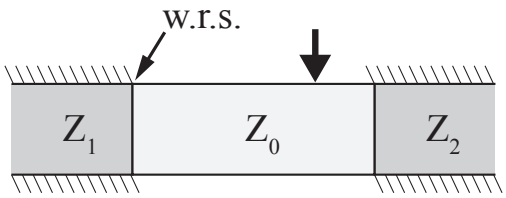

Figure 1. *A schematic of the basic arrangement of an impedance pump. The impedances of respective segments are denoted by Z_0, Z_1 and Z_2, the boundaries between these segments creates two wave reflection sites (w.r.s). The arrow designates the location of the excitation.*

ence of one or more wave reflection sites and an excitation located asymmetrically with respect to the fluidic impedance of the system. A schematic of the basic requirements for an impedance pump can be seen in Figure 1. In practice, the pump is formed by coupling a compressible material at either end with material differing in compliance or geometry in order to reflect wave energy. Figure 1 depicts these wave reflection sites through a distinct mismatch in fluid impedance represented by Z_0, Z_1 and Z_2. Commonly in its implementation Z_1 and Z_2 are of identical materials and geometries and asymmetry is imposed by an offset in the excitation location along the length of the compressible section, Z_0. Excitation in the case of meso- and micro-scale impedance pumps is commonly provided through electromagnetic or piezoelectric actuation due to their ease of implementation however, any actuation scheme that provides sufficient frequency dynamics and displaces the wall of the compressible section can be used. A more complete description of the mechanism of impedance pumping can be found in the literature [15, 24].

3 Design considerations for impedance pumps in space

The extreme environment of space presents many challenges when designing pumps. Pumps not only must meet the performance and lifetime requirements of space operation but also be able to withstand the impacts of solar radiation as well as function in the low pressures and temperatures of space. Reliable space based fluid systems must also resist biofouling and the growth of contaminating bacteria that can harm water quality and degrade performance [25]. In addition to mitigating the impacts of space operation, pumps must also provide high efficiencies and meet the cost, size, and weight requirements of the payload.

The impedance pump is a valveless pump and therefore, has no internal moving parts such as valves or rotary mechanisms which often result in failure particularly, in the harsh environment of space. The impedance pump also requires only a single actuator and can be controlled by frequency making it easy to actuate and drive. The resonant wave based mechanism by which it operates can make the pump highly efficient at converting input power to fluid work, meaning high performance can be attained with minimal power cost. While there is a wide array of needs for pumps aboard spacecraft, the impedance pump mechanism has been demonstrated to be robust to changes in size scale and material properties [24]. In this regard, given that the pump has minimal required components and most of the weight results from the components required to drive the actuator, with careful design impedance pumps can be implemented to add only minimal weight increase to space based fluid management systems. As a valveless pump the impedance pump will not pump air. The pumping mechanism however has been observed to be tolerant to two-phase flows, which are common aboard spacecraft. In designing impedance pumps for space, care would therefore need to be exercised to ensure that bubbles present in the flow do not have the tendency to stick to the interior of the pump where they might merge and create a blockage, or in general to ensure that bubbles carried by the flow are adequately small relative to the inner diameter of the pump. Additionally changes in stiffness resulting from variations in transmural pressure have been shown to shift the resonant frequency of the pump [15]. Similar behavior would likely be observed if the materials comprising the pump were not tolerant to the low temperatures of space. Consequently, materials should be chosen which exhibit stable properties over the expected range of operating temperatures. Furthermore in choosing materials to construct impedance pumps for space applications, consideration would also need to be made to minimize permeability and resist fluid loss. These are metrics by which any material would be chosen for fluid based applications in space. However with regards to the impedance pump, if temperature tolerant materials were identified, a reasonable solution is a hermetically sealed case protecting the pump from the vacuum and radiation of the space environment.

4 Results

4.1 The behavior of impedance pumps

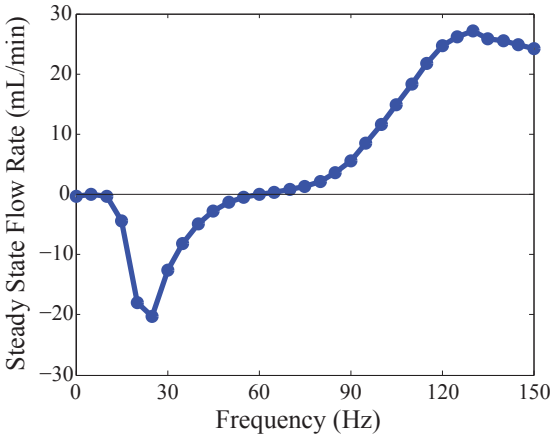

FIGURE 2. *A typical flow response of an impedance pump showing resonant flow peaks and bidirectional flow as seen by examining the flow response at 25 Hz and 130 Hz where the flow rate is -20 mL/min and 27 mL/min, respectively.*

Impedance pumps are commonly characterized in a flow loop that in addition to the parameters associated with pump actuation enables both the flow rate and pressure difference across the pump to be measured. Flow rates are evaluated using a Transonic flow meter model TS410 with a ME 2 PXN flow probe. Pressure is recorded using two differential pressure transducers (PX26) located on either side of the pump. The best performance is achieved when the resonant frequencies of the actuator coincide with that of the pump. In order to understand and design the required actuator response, actuator performance is decoupled from the material response during testing. This is enabled through the use of a voice coil actuator providing a fixed displacement over a wide range of frequencies. Figure 2 shows a typical frequency response of the pump and many characteristics of its flow output.

The flow response in Figure 2 was produced with an impedance pump made of a silicone tube with a length of 15 mm, with an inner diameter of 2 mm and a wall thickness of 780 µm coupled on either end to glass tubes with a 2 mm outer diameter and 1 mm inner diameter. The change in material compliance between the silicone tube and the glass creates two wave reflection sites. Given that both wave reflection sites have similar impedance, the pump is excited at a position of 12.4 mm with respect to the left-hand-side of the pump. If the impedance pump was actuated directly along the midline of the tube length zero net flow would be produced, due to a lack of asymmetry. A peak-to-peak amplitude of 400 µm was applied around the transverse axis of the pump at frequencies spanning 0 to 150 Hz. Positive flow as measured is flow from the left-hand-side to the right-hand-side of the pump. The maximum flow rate of 27 mL/min can clearly be seen at around 130 Hz as represented in the flow response curve. Another trait of impedance pump is bidirectionality, meaning the pump can output flow in both directions. In this example, the impedance pump exhibits negative flow between the frequency range of 10 Hz and 60 Hz and a positive flow above 60 Hz up to the maximum input frequency of the experimental actuator. Examining Figure 2, it can be seen that the maximum negative flow rate occurs at 25 Hz where the flow is -20mL/min and the maximum forward flow frequency occurs at 130 Hz where the flow rate is 27 mL/min. The pressure output of an impedance pump follows a similar trend as the flow response curve shown in Figure 2. In this regard, the maximum power output of the pump also occurs at resonance and therefore represents the optimal frequency at which to convert actuator work to fluid work.

4.2 Impedance pumps for thermal management

Here we will examine the potential of the bioinspired impedance pump for thermal management in space. The system consisted of a pump constructed and driven similarly to that described in the previous section and included a custom designed micromachined brass heatsink with a channel depth of 100 µm. The heatsink was attached to the backside of a 100 Ω power resistor in order to dissipate a heat flux of 10 W/cm^2. Water at room temperature was pumped from a reservoir across the heatsink depositing the heated fluid in a second reservoir. Although a closed loop with a radiator to dispose of the heat would be ideal, the aforementioned experimental scenario was similar to a situation where the fluid is jettisoned after being used for heat removal. The temperature distribution on the heatsink was monitored using a FLIR Phoenix DTS thermal camera. After 10 seconds of resistive heating, the pump was turned on at a flow rate of 6 mL/min. At 6 mL/min the pressure drop across the heatsink was measured to be 0.6 kPa. Figure 3A is a thermal image of the heatsink roughly 50

 DOI: 10.2420/AF06.2013.9

Table 1. *A summary of the performance specifications of common small-scale pump technologies.*

Pumping technology	Actuation method	P_{max} [kPa]	Q_{max} [mL/min]	Power [mW]	$\eta_{thermodynamic}$ [%]
Impedance	electromagnetic	20	10	21	4.0
Electroosmotic [8]	-	33	0.015	0.42	0.49
Electroosmotic [16]	-	160	7	2000	0.23
Electrohydrodynamic [23]	injection-type	2.5	14	420	0.034
Microgear pump [10]	magnetic motor	14	0.35	500	0.0041
Valveless diffusion [20]	piezoelectric	16	16	72	1.5

seconds into the experiment. Figure 3B is an inset plot of the temperature of two points, one located on the surface of the heatsink and the other located on the outlet tube (indicated by the two crosses in the thermal image). In Figure 3B Region of interest (ROI) 0 indicates the temperature on the surface of the heat sink whereas, ROI 1 indicates the temperature of the outlet tube.

The general objective of single-phase forced convection thermal management systems is to remove the maximum amount of heat energy for a given volume of fluid per unit time. The major power cost of such thermal management systems is the pump. The pump is required to provide the fluid work required to meet the pressure demands of the system while maintaining adequate volume flow rate. The efficiency of the pumping mechanism is therefore a key metric in determining the efficacy of forced convection single-phase thermal management systems. Table 1 examines the performance of the impedance pump versus other potential pump technologies available for thermal management. P_{max} is the maximum pressure output of the pump and likewise Q_{max} is the maximum flow rate. The thermodynamic efficiency, $\eta_{thermodynamic}$, is defined as the ratio of fluid work output to power input for the pump. It can be noted in Table 1 that the impedance pump delivers relatively high efficiencies in terms of the ratio of fluid work done by the pump to power input to the actuator.

5 Discussion

Impedance pumps have been made on size scales ranging from a few centimeters to tens of microns producing flow rates from liters per minute to microliters per minute, respectively, and therefore are a viable option for many pump driven applications. Due to the simplicity of the governing principle, any tube, if compressible, can be turned into a valveless pump. This presents an opportunity for redundancy in space based fluid management, eliminating system-wide failures when a pump component fails. In this regard, impedance pumps not only have the ability to drive systems in space but also can be used to supplement existing pump systems in case of performance degradation during space flight. The flow results presented in Figure 2 reveal many characteristics typical of impedance pumps such as flow reversals and frequency dependent flow peaks, making available a wide range of potential flow outputs with a single pump.

Micro impedance pumps with characteristic diameters of around 100 μm generally have outputs in the tens of microliters per minute making them widely useful in a number of biotech driven applications such as theranostic applications for astronauts providing a means for both drug delivery and aid in diagnostic efforts for astronaut health. Impedance pumps could also be implemented as standalone systems for thermal management of electronics or body temperature regulation for astronauts. As demonstrated by Figure 3, even without design optimization, the impedance pump has the potential to remove moderate heat loads for cooling electronics. The effect of convective thermal transport driven the by the impedance pump is clearly visible in the inset plot on the right in Figure 3B. During the first 10 seconds of the experiment the surface temperature of the heat sink plateaus at around 34 °C. After the pump is activated this temperature quickly drops and the temperature at the outlet tube peaks before decreasing, as stagnant fluid which remained in the heatsink for the first 10 seconds is swept out and flow is maintained. With improvements to both the heatsink and the pump, such systems would most likely possess the capability to exceed the reported power density of 10 W/cm^2 in the experiment and approach the likely 25 W/cm^2 power densities of next generation electronics and instrumentation aboard microspacecraft [3].

Efficiency and low power consumption are critical

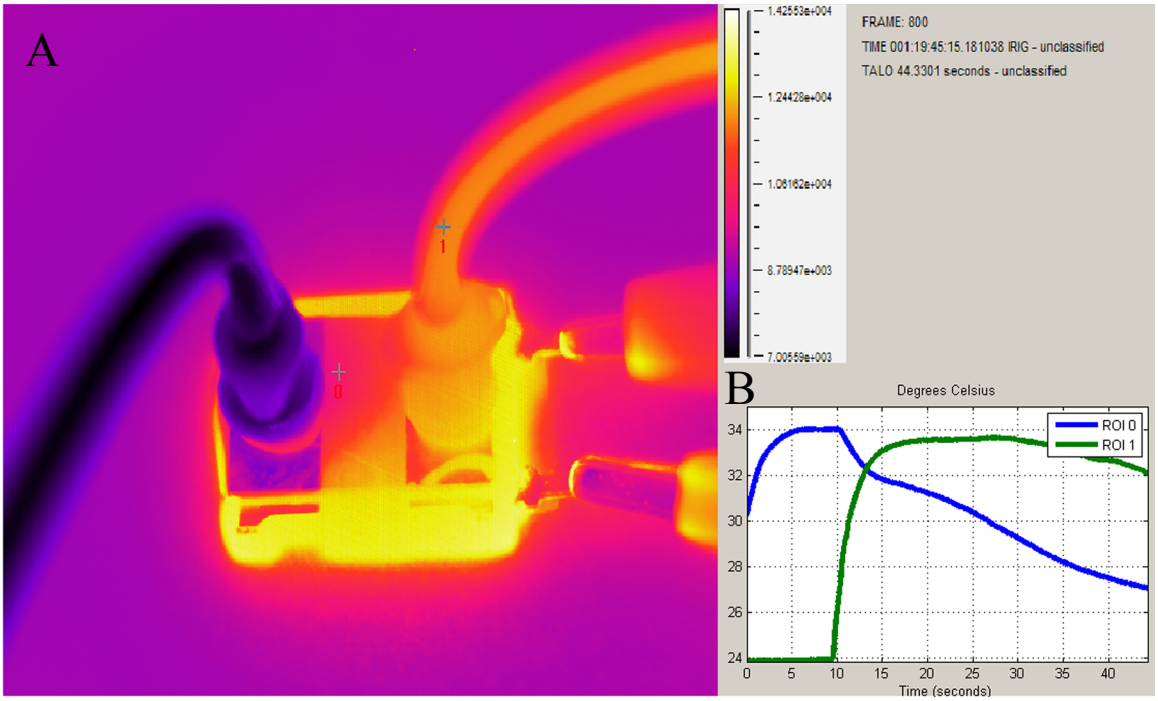

Figure 3. *(A) A thermal camera image of a heatsink attached to a resistor dissipating 10 W/cm^2 being cooled by an impedance pump with a mean output flow rate of 6 mL/min. (B) A plot showing the temperatures of two ROIs depicted by the cross-marks in the thermal camera image versus time. ROI 0 corresponds to the temperature on the surface of the heatsink whereas ROI 1 corresponds to the temperature on the surface of the outlet tube.*

aboard spacecraft where power is often only available through onboard fuel reserves or solar power generation. Due to the resonant wave based mechanism by which the impedance pump operates, properly designed pumps can be highly efficient when compared to other micropump technologies. Computational models of the impedance pump have demonstrated that as much as 75% of the mechanical work done by the actuator on the pump can be directly converted to fluid work [1]. Such analysis may lend some insight into why nature chose to utilize an impedance pump through its very early stages of development. Although no study exists where the response of the actuator has been matched to that of the pump, the impedance pump still exhibits high efficiencies when compared to other pump technologies with similar package sizes. In contrast to other mechanisms, Table 1 shows the impedance pump has the potential to significantly increase the efficiency of fluid power conversion in space missions while delivering relatively high flow rates and pressures.

6 Conclusion

As a bioinspired pump whose mechanism is modeled after the embryonic vertebrate heart the impedance pump holds great promise to provide fluid flow in a wide array of applications for pumps aboard spacecraft. In particular, the versatility in format and lack of internal moving parts make it a viable candidate for thermal management of electronics or standalone liquid cooling underneath the protective clothing used in space to mitigate the effects of fatigue on astronauts. The impedance pump mechanism has been demonstrated to be scalable and, as a result, has been designed to deliver a wide range of flow rates from microliters to liters per minute. The 2 mm tubular pump presented in this manuscript displayed many characteristics typical of impedance pumps including flow reversals and resonant flow peaks in response to changes in the excitation input frequency. A preliminary study examining the impedance pump for thermal management applications utilizing a microchannel heatsink has demonstrated the capability of impedance pumps to provide levels of heat flux removal

 DOI: 10.2420/AF06.2013.9

which approach those projected for the next generation of microspacecraft [3]. With further testing and development of space based designs, impedance pumps have the potential to be a highly effective solution for fluid management in future space missions.

References

[1] I. Avrahami and M. Gharib. Computational studies of resonance wave pumping in compliant tubes. *Journal of Fluid Mechanics*, 608:139–160, 2008.

[2] S. Benner and M. Martins. Development of a heat-driven pulse pump for spacecraft applications. ii. In *Proceedings of the 32nd Intersociety Energy Conversion Engineering Conference (IECEC-97)*, volume 2, pages 1482 – 1485, 1997.

[3] G. Birur, T. Waniewski Sur, A. Paris, P. Shakkottai, A. Green, and S. Haapanen. Micro/nano spacecraft thermal control using a mems-based pumped liquid cooling system. pages 196–206, 2001.

[4] A. Borzi and G. Propst. Numerical investigation of the liebau phenomenon. *Zeitschrift Fur Angewandte Mathematik Und Physik*, 54(6):1050–1072, 2003.

[5] R. Burian, A. Hetem, J. Miraglia, and C. Caetano. Parametric design of rocket engine turbopumps with genetic algorithms. In *MIPRO, 2011 Proceedings of the 34th International Convention*, pages 925 –929, May 2011.

[6] D. Butler, J. Ku, T. Swanson, and A. Obenschain. Loop heat pipes and capillary pumped loops: An applications perspective. Technical report, NASA, 2001.

[7] H.-T. Chang, C.-Y. Lee, and C.-Y. Wen. Design and modeling of electromagnetic actuator in mems-based valveless impedance pump. *Microsystem Technologies*, 13(11):1615–1622, 2007.

[8] C. Chen. A planar electroosmotic micropump. *Journal of microelectromechanical systems*, 11(6):672–683, 2002. 1057-7157.

[9] P.-C. Chen and W.-K. Lin. The application of capillary pumped loop for cooling of electronic components. *Applied Thermal Engineering*, 21(17):1739–1754, 2001.

[10] A. Dewa, K. Deng, D. Ritter, C. Bonham, H. Guckel, and S. Massood-Ansari. Development of liga-fabricated, self-priming, in-line gear pumps. In *International Conference on Solid State Sensors and Actuators*, volume 2, pages 757 – 760, 1997.

[11] A. Flouris and S. Cheung. Design and control optimization of microclimate liquid cooling systems underneath protective clothing. *Ann Biomed Eng*, 34(3):359–72, 2006.

[12] A. Forouhar, M. Liebling, A. Hickerson, A. Nasiraei-Moghaddam, J.-H. Tsai, J. Hove, S. Fraser, M. Dickinson, and M. Gharib. The embryonic vertebrate heart tube is a dynamic suction pump. *Science*, 312(5774):751–753, 2006.

[13] S. Gaddis, S. Hudson, and P. Johnson, editors. *Cold flow testing of the Space Shuttle Main Engine alternate turbopump development high pressure fuel turbine model*, June 1992.

[14] A. Hickerson. *An experimental analysis of the characteristic behaviors of an impedance pump*. PhD thesis, 2005.

[15] A. Hickerson, D. Rinderknecht, and M. Gharib. Experimental study of the behavior of a valveless impedance pump. *Experiments in Fluids*, 38(4):534–540, 2005.

[16] L. Jiang, J. Mikkelsen, J.-M. Koo, D. Huber, S. Yao, L. Zhang, P. Zhou, J. Maveety, R. Prasher, J. Santiago, T. Kenny, and K. Goodson. Closed-loop electroosmotic microchannel cooling system for vlsi circuits. *IEEE Transactions on Components and Packaging Technologies*, 25(3):347 – 355, 2002.

[17] E. Jung and C. Peskin. Two-dimensional simulations of valveless pumping using the immersed boundary method. *SIAM J. Sci. Comput.*, 23(1):19–45, 2001.

[18] C.-Y. Lee, H.-T. Chang, and C.-Y. Wen. A mems-based valveless impedance pump utilizing electromagnetic actuation. *Journal of Micromechanics and Microengineering*, 18(3):035044, 2008.

[19] G. Liebau. Uber ein ventilloses pumpprinzip. *Naturwissenschaften*, 41(14):327–327, 1954.

[20] A. Olsson, G. Stemme, and E. Stemme. A valveless planar fluid pump with two pump chambers. *Sensors and actuators. A, Physical*, 46-47:549–556, 1995.

[21] J. Ottesen. Valveless pumping in a fluid-filled closed elastic tube-system: one-dimensional theory with experimental validation. *Journal of Mathematical Biology*, 46(4):309–332, 2003.

[22] K. Patel, M. Bartsch, M. McCrink, J. Olsen, B. Mosier, and R. Crocker. Electrokinetic pumping of liquid propellants for small satellite microthruster applications. *Sensors and Actuators B: Chemical*, 132(2):461–470, 2008.

[23] A. Richter. A micromachined electrohydrodynamic (ehd) pump. *Sensors and actuators. A, Physical*, 29(2):159–168, 1991.

[24] D. Rinderknecht, A. Hickerson, and M. Gharib. A valveless micro impedance pump driven by electromagnetic actuation. *Journal of Micromechanics and Microengineering*, 15(4):861–866, 2005.

[25] E. Thomas, M. Weislogel, and D. Klaus. Design considerations for sustainable spacecraft water management systems. *Advances in Space Research*, 46(6):761–767, 2010.

[26] G. Wang, D. Mishkinis, and D. Nikanpour. Capillary heat loop technology: Space applications and recent canadian activities. *Applied Thermal Engineering*, 28(4):284–303, 2008.

[27] C. Wen, C. Cheng, C. Jian, T. Nguyen, C. Hsu, and Y. Su. A valveless micro impedance pump driven by pzt actuation. *Materials Science Forum*, 505-507:127–132, 2006.

 DOI: 10.2420/AF06.2013.9

Acta Futura 6 (2013) 17-24
DOI: 10.2420/AF06.2013.17

Acta Futura

Organic photovoltaic cells for space applications

Eva M. Herzig,
Lehrstuhl für Funktionelle Materialien, Technische Universität München James-Franck-Str.1, 85748 Garching (Germany)
Peter Müller-Buschbaum *
Network for Renewable Energy, Munich School of Engineering, Technische Universität München, Boltzmannstr 17, 85748 Garching (Germany)

Abstract. Solar cell technology is already widely used in space applications. The steady development of organic photovoltaic cells based on polymers or small organic molecules has now achieved competitive efficiencies and long enough lifetimes to offer new possibilities for potential future space applications. A high efficiency per mass and a wide range of tunability for these solar cells make this novel technology attractive. Light-weight and flexible solar cells with an absorption range adjusted for extraterrestrial conditions offer the opportunity to optimize the future design of space solar power.

1 Introduction

Today solar cells are routinely used in aerospace applications [1, 2]. Solar cells are attractive as power supply in space applications because no fuel transport is required and there is also no need to deal with any resultant waste. Significant progress has been made for silicon-based and other specially designed solid-state solar cells achieving very high power conversion efficiencies. For these reasons solid-state solar cells are commonly in operation in space today. However, energy density, i. e. the power conversion efficiency per mass, remains a challenge for the relatively heavy solid-state solar modules.

Driven by the necessity of very light weight solar cells the emerging organic photovoltaic (OPV) technology can be a possible solution. Depending on the definition, OPV devices cover solar cells purely made of organic compounds as well as hybrid solar cells which combine organic and inorganic materials [6, 8]. The solar energy converting, active layer in OPV devices therefore consists of either polymers or small organic molecules. Due to the very high absorption of such organic compounds the active layer is only about 100 nm thick. Given the low density of polymers or small organic molecules in comparison to solid-state materials of common solar cells (e.g. Si, Ge, GaAs, GaInAs, GaInP) this results in a strong weight reduction. Moreover, the active layer can be applied on various substrates or surfaces, including thin foils, which results in extremely light weight solar cells. Thus weight is further reduced in comparison to common state-of-the-art solar cells which are deposited on rigid and solid substrates. Furthermore, OPV cells are very shape versatile due to wet-chemical processing routes [3, 15]. This together with mechanical flexibility as shown in figure 1 will also be of advantage in space applications where stowing and unfolding the solar panels plays an important role. For OPV to be attractive in general applications outside the laboratory long enough lifetimes and sufficiently high efficiencies are required. Due to the intensive research on OPV devices the fundamental understanding has significantly

*Corresponding author e-mail: muellerb@ph.tum.de

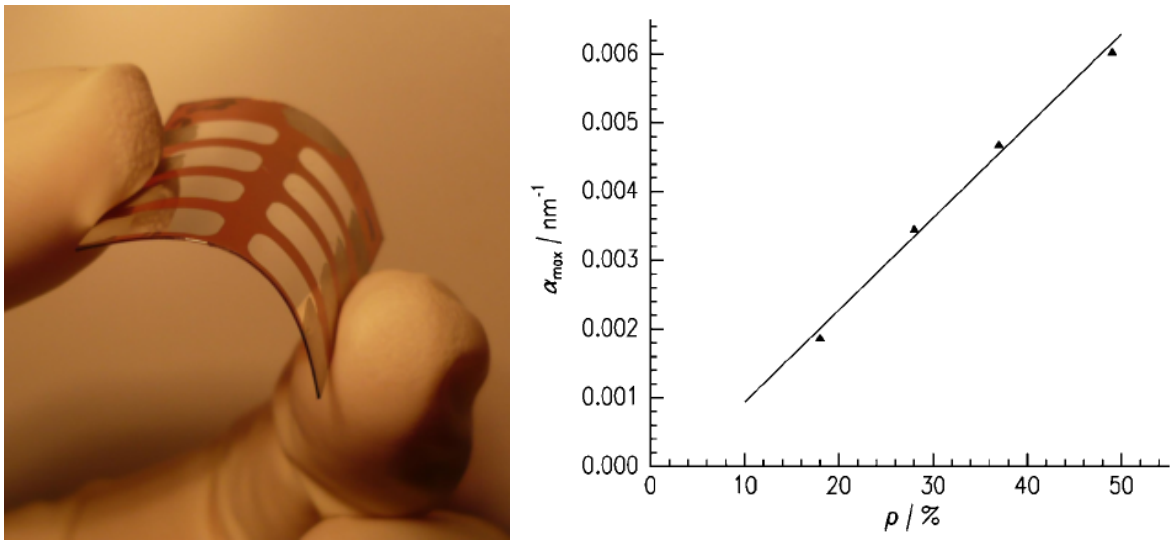

Figure 1. *Left: Photograph of polymer:fullerene solar cell on flexible PET substrate. Right: Absorbance maximum* α_{max} *of a nanostructured polypyrrole film as a function of the rate of coverage. Copyright 2009 Wiley-VCH Verlag GmbH & Co. KGaA, Weinheim. From ref. [28].*

increased in the past years. In this short introduction we would like to show that OPV is now on the verge of becoming an extremely powerful method for solar energy conversion, with potential even for as demanding applications as space missions.

Degradation processes in OPV are dominantly driven by the interaction of oxygen or water with the organic molecules during light exposure [9, 13, 25] i. e. degradation occurs predominantly during the operation of the solar cell. This effect is being successfully tackled by chemically improving the stability of the organic molecules or by encapsulation such that stability that exceeds 1000 hours has already been shown for terrestrial OPV cells [12]. Considering the lack of oxygen and water in space this decay mechanism will not be present in space applications, promising high stability against degradation. Of course, outside the atmosphere new degradation factors come into play. For example, x-ray exposure can lead to internal charge up decreasing performance. However, it is also possible to overcome this phenomenon by exchanging the electrode material [16].

Efficiency of OPV devices has grown significantly over the last years. Today's highest efficiencies already exceed 10% [7] and companies are starting to develop large-scale production for OPV devices [32].

The main shortcomings of OPV are therefore diminishing. In addition, OPV offers a wide range of control over solar cell parameters allowing the tuning of the system to the particular needs of the application. In the following the possibilities for tuning OPV cells for potential space applications are introduced.

2 Organic photovoltaic systems

With the discovery of conducting polymers different research fields needed to collaborate to merge the understanding on electrical and structural properties to achieve high performing devices. Over the last years a very large number of different semi-conducting polymers and small molecules has been used for the fabrication of OPV cells. Polymers are long molecules that can either be highly aligned (similar like spaghetti in their package) or disordered (such as cooked spaghetti on a plate). Since polymers can be very long, one molecule can even participate with one end in an ordered region while the other end is curled and tangled up with other polymers. The conjugated backbone of the polymer is where charge transport can take place, but to improve solubility or other properties, side chains are attached to the long backbone. This in turn influences the possible ordering of the polymers. Small molecules can be flat, spherical or elongated and equally exist in ordered (i.e. crystalline) or disordered (i.e. amorphous) phases. Most commonly a mixture of both exists, resulting in

 DOI: 10.2420/AF06.2013.17

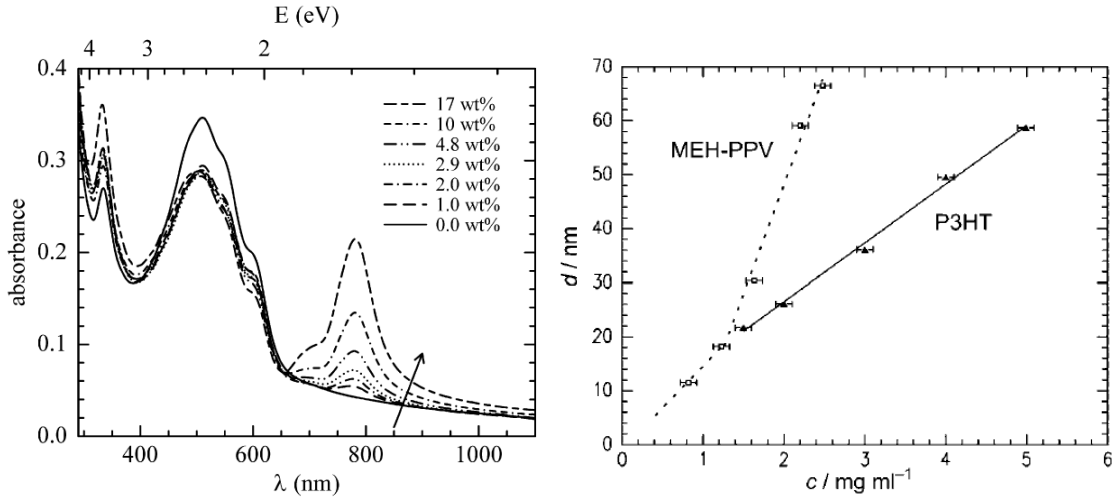

Figure 2. *Left: Wavelength dependent absorbance of ternary P3HT:PCBM:OPc blend films with different dye (OPc) content. The arrow indicates increasing dye content. Copyright 2011 Elsevier B.V.. From ref. [27]. Right: Thickness of polymer film versus concentration spin coated from trichloromethane solutions. Open squares are MEH-PPV films and triangles are P3HT films. Lines are drawn as guide to the eye illustrating the linear dependence. Copyright 2009 Wiley-VCH Verlag GmbH & Co. KGaA, Weinheim. From ref. [30].*

crystallites embedded in a matrix of amorphous material. Depending on the chosen system, the active layer is formed via evaporation or solution based techniques like spin-coating, spraying or printing [15]. Generally, these organic molecules and polymers dominantly consist of carbon, oxygen, nitrogen and hydrogen and a few slightly heavier or more electronegative atoms like sulphur, silicon or fluorine. Altogether the mass density is typically close to 1.

For an organic solar cell to have excellent performance, the first step is – as for any solar cell – to maximize the amount of absorbed light. Ideally this is optimized to the available intensity and wavelength of the incident light. Charge generation, however, is different to common solid-state solar cells. To produce current out of the charges created during the absorption process in OPV, these charges must be effectively separated and then efficiently transported through the active layer avoiding losses. Finally, pathways to the adequate electrode are required to allow the build up of a potential. This requires a continuous transport network similar to neural networks or supply networks in biological species. The key for optimum solar cell performance in OPV lies in the choice of the two organic components – one acceptor, one donator – with matching optical and electronic properties and the choice of the optimum morphology for that pair [31].

One of the most thoroughly studied systems in OPV is the solution processed polymer:fullerene blend P3HT (poly-(3-hexylthiophene-2,5-diyl)):PCBM ([6,6]-phenyl C_{61} butyric acid methyl ester) [5, 10, 11, 20, 22]. The fullerene PCBM is a small, spherical molecule which is a lot smaller than the polymer P3HT. A lot of important information for the fundamental understanding of OPV devices has been gained from the system P3HT:PCBM, although the highest efficiencies so far have been obtained with small molecule systems or newly synthesized polymers [7, 32]. In the following we will focus on the model system of polymer:fullerene systems, namely P3HT:PCBM, to show the possibilities that OPV offers for specialized solar cell applications.

2.1 Optical absorption tuning

The solar spectrum reaching the device differs whether or not it has been filtered by the atmosphere or any protecting layers. The absorption properties of an OPV system depend on the chemical structure of the organic molecules or polymers used and the molecular arrangement within the final active layer. This can be exploited to tune and optimize the absorption behavior for the desired application via various routes.

For example, chemically altering the side chain length of thiophene-based conducting polymers changes the shape and intensity of the absorption profile within the main absorption range [24], while changing the molecular structure of the conjugated backbone can shift the wavelength range of absorption and alter its width [23].

Since the absorption properties depend on the band gap of the material and the band gap is in turn influenced by the conjugation length, i.e. the defect free length of the conjugated backbone, a tuning via the conjugation length is also possible as shown in figure 1. Due to the enforced nanostructure the conjugation length is directly influenced resulting in a linear change of the absorption maximum without any chemical alteration [28].

A huge array of changing and increasing the range of absorption is accessible via the addition of a third component. This is exemplified in figure 2 with the addition of a dye. The addition of this third component leads to the development of a new absorption range at higher wavelengths. The choice of the third component determines the new range and can be tuned to satisfy the need of the application.

Of course the absorption will also increase when there is a larger amount of absorbing material available, i.e. depending on the thickness of the active layer. A precise repeatability and adequate choice of layer thickness is therefore essential. The most widely used technique for producing thin polymer films is spin-coating. In spin-coating the thickness of the film can easily be tuned because of the intrinsic property that the film thickness is linearly dependent on the concentration of the solution from which the active layer is deposited [30]. Fixing the concentration of the solution and the spin-coating conditions therefore results in a very well controlled film thickness. Figure 2 shows the linear behavior of film thickness with concentration for P3HT and a second semi-conducting polymer poly[(1-methoxy)-4-(2-ethylhexyloxy)-p-phenylenevinylene (MEH-PPV). For P3HT the viscosity of the solution is negligible in the investigated concentration range. In contrast, MEH-PPV shows a more complex behavior. Its chemical structure leads to an entanglement of chains already at low concentrations such that viscosity influences the thickness at higher concentrations. In both regimes a linear film thickness dependence is present, however, the slope is different. Thus with the knowledge as displayed in figure 2 the film thickness can be easily controlled. This also holds for polymer blend solutions.

The possibility to deliberately adjust the absorption behavior of the OPV system is a strong advantage for highly specialized applications.

2.2 Importance of morphology

To obtain the highest efficiency from the opto-electronically tuned system, control over the morphology on different length scales is required. From the working principle of an organic solar cell three main points have to be fulfilled by the morphology of the active layer. Firstly, the donor and acceptor domains need to be in close proximity such that the coulombically bound charge pair created during the absorption of light can reach the donor-acceptor interface. This is necessary because only there it is energetically favorable to separate the charges. The lifetimes of these so called excitons is short and the resulting diffusion lengths have been found to be in the range of a few 10 nm [26]. Consequently, domain separations on the order of this length scale are necessary in the active layer. Secondly, the separated charges can only be transported successfully through the film if the conductivities of the materials are high enough. This is particularly challenging for the hole conducting material such as P3HT, where the charge transport occurs in the conjugated backbone and via overlapping π-orbitals. It requires a high molecular order, i.e. crystallinity, within the hole-conducting polymer to allow successful overlap of the π-orbitals of adjacent polymer chains. Lastly, it is necessary that continuous pathways exist to the relevant electrodes to make the extraction of the charges possible.

Factors which can control the morphology of the OPV thin films are the blending ratio, post-production treatments, additives or solvents used [31]. It is important to note that the molecular order and domain separations are closely linked, requiring a collective optimization.

The blending ratio in a binary system influences the domain separation [21]. Therefore, for a new system the best performing blending ratio needs to be established and can vary significantly between systems [17, 30, 33]. Post-production methods like temperature annealing lend mobility to the formerly arrested system and therefore allow for molecular reorganization and smoothing of the interfaces. Although this implies a decrease in the available interfacial area for charge separation the gain in conductivity via formation of crystalline regions usually dominates [14]. Since glass transition temperatures, i.e. the temperature boundary between mobile or non-mobile situations, depend on molecular struc-

 DOI: 10.2420/AF06.2013.17

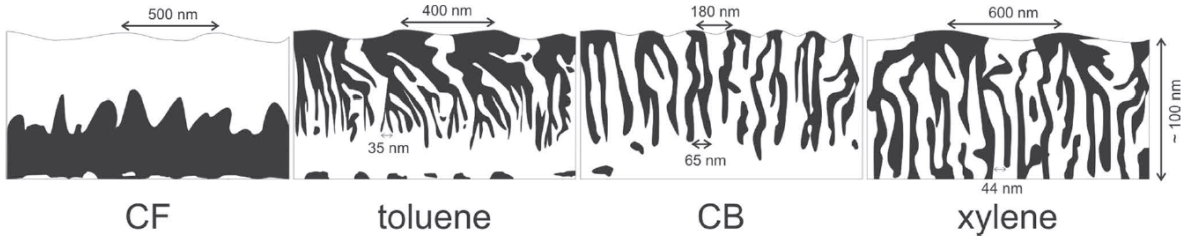

Figure 3. *Schematic morphology of annealed P3HT:PCBM films spin coated from chloroform (CF), toluene, chlorobenzene (CB) and xylene solutions, reconstructed using results from AFM, XRR and GISAXS investigations. Simplified model where black areas correspond to pure PCBM phases and white to pure P3HT phases. Copyright 2011 Wiley-VCH Verlag GmbH & Co. KGaA, Weinheim. From ref. [26].*

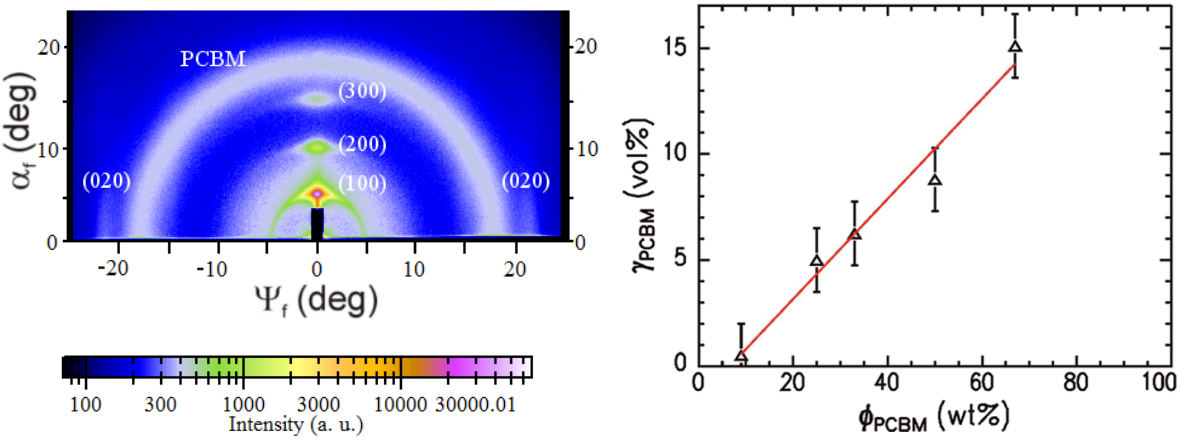

Figure 4. *Left: Grazing incidence wide angle x-ray scattering image with the out-of plane angle* ψ *and the exit angle* α_f *with respect to the scattering plane defined by the incoming x-ray beam perpendicular to the surface of a P3HT:PCBM blend film. The clear peaks indicate that the P3HT is highly ordered. Right: Fraction of molecularly dissolved PCBM in P3HT matrix depending on total PCBM content. If taking into account that there is no PCBM in crystalline P3HT regions, the PCBM content in the amorphous P3HT is even higher. Copyright 2012 American Chemical Society. From ref. [29].*

ture and vary for pure and blended systems, appropriate post-production treatment also needs to be individually tuned for each new system. For some systems post-production methods can be replaced with additives that preferentially dissolve one of the two blend components. This has led to successful morphological control for low band gap polymers [18, 19].

Also the use of different solvents for the spin-coating process can significantly influence the morphology of an otherwise identical system [26] as shown in figure 3. The sketches show the combination of results obtained from surface sensitive and bulk examination methods in the vertical and lateral direction. Solubility driven cluster formation of PCBM and pre-ordering during spin coating prior to post production treatments is observed. Additionally, the increasing boiling points of the solvents used lead to longer drying times during spin coating, resulting in increased crystal sizes. It is important to note that the surface morphology not necessarily represents the morphology of the inner film as shown in the sketches.

Direct evidence of crystallinity (i. e. the ordered part of the active layer) can be obtained from grazing incidence wide angle scattering (GIWAXS) as shown in figure 4. Only if strong ordering is present in the scattering data, special features such as peaks or rings are observable. The ring in intensity in figure 4 shows that PCBM is crystalline but has no preferred orientation, i.e. a powder of small PCBM crystals is present within the P3HT:PCBM film. The sharp intensity peaks (Bragg

peaks) denoted (100), (200) and (300) correspond to the backbone separation in the side chain direction and its higher orders. The (020) feature shifted 90° to the (100) peak is related to the backbone separation along the π-conjugation direction. Such clear peaks are only observable for highly ordered systems. Contributions from disordered (e.g. molecularly dissolved fullerene) or amorphous material (e.g. non-crystalline polymer) contribute to the background and are not easily quantified. To measure the fraction of crystalline content opto-electronic methods can be used [4, 34].

As pointed out earlier the partaking components will not be fully crystalline but coexist with amorphous material. Therefore, although in a binary system only two components are present, the resulting domains can have more than two phases. For example, in the P3HT:PCBM blend crystalline P3HT exists within a matrix of amorphous P3HT that contains a significant amount of PCBM and larger PCBM domains. The amount of PCBM within the amorphous P3HT varies with the overall PCBM content as shown in figure 4 [29].

All these examples show that the extensive research over the last years has brought significant understanding. The key parameters for optoelectronic properties and structure are identified. Although the films require complex, multi-length scale architecture, substantial knowledge has been established on how to systematically tune the systems. Now is the time to steer pioneering work into highly specialized applications of the near future.

3 Conclusion

Today solid state solar cells are successfully used in space applications. The emerging OPV devices offer new possibilities due to a wide range of control and tunability to optimize the solar cells for space applications. The driving advantage for using OPV in space will be the extremely light weight of OPV devices. Additional benefits are mechanical flexibility and shape versatility. Absorption ranges can be tuned and a good understanding on morphological control exists. Only few additional challenges have to be overcome for OPV to be a successful candidate for power supply in space. For example, investigations under extremely strong illumination without the presence of oxygen or water are still necessary. Stability to the bombardment of particles usually filtered by the atmosphere also needs to be examined. Overall, recent developments suggest that overcoming the challenges of OPV systems will be extremely rewarding and will pave our future.

4 Acknowledgements

EMH gratefully acknowledges financial support from the Munich School of Engineering.

References

[1] S. G. Bailey and D. J. Flood. Space photovoltaics. *Progress in Photovoltaics: Research and Applications*, 6(1):1–14, 1998.

[2] E. Birkmire, R. W.; Eser. Polycrystalline thin film solar cells: Present status and future potential. *Annual Review of Materials Science*, 27:625–653, 1997.

[3] C. J. Brabec, J. A. Hauch, P. Schilinsky, and C. Waldauf. Production aspects of organic photovoltaics and their impact on the commercialization of devices. *MRS Bulletin*, 30:50 – 52, 2005.

[4] J. Clark, J. C. Chang, F. C. Spano, R. C. Friend, and C. Silva. Determining exciton bandwidth and film microstructure in polythiophene films using linear absorption spectroscopy. *Applied Physics Letters*, 94(16):163306, 2009.

[5] B. A. Collins, J. R. Tumbleston, and H. Ade. Miscibility, crystallinity, and phase development in p3ht/pcbm solar cells: Toward an enlightened understanding of device morphology and stability. *The Journal of Physical Chemistry Letters*, 2(24):3135–3145, 2011.

[6] C. Deibel and V. Dyakonov. Polymer-fullerene bulk heterojunction solar cells. *Reports on Progress in Physics*, 73(9):096401, 2010.

[7] M. A. Green, K. Emery, Y. Hishikawa, W. Warta, and E. D. Dunlop. Solar cell efficiency tables (version 40). *Progress in Photovoltaics: Research and Applications*, 20(5):606–614, 2012.

[8] S. Günes, H. Neugebauer, and N. S. Sariciftci. Conjugated polymer-based organic solar cells. *Chemical Reviews*, 107(4):1324–1338, 2007. PMID: 17428026.

 DOI: 10.2420/AF06.2013.17

[9] H. Hintz, H.-J. Egelhaaf, H. Peisert, and T. Chassé. Photo-oxidation and ozonization of poly(3-hexylthiophene) thin films as studied by uv/vis and photoelectron spectroscopy. *Polymer Degradation and Stability*, 95(5):818 – 825, 2010.

[10] H. Hoppe and N. S. Sariciftci. Morphology of polymer/fullerene bulk heterojunction solar cells. *J. Mater. Chem.*, 16:45–61, 2006.

[11] H. Hoppe and N. S. Sariciftci. Polymer solar cells. In S. Marder and K.-S. Lee, editors, *Photoresponsive Polymers II*, volume 214 of *Advances in Polymer Science*, pages 1–86. Springer Berlin / Heidelberg, 2008.

[12] M. Jørgensen, K. Norrman, S. A. Gevorgyan, T. Tromholt, B. Andreasen, and F. C. Krebs. Stability of polymer solar cells. *Advanced Materials*, 24(5):580–612, 2012.

[13] M. Jørgensen, K. Norrman, and F. C. Krebs. Stability/degradation of polymer solar cells. *Solar Energy Materials and Solar Cells*, 92(7):686 – 714, 2008.

[14] Y. Kim, S. A. Choulis, J. Nelson, D. D. C. Bradley, S. Cook, and J. R. Durrant. Device annealing effect in organic solar cells with blends of regioregular poly(3-hexylthiophene) and soluble fullerene. *Applied Physics Letters*, 86(6), 2005.

[15] F. C. Krebs. Fabrication and processing of polymer solar cells: A review of printing and coating techniques. *Solar Energy Materials and Solar Cells*, 93(4):394 – 412, 2009. Processing and Preparation of Polymer and Organic Solar Cells.

[16] A. Kumar, N. Rosen, R. Devine, and Y. Yang. Interface design to improve stability of polymer solar cells for potential space applications. *Energy Environ. Sci.*, 4:4917–4920, 2011.

[17] C.-K. Lee, C.-W. Pao, and C.-W. Chu. Multiscale molecular simulations of the nanoscale morphologies of p3ht:pcbm blends for bulk heterojunction organic photovoltaic cells. *Energy Environ. Sci.*, 4:4124–4132, 2011.

[18] Y. Liang, Z. Xu, J. Xia, S.-T. Tsai, Y. Wu, G. Li, C. Ray, and L. Yu. For the bright future – bulk heterojunction polymer solar cells with power conversion efficiency of 7.4 *Advanced Materials*, 22(20):E135–E138, 2010.

[19] S. J. Lou, J. M. Szarko, T. Xu, L. Yu, T. J. Marks, and L. X. Chen. Effects of additives on the morphology of solution phase aggregates formed by active layer components of high-efficiency organic solar cells. *Journal of the American Chemical Society*, 133(51):20661–20663, 2011.

[20] W. Ma, C. Yang, X. Gong, K. Lee, and A. J. Heeger. Thermally stable, efficient polymer solar cells with nanoscale control of the interpenetrating network morphology. *Advanced Functional Materials*, 15(10):1617–1622, 2005.

[21] R. Meier, M. A. Ruderer, A. Diethert, G. Kaune, V. Körstgens, S. V. Roth, and P. Müller-Buschbaum. Influence of film thickness on the phase separation mechanism in ultrathin conducting polymer blend films. *The Journal of Physical Chemistry B*, 115(12):2899–2909, 2011.

[22] A. J. Moulé and K. Meerholz. Controlling morphology in polymer-fullerene mixtures. *Advanced Materials*, 20(2):240–245, 2008.

[23] D. Mühlbacher, M. Scharber, M. Morana, Z. Zhu, D. Waller, R. Gaudiana, and C. Brabec. High photovoltaic performance of a low-bandgap polymer. *Advanced Materials*, 18(21):2884–2889, 2006.

[24] L. H. Nguyen, H. Hoppe, T. Erb, S. Günes, G. Gobsch, and N. S. Sariciftci. Effects of annealing on the nanomorphology and performance of poly(alkylthiophene):fullerene bulk-heterojunction solar cells. *Advanced Functional Materials*, 17(7):1071–1078, 2007.

[25] A. Rivaton, S. Chambon, M. Manceau, J.-L. Gardette, N. Lemaître, and S. Guillerez. Light-induced degradation of the active layer of polymer-based solar cells. *Polymer Degradation and Stability*, 95(3):278 – 284, 2010. Special Issue: MoDeSt 2008.

[26] M. A. Ruderer, S. Guo, R. Meier, H.-Y. Chiang, V. Körstgens, J. Wiedersich, J. Perlich, S. V. Roth, and P. Müller-Buschbaum. Solvent-induced morphology in polymer-based systems for organic photovoltaics. *Advanced Functional Materials*, 21(17):3382–3391, 2011.

[27] M. A. Ruderer, M. Hinterstocker, and P. Müller-Buschbaum. Structure in ternary blend systems for

organic photovoltaics. *Synthetic Metals*, 161(17 - 18):2001 – 2005, 2011.

[28] M. A. Ruderer, M. Hirzinger, and P. Müller-Buschbaum. Photoactive nanostructures of polypyrrole. *ChemPhysChem*, 10(15):2692–2697, 2009.

[29] M. A. Ruderer, R. Meier, L. Porcar, R. Cubitt, and P. Müller-Buschbaum. Phase separation and molecular intermixing in polymer-fullerene bulk heterojunction thin films. *The Journal of Physical Chemistry Letters*, 3(6):683–688, 2012.

[30] M. A. Ruderer, E. Metwalli, W. Wang, G. Kaune, S. V. Roth, and P. Müller-Buschbaum. Thin films of photoactive polymer blends. *ChemPhysChem*, 10(4):664–671, 2009.

[31] M. A. Ruderer and P. Müller-Buschbaum. Morphology of polymer-based bulk heterojunction films for organic photovoltaics. *Soft Matter*, 7:5482–5493, 2011.

[32] R. F. Service. Outlook brightens for plastic solar cells. *Science*, 332(6027):293, 2011.

[33] S. E. Shaheen, C. J. Brabec, N. S. Sariciftci, F. Padinger, T. Fromherz, and J. C. Hummelen. 2.5% efficient organic plastic solar cells. *Applied Physics Letters*, 78(6):841–843, 2001.

[34] F. C. Spano. The spectral signatures of frenkel polarons in h- and j-aggregates. *Accounts of Chemical Research*, 43(3):429–439, 2010. PMID: 20014774.

 DOI: 10.2420/AF06.2013.17

Acta Futura 6 (2013) 25-35
DOI: 10.2420/AF06.2013.25

Acta Futura

Cyborgs in Space

Kevin Warwick*
School of systems engineering, University of Reading, Whiteknights, Reading, RG6 6AY (UK)

Abstract.
Practical realisation of Cyborgs opens up significant new opportunities in many fields. In particular when it comes to space travel many of the limitations faced by humans, in stand-alone form, are transposed by the adoption of a cyborg persona. In this article a look is taken at different types of Brain-Computer interface which can be employed to realise Cyborgs, biology-technology hybrids. The approach taken is a practical one with applications in mind, although some wider implications are also considered. In particular results from experiments are discussed in terms of their meaning and application possibilities. The article is written from the perspective of scientific experimentation opening up realistic possibilities to be faced in the future rather than giving conclusive comments on the technologies employed. Human implantation and the merger of biology and technology are though important elements.

1 Introduction

Science fiction has looked, over many years, to a future in which robots are intelligent and cyborgs – a human/machine merger – are commonplace – The Terminator, The Matrix, Blade Runner and I, Robot are all good examples of this. However, until recently, any serious consideration of what this might actually mean in the future real world was not necessary because it was only science fiction and not in any way scientific reality. Now however science has not only done a catching up exercise but, in bringing about some of the ideas initially thrown up by science fiction, has introduced practicalities that the original story lines did not extend to (and in some cases still have not extended to).

What we consider here are relevant experiments in linking biology and technology together in a cybernetic fashion. Key to this is that it is the overall final system that is important. Where a brain is involved, which surely it is, it should not be seen as a stand alone entity but rather as part of the overall system – adapting to the system's needs. In particular we take a look here at what such hybrid systems could possibly contribute within the field of space travel.

Whilst there is clear overlap between the experiments described, they also throw up individual considerations. To set the scene and give suitable background on the subject, a description of practical investigations is firstly given and then pertinent issues on the topic are discussed. Points have been raised with a view to near term future technical advances and what these might mean in a practical scenario. It has certainly not been the case of an attempt to present a fully packaged conclusive document, rather the aim has been to open up the range of research carried out and to look at some of its implications.

*Corresponding author. E-mail: k.warwick@reading.ac.uk

2 Robots with Biological Brains

Firstly we consider an area that might not immediately be thought of. Initially when one thinks of brain-computer interaction then it is usually in terms of a brain already functioning and settled within a body – normally a human body. Here however we consider the possibility of a fresh merger where a brain is grown from scratch and is subsequently given a body in which to operate.

When one thinks of a robot it may be a little wheeled device that springs to mind [2] or perhaps a metallic head that looks roughly human-like [3]. Whatever the physical appearance our concept tends to be that the robot might be operated remotely by a human, as in the case of a bomb disposal robot, is being controlled by a simple computer programme, or even may be able to learn with a microprocessor/computer as its brain. In all these cases we regard the robot simply as a machine. But what if the robot has a biological brain made up of brain cells (neurons), possibly even human neurons?

Neurons cultured under laboratory conditions on an array of non-invasive electrodes provide an attractive alternative with which to realise a new form of robot controller. An experimental control platform, a robot body, can move around in a defined area purely under the control of such a network/brain and the effects of the brain, controlling the body, can be witnessed. This is not only extremely interesting from a robotics perspective but it also opens up a new approach to the study of the development of the brain itself because of its sensory-motor embodiment. Investigations can therefore be carried out into memory formation and reward/punishment scenarios.

Typically culturing networks of brain cells (around 100,000 to 150,000 at present) in vitro commences by separating neurons obtained from foetal rodent cortical tissue using enzymes. The neurons are then grown (cultured) in a specialised chamber, in which they can be provided with suitable environmental conditions (e.g. appropriate temperature) and fed with minerals and nutrients. An array of electrodes embedded in the base of the chamber (a Multi Electrode Array; MEA) acts as a bi-directional electrical interface to/from the culture. The neurons in such cultures spontaneously connect, communicate and develop, within a few weeks giving useful responses for typically 3 months at present.

At present the culture is grown in a glass specimen chamber lined with a planar '8x8' Multi Electrode Array which can be used for real-time recordings (see Figure 1). It is possible to separate the firings of small

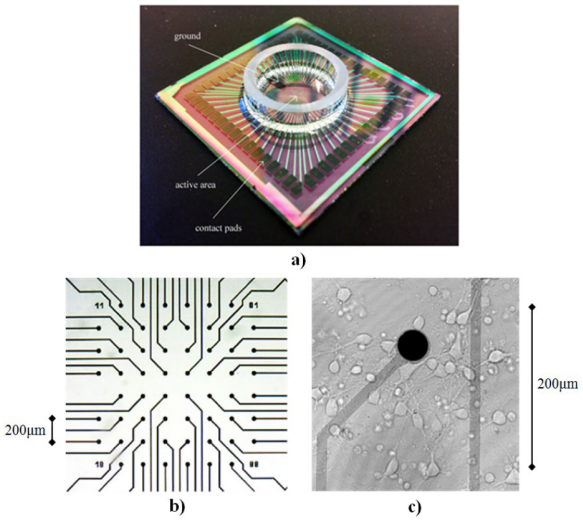

Figure 1. *a) A Multi Electrode Array (MEA) showing the electrodes. b) Electrodes in the centre of the MEA seen under an optical microscope. c) An MEA at x40 magnification, showing neuronal cells in close proximity to an electrode.*

groups of neurons, by monitoring the output signal on the electrodes. In this way a picture of the global activity of the entire network can be formed. It is also possible to electrically stimulate the culture, using biphasic electrical pulses, via any of the electrodes to induce neural activity. The multi-electrode array therefore forms a bi-directional interface to the cultured neurons [4, 6].

After initial growth and brain development lasting around 10 days the culture can be coupled to its physical robot body [28]. Sensory data fed back from the robot is subsequently delivered to the culture, thereby closing the robot-culture loop. Thus, signal processing can be broken down into two discrete sections (a) "culture to robot", in which live neuronal activity is used as the decision making mechanism for robot control, and (b) "robot to culture", which involves an input mapping process, from robot sensor to stimulate the culture.

The actual number of neurons in a culture depends on natural density variations in seeding. The electrochemical activity of the culture is sampled and this is used as input to the robot's wheels. Meanwhile the robot's (ultrasonic) sensor readings are converted into stimulation signals received by the culture, thereby closing the loop.

An existing neuronal pathway is identified by searching for strong relationships between pairs of electrodes. Such pairs are defined as those electrode combinations in which neurons close to one electrode respond to stim-

 DOI: 10.2420/AF06.2013.25

ulation from the other electrode at which the stimulus was applied more than 60% of the time and respond no more than 20% of the time to stimulation on any other electrode. A rough input-output response map of the culture can then be created by cycling through all electrodes. In this way, a suitable input/output electrode pair can be chosen in order to provide an initial decision making pathway for the robot. This is employed to control the robot body – for example if the ultrasonic sensor is active and we wish the response to cause the robot to turn away from the object being located ultrasonically (possibly a wall) in order to keep moving.

For experimentation purposes, the robot follows a forward path until it reaches a wall, at which point the front sonar value decreases below a threshold, triggering a stimulating pulse. If the responding/output electrode registers activity the robot turns to avoid the wall. In experiments the robot turns spontaneously whenever activity is registered on the response electrode. The most relevant result is the occurrence of the chain of events: wall detection – stimulation – response. From a neurological perspective it is of course also interesting to speculate why there is activity on the response electrode when no stimulating pulse has been applied.

As an overall control element for direction and wall avoidance the cultured network acts as the sole decision making entity within the overall feedback loop. Clearly one important aspect then involves neural pathway changes, with respect to time, in the culture between the stimulating-recording electrodes.

Learning and memory investigations are generally at an early stage. However the robot appears to improve its performance over time in terms of its wall avoidance ability in the sense that neuronal pathways that bring about a satisfactory action tend to strengthen purely through the process of being habitually performed – learning due to habit. The number of confounding variables is however considerable and the plasticity process, which occurs over quite a period of time, is (most likely) dependent on such factors as initial seeding and growth near electrodes as well as environmental transients such as temperature and humidity. Learning by reinforcement – rewarding good actions and punishing bad is much more of an investigative research effort at this time.

On many occasions the culture responds as expected, on other occasions it does not, and in some cases it provides a motor signal when it is not expected to do so. But does it "intentionally" make a different decision to the one we would have expected? We cannot tell.

In terms of robotics, it has been shown by this research that a robot can successfully have a biological brain to make all its "decisions". The 150,000 neuron size is merely due to the present day limitations of the experimentation described. Indeed 3 dimensional structures are already being investigated. Increasing the complexity from 2 dimensions to 3 dimensions realises a figure of approximately 30 million neurons for the 3 dimensional case – not yet reaching the 100 billion neurons of a "perfect" human brain, but well in tune with the brain size of many other animals.

This area of research is expanding rapidly. Not only is the number of cultured neurons increasing, but the range of sensory input is being expanded to include audio, infra red and even visual. Such richness of stimulation will no doubt have a dramatic effect on culture development. The potential of such systems, including the range of tasks they can deal with, also means that its physical body can take on different forms. There is no reason, for example, that the body could not be a two legged walking robot, with rotating head and the ability to walk around in a building.

It is certainly the case that understanding neural activity becomes more difficult as the culture size increases. With a 3 dimensional structure, monitoring activity deep within the central area, as with a human brain, becomes extremely complex, even with needle-like electrodes. In fact the present 150,000 neuron cultures are already too complex at present for us to gain an overall insight.

When they are grown to sizes such as 30 million neurons and beyond, clearly the problem is significantly magnified. Looking a few years out, it seems quite realistic to assume that such cultures will become larger, potentially growing into sizes of billions of neurons. On top of this, the nature of the neurons may be diversified. At present rat neurons are generally employed in studies. However human neurons are also now being cultured, enabling robots each with a human neuron brain. Clearly when this brain consists of billions of neurons, many social and ethical questions will need to be asked [24].

For example - If the robot brain has roughly the same number of human neurons as a typical human brain then could/should it have similar rights to humans? Also - What if such creatures had far more human neurons than in a typical human brain – e.g. a million times more – would they make all future decisions rather than regular humans?

DOI: 10.2420/AF06.2013.25

Space Travel via a Cultured Brain

However this technology does open up significant opportunities when we look at space travel. Sending living humans through the considerable distances required for space travel, especially if we wish to explore outside our own solar system, is extremely problematic – 1. Due to the time taken potentially extending well over a lifetime or two: 2. Due to the requirements to keep a human alive for such a period in a stand-alone environment: 3. Due to the considerable unknown hazards that could potentially be faced on arrival: 4. Due to the rigours on the human body during the trip, e.g. effects of gravity loss on the body and brain.

The possibility is open here to freeze human neurons for the period of travel and to defrost them when within the gravitational pull of the distant planet. Robot technology could be employed to culture the neurons and embody them on arrival and not before. All that would be required would be a method to retain their feedstock in a reasonable state over the necessary time. Educational aspects could be provided to cause the newly embodied brain to investigate the planet as desired and to communicate any results in a suitable fashion.

Advantages of such space travel are considerable. Costs to send such creatures to a distant planet would be very little different to sending a mere technological robot. Certainly such costs would be far less than sending a human expedition. Further, if anything was to go wrong either on arrival or during the journey then no life, in the normal sense of the word, would be lost, hence there would be little or no negative political outcry.

3 General Purpose Brain Implants

In this section we consider as a start point a regular human body and brain. It is certainly possible even now to employ implants within the human brain to attempt to counteract the effects of neurological problems [16, 30, 29], i.e. the use of implants for therapeutic purposes. Even in such cases it is quite possible to consider employing such technology to give individuals abilities not normally possessed by humans. Human Enhancement! Here however we look at the possibility of neural implants being employed directly to extend human capabilities.

With general brain-computer interfaces the therapy - enhancement situation is complex. In some cases it is possible for those who have suffered an amputation or have received a spinal injury due to an accident, to regain control of devices via their (still functioning) neural signals [7]. Meanwhile stroke patients can be given limited control of their surroundings, as indeed can those who have such as motor neurone disease.

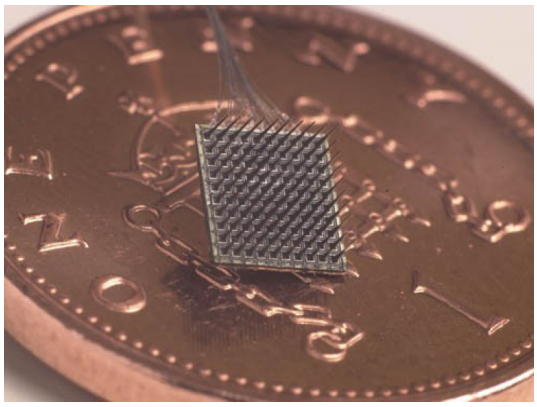

Figure 2. *A 100 electrode, 4X4mm Microelectrode Array, shown on a UK 1 pence piece for scale.*

Even with these cases the situation is not exactly simple, as each individual is given abilities that no normal human has – for example the ability to move a cursor around on a computer screen from neural signals alone [11]. The same quandary exists for blind individuals who are allowed extra sensory input, such as sonar (a bat-like sense) – it doesn't repair their blindness but rather allows them to make use of an alternative sense.

Some of the most impressive human research to date has been carried out using the microelectrode array, shown in Figure 2 [14, 25, 8]. The individual electrodes are 1.5 mm long and taper to a tip diameter of less than 90 microns. Although a number of trials not using humans as a test subject have occurred, human tests are at present limited to two groups of studies. In the second of these the array has been employed in a recording only role, most notably recently as part of (what was called) the "Braingate" system.

Essentially electrical activity from a few neurons monitored by the array electrodes was decoded into a signal to direct cursor movement. This enabled an individual to position a cursor on a computer screen, using neural signals for control combined with visual feedback. The same technique was later employed to allow the individual recipient, who was paralysed, to operate a robot arm [10]. The first use of the microelectrode array (shown in Figure 2) has though considerably broader implications which extend the capabilities of the human

 DOI: 10.2420/AF06.2013.25

recipient.

Actually deriving a reliable command signal from a collection of captured neural signals is not necessarily a simple task, partly due to the complexity of signals recorded and partly due to time constraints in dealing with the data. In some cases however it can be relatively easy to look for and obtain a system response to certain anticipated neural signals – especially when an individual has trained extensively with the system. In fact neural signal shape, magnitude and waveform with respect to time are considerably different to the other signals that it is possible to measure in this situation.

The interface through which a user interacts with technology provides a distinct layer of separation between what the user wants the machine to do, and what it actually does. This separation imposes a cognitive load that is proportional to the difficulties experienced. The main issue is interfacing the human motor and sensory channels with the technology in a reliable, durable, effective, bi-directional way. One solution is to avoid this sensorimotor bottleneck altogether by interfacing directly with the human nervous system.

An individual human so connected can potentially benefit from some of the advantages of machine/artificial intelligence, for example rapid and highly accurate mathematical abilities in terms of "number crunching", a high speed, almost infinite, internet knowledge base, and accurate long term memory. Additionally, it is widely acknowledged that humans have only five senses that we know of, whereas machines offer a view of the world which includes infra-red, ultraviolet, ultrasonic signals, to name but a few.

Humans are also limited in that they can only visualise and understand the world around them in terms of a limited 3 dimensional perception, whereas computers are quite capable of dealing with hundreds of dimensions. Perhaps most importantly, the human means of communication, essentially transferring a complex electro-chemical signal from one brain to another via an intermediate, often mechanical slow and error prone medium (e.g. speech), is extremely poor, particularly in terms of speed, power and precision. It is clear that connecting a human brain, by means of an implant, with a computer network could in the long term open up the distinct advantages of machine intelligence, communication and sensing abilities to the implanted individual.

As a step towards a more broader concept of brain-computer interaction, in the first study of its kind, the microelectrode array (as shown in Figure 2) was implanted into the median nerve fibers of a healthy human individual (the author) during two hours of neurosurgery in order to test bidirectional functionality in a series of experiments. A stimulation current directly into the nervous system allowed information to be sent to the user, while control signals were decoded from neural activity in the region of the electrodes [26]. In this way a number of experimental trials were successfully concluded [27]. In particular:

1. Extra sensory (ultrasonic) input was successfully implemented.
2. Extended control of a robotic hand across the internet was achieved, with feedback from the robotic fingertips being sent back as neural stimulation to give a sense of force being applied to an object (this was achieved between Columbia University, New York (USA) and Reading University, England).
3. A primitive form of telegraphic communication directly between the nervous systems of two humans (the author's wife assisted) was performed [27].
4. A wheelchair was successfully driven around by means of neural signals.
5. The colour of jewellery was changed as a result of neural signals – also the behavior of a collection of small robots.

In most, if not all, of the above cases it could be regarded that the trial proved useful for purely therapeutic reasons, e.g. the ultrasonic sense could be useful for an individual who is blind or the telegraphic communication could be very useful for those with certain forms of Motor Neurone Disease. However each trial can also be seen as a potential form of enhancement beyond the human norm for an individual.

The author did not need to have the implant for medical purposes to overcome a problem but rather for scientific exploration. The question then arises as to how far should things be taken? Clearly enhancement by means of Brain-Computer Interfaces opens up all sorts of new technological and intellectual opportunities, however it also throws up a raft of different ethical considerations that need to be addressed directly.

When ongoing experiments of the type just described involve healthy individuals where there is no reparative element in the use of a brain computer interface, but rather the main purpose of the implant is to enhance an individual's abilities, it is difficult to regard the operation as being for therapeutic purposes. Indeed the author, in

carrying out such experimentation, specifically wished to investigate actual, practical enhancement possibilities [26, 27]. From the trials it is clear that extra sensory input is one practical possibility that has been successfully trialled, however improving memory, thinking in many dimensions and communication by thought alone are other distinct potential, yet realistic, benefits, with the latter of these also having been investigated to an extent. To be clear – all these things appear to be possible (from a technical viewpoint at least) for humans in general.

As we presently stand, to get the go ahead for an implantation in each case (in the UK anyway), requires ethical approval from the local hospital authority in which the procedure is to be carried out, and, if it is appropriate for a research procedure, also approval from the research and ethics committee of the establishment involved. This is quite apart from Devices Agency approval if a piece of equipment, such as an implant, is to be used on many individuals. Interestingly no general ethical clearance is needed from any societal body – yet the issues are complex.

If we now consider the possibilities with this type of implant when it comes to space travel then these are quite different in comparison with those considered earlier for the brain grown within a robot body. In this case any technology is regarded by the recipient as merely being a new bi-directional extension to their body, rather akin to another leg or arm. In reality however the extension can take on any desired technical form. It certainly does not have to be an actual leg or arm, rather it can be a wheeled device or a building. Whatever form it takes, the individual whose brain is connected into it as the sole controlling element, regards it as being themselves.

Space Travel via Implants

If now we consider space travel the opportunity exists for the individual person to remain on planet earth – they do not need to travel – but their new body parts can travel to distant solar systems. By means of an implant, as discussed here, once the required items of technology have safely landed on a distant planet then the connection can be made with the individual who has remained on earth.

In this way, whilst the individual is safe on earth, their new body parts can investigate the planet of choice as though the individual was there themselves. The one negative in this plan is the potential significant time lag between a signal being transmitted from the brain of the individual on earth, bringing about an action in the distant body part and receiving a response from any sensors on the body part. Practical experiments to this end have thus far only involved such a loop from Columbia University, New York to/from Reading University, England [27]. However from such experience it can be reported that the human brain can cope with the different parameters that arise.

It has to be acknowledged though that the time lag between the actuation and sensing in terms of controlling devices in space by means of an implant is a significant problem. Unless our present understanding of physics changes then there appears to be no way of avoiding this. So either brain coupled control of devices in space from earth will be limited to low to medium space orbits or for such control in distant solar systems then the time delays involved will be considerable.

Once again however there is an enormous cost saving for this type of space travel when compared to manned missions. Whilst a neural implantation is indeed required, the costs are as nothing to those of space travel. Time is also important here. The individual involved can lead a perfectly normal life until their distant body parts are switched on. Space travel would, very likely, have tied up those travelling for many years.

Dangers are also significantly reduced with this method. Although a neural implant is required, as of yet, there have been no reported problems with this type of implant. Indeed it is several years since the author experienced the implant and there are no mal-effects whatsoever to report. Space travel meanwhile, even after considerable expense, has many associated hazards. This must be coupled with the potential extra hazards of travelling further, for longer, than ever before and visiting, for the first time, new, relatively unknown, planets.

One other question that might be raised with regard to an implant of this type is the potential durability of the connection between the human nervous system and technology. It has to be admitted that in terms of experimentation involving an able bodied individual then the length of functionality reported is just over 3 months, this limitation being due to the length of the experiment rather than a problem with the implant [22]. However it has been found that the microelectrode array can provide a reliable computer interface to an individual with tetraplegia 1000 days after implantation [19].

 DOI: 10.2420/AF06.2013.25

4 Non-Invasive Brain-Computer Interfaces

The most studied Brain-Computer Interface is perhaps that involving Electroencephalography (EEG) and this is due to several factors. Firstly it is (as the heading says) non-invasive, hence there is no need for surgery with potential infection and/or side effects. As a result ethical approval requirements are significantly less and, due to the ease of electrode availability, costs are significantly less than other methods.

It is also a portable procedure, involving electrodes which are placed on to the outside of a person's head and can be set up in a lab with relatively little training and little background knowledge and taking little time – it can be done then and there, on the spot. As a consequence of this to some researchers, not so well versed in the field, one sometimes often encounters the feeling that BCI = EEG = BMI (Brain-Machine Interface), i.e. to some it appears that EEG collected via scalp electrodes is the only form of BCI.

The number of electrodes employed for experimental purposes can vary from a small number, 4 to 6, to the most commonly encountered 26-30, to well over 100 for those attempting to achieve better resolution. As a result it may be that individual electrodes are attached at specific locations or a cap is worn in which the electrodes are pre-positioned. The care and management of the electrodes also varies considerably between experiments from those in which the electrodes are positioned dry and external to hair to those in which hair is shaved off and gels are used to improve the contact made.

Some studies are employed more in the medical domain, for example to study the onset of Epileptic seizures in patients. However the range of applications is widespread. A few of the most typical and/or interesting are included here as much to give an idea of possibilities and ongoing work rather than for a complete overview of the present state of play.

Typical are those in which subjects learn to operate a computer cursor in this fashion [21]. It must be pointed out here however that, even after significant periods of training (many months), the process is slow and usually requires several attempts before success is achieved. Along much the same lines, numerous research groups have used EEG recordings to switch on lights, control a small robotic vehicle and control other analogue signals [13, 20]. A similar method was employed, with a 64-electrode skull cap, to enable a quadriplegic to learn to carry out simple hand movement tasks by means of stimulation through embedded nerve controllers [12].

It is possible also to consider the uniqueness of specific EEG signals, particularly in response to associated stimuli, potentially as an identification tool [15]. Meanwhile interesting results have been achieved using EEG for the identification of intended finger taps, whether the taps occurred or not, with high accuracy. This is useful as a fast interface method as well as a possible prosthetic method [5].

Whilst EEG experimentation is relatively cheap, portable and easy to set up, in a completely different light, yet still within the category of non-invasive techniques, both functional Magnetic Resonance Imaging (fMRI) and Magnetoencephalography (MEG) have also been successfully employed. fMRI brain scans use a strong, permanent magnetic field to align nuclei in the brain region being studied to ascertain blood flow at specific times in response to specific stimuli. As was reported earlier they can therefore be used as a marker to figure out where there is activity in the brain when an individual thinks about moving their hand.

The equipment is though necessarily cumbersome and relatively expensive. As a result of the cost and equipment availability, experimentation in this area is by no means as widespread as that for EEG. Results have nevertheless been obtained in reconstructing images from such scans [17] and matching visual patterns from watching videos with those obtained in a time stamped fashion from the fMRI scans being recorded [1].

Space Travel via EEG

It is not so immediately obvious to assign advantages in space travel to this type of brain-computer interaction. If we can learn to recognise more easily and accurately intent from neural signals then potentially the technique could be of some use remotely. But without the concept of feedback and hence feelings, it is difficult to see how travelling astronauts could immediately be replaced in this way.

Nevertheless the potential for monitoring the brain activity of astronauts by means of this technology is clear. This is especially pertinent in order to research the effects of the long term lack of earth's gravity on brain functioning. A good review of the overall potential of such interfaces in space travel can be found in [18].

5 Subdermal Magnetic Implants

One final area to be considered here is that of subdermal magnetic implants [9]. This involves the controlled stimulation of mechanoreceptors by an implant manipulated through an external electromagnet. A suitable magnet and implant site are required for this along with an external interface for manipulating the implant. Clearly issues such as magnetic field strength sensitivity and frequency sensitivity are important.

Implantation is an invasive procedure and hence implant durability is an important requirement. Only permanent magnets retain their magnetic strength over a very long period of time and are robust to various conditions. This restricts the type of magnet that can be considered for implantation to permanent magnets. Hard ferrite, Neodymium and Alnico are easily available, low cost permanent magnets suitable for this purpose.

The magnetic strength of the implant magnet contributes to the amount of agitation the implant magnet undergoes in response to an external magnetic field and also determines the strength of the field that is present around the implant location.

The skin on the human hand contains a large number of low threshold mechanoreceptors that allow humans to experience in great detail the shape, size and texture of objects in the physical world through touch. The highest density of mechanoreceptors is found in the fingertips, especially of the index and middle fingers. They are responsive to relatively high frequencies and are most sensitive to frequencies in the range 200Hz-300Hz.

For reported experiments [9], the pads of the middle and ring fingers were the preferred sites for magnet implantation. A simple interface containing a coil mounted on a wire-frame and wrapped around each finger was designed for generating the magnetic fields to stimulate movement in the magnet within the finger. The general idea being that the output from an external sensor is used to control the current in the wrapped coil. So as the signals detected by the external sensor change, these in turn are reflected in the amount of vibration experienced through the implanted magnet.

A number of application areas have already been experimented on, as reported in [9]. The first being ultrasonic range information. This scenario connects the magnetic interface to an ultrasonic ranger for navigation assistance. Distance information from the ranger was encoded via the ultrasonic sensor as variations in frequency of current pulses, which in turn were passed on to the electromagnetic interface.

It was found that this mechanism allowed a practical means of providing reasonably accurate information about the individual's surrounding towards navigational assistance. The distances were intuitively understood within a few minutes of use and were enhanced by distance "calibration" through touch and sight.

A further application involves reading Morse signals. This application scenario applies the magnetic interface towards communicating text messages to humans using an encoding mechanism suitable for the interface. Morse code was chosen for encoding due to its relative simplicity and ease of implementation.

In this way text input can be encoded as Morse code and the dots and dashes transmitted to the interface. The dots and dashes can be represented as either frequency or magnetic field strength variations.

Space Travel using Magnetic Implants

The invasiveness of such implants is relatively trivial. Indeed many who have piercings see the necessary operation as of no concern whatsoever. Clearly we are not looking here at a new form of motor control but rather a way to sense other signals not normally sensed by humans – infra red being a good, immediate example.

In this case therefore it may be simply an extra tool for an astronaut. Rather than use technology to take measurements of different signals they could potentially, with an implant or two of this type in place, experience sensations themselves of the different signals measureable on another planet. In particular, if it was felt likely that certain signals, if they rise above a previously defined threshold, could spell danger for that person, so the implant could prove to be very useful as an early warning indicator of danger.

6 Conclusions

In this article a look has been taken at several different types of brain-computer interface. Experimental cases have been reported on in order to indicate how humans can merge with technology in this way – thereby throwing up a plethora of social considerations as well as technical issues. In each case reports on actual practical experimentation results have been given, rather than merely some theoretical concepts.

In particular when considering robots with biological brains, this could ultimately mean perhaps human brains operating in a robot body. Therefore, should such a robot be given rights of some kind? If one was

 DOI: 10.2420/AF06.2013.25

switched off would this be deemed as cruelty to robots? More importantly at this time – should such research forge ahead regardless? Before too long we may well have robots with brains made up of human neurons that have the same sort of capabilities as those of the human brain and the ethical aspects of such an eventuality need to be discussed.

Meanwhile in the section considering a more general purpose invasive brain implant as well as implant employment for therapy a look was taken at the potential for human enhancement. Already extra-sensory input has been scientifically achieved, extending the nervous system over the internet and a basic form of thought communication. If many humans upgrade and become part machine (Cyborgs) then that could have a significant impact also on those who do not. Indeed if ordinary (non-implanted) humans are left behind as a result then this could bring about the digital divide. It will be interesting for each person to consider that if any individual could be enhanced, would they even question it [23]?

Then came a section on the much more standard EEG electrodes which are positioned externally and which therefore are encountered much more frequently. Unfortunately the resolution of such electrodes is relatively poor and they are indeed only useful for monitoring and not stimulation. Hence issues surrounding them are somewhat limited. We may well be able to use them to learn a little more about how the brain operates but it is difficult to see them every being used for highly sensitive control operations when several million electrodes feed into the information transmitted by each electrode.

Finally a quick look was taken at sub-dermal magnetic implants. This type of connection has, until recently been investigated more by body modification artists rather than scientists and hence application areas are still relatively few. Whilst involving an invasive procedure it still is relatively straightforward in comparison with such as Deep Brain Stimulation or Multi Electrode Arrays fired into the nervous system. It is expected therefore that this will become an area of considerable interest over the next few years with many more potential application areas being revealed.

As well as taking a look at the procedures involved, the aim in this article has been to have a look at some of the ethical and social issues as well. Some technological issues have though also been pondered on in order to open a window on the direction that developments are heading. In each case however a firm footing has been planted on actual practical technology rather than on speculative ideas. In a sense the overall idea is to open up a sense of reflection such that further experimentation can be guided by the informed feedback that results.

In each case the possibilities of how this technology could play a part in space travel has been considered. In this respect the first two examples proved to be potentially most useful and certainly disruptive. It is felt that both culturing brains and embodying them within a robot body and the use of neural implants offer significant advantages, for mainly cost and safety reasons, in comparison with the present manned space travel programmes.

References

[1] M. S. Beauchamp, K. E. Lee, J. V. Haxby, and A. Martin. fMRI responses to video and point-light displays of moving humans and manipulable objects. *Journal of Cognitive Neuroscience*, 15(7):991–1001, 2003.

[2] G. A. Bekey. *Autonomous robots*. MIT Press, 2005.

[3] R. A. Brooks. *Robot*. Penguin, 2002.

[4] M. Chiappalone, A. Vato, L. Berdondini, M. Koudelka-Hep, and S. Martinoia. Network dynamics and synchronous activity in cultured cortical neurons. *International journal of neural systems*, 17(2):87–103, 2007.

[5] I. Daly, S. J. Nasuto, and K. Warwick. Single tap identification for fast BCI control. *Cognitive Neurodynamics*, 5(1):21–30, 2011.

[6] T. B. DeMarse, D. A. Wagenaar, A. W. Blau, and S. M. Potter. The neurally controlled animat: biological brains acting with simulated bodies. *Autonomous Robots*, 11(3):305–310, 2001.

[7] J. P. Donoghue, A. Nurmikko, G. Friehs, and M. Black. Development of neuromotor prostheses for humans. *Supplements to Clinical neurophysiology*, 57:588–602, 2004. Chapter 63 in Advances in Clinical Neurophysiology.

[8] M. Gasson, B. Hutt, I. Goodhew, P. Kyberd, and K. Warwick. Invasive neural prosthesis for neural signal detection and nerve stimulation. *International journal of adaptive control and signal processing*, 19(5):365–375, 2005.

[9] J. Hameed, I. Harrison, M. N. Gasson, and K. Warwick. A novel human-machine interface using subdermal magnetic implants. In *Proc. IEEE International Conference on Cybernetic Intelligent Systems*, pages 106–110, 2010.

[10] L. R. Hochberg, M. D. Serruya, G. M. Friehs, J. A. Mukand, M. Saleh, A. H. Caplan, A. Branner, D. Chen, R. D. Penn, and J. P. Donoghue. Neuronal ensemble control of prosthetic devices by a human with tetraplegia. *Nature*, 442:164–171, 2006.

[11] P. Kennedy, D. Andreasen, P. Ehirim, B. King, T. Kirby, H. Mao, and M. Moore. Using human extra-cortical local field potentials to control a switch. *Journal of neural engineering*, 1(2):72–77, 2004.

[12] N. Kumar. Brain computer interface. Cochin University of Science & Technology Report, Kochi-682022, 2008.

[13] J. Millan, F. Renkens, J. Mourino, and W. Gerstner. Non-invasive brain-actuated control of a mobile robot by human EEG. *IEEE Transactions on Biomedical Engineering*, 51(6):1026–1033, 2004.

[14] C. T. Nordhausen, E. M. Maynard, and R. A. Normann. Single unit recording capabilities of a 100 microelectrode array. *Brain research*, 726(1-2):129–140, 1996.

[15] R. Palaniappan. Two-stage biometric authentication method using thought activity brain waves. *International Journal of Neural Systems*, 18(1):59–66, 2008.

[16] M. M. Pinter, M. Murg, F. Alesch, B. Freundl, R. J. Helscher, and H. Binder. Does deep brain stimulation of the nucleus ventralis intermedius affect postural control and locomotion in parkinson's disease? *Movement Disorders*, 14(6):958–963, 1999.

[17] G. Rainer, M. Augath, T. Trinath, and N. K. Logothetis. Nonmonotonic noise tuning of BOLD fMRI signal to natural images in the visual cortex of the anesthetized monkey. *Current Biology*, 11(11):846–854, 2001.

[18] L. Rossini, D. Izzo, and L. Summerer. Brain-machine interfaces for space applications. In *Proc. IEEE International Conference on Engineering in Medicine and Biology*, pages 520–523. IEEE, 2009.

[19] J. D. Simeral, S. P. Kim, M. J. Black, J. P. Donoghue, and L. R. Hochberg. Neural control of cursor trajectory and click by a human with tetraplegia 1000 days after implant of an intracortical microelectrode array. *Journal of Neural Engineering*, 8(2):025027, 2011.

[20] K. Tanaka, K. Matsunaga, and H. O. Wang. Electroencephalogram-based control of an electric wheelchair. *Robotics, IEEE Transactions on Robotics*, 21(4):762–766, 2005.

[21] L. J. Trejo, R. Rosipal, and B. Matthews. Brain-computer interfaces for 1-D and 2-D cursor control: designs using volitional control of the EEG spectrum or steady-state visual evoked potentials. *IEEE Transactions on Neural Systems and Rehabilitation Engineering*, 14(2):225–229, 2006.

[22] K. Warwick. I, Cyborg. *University of Illinois Press*, 2004.

[23] K. Warwick. The promise and threat of modern cybernetics. *Southern Medical Journal*, 100(1):112–115, 2007.

[24] K. Warwick. Implications and consequences of robots with biological brains. *Ethics and information technology*, 12(3):223–234, 2010.

[25] K. Warwick and M. Gasson. Practical interface experiments with implant technology. In *"Computer Vision in Human-Computer Interaction", Lecture Notes in Computer Science*, volume 3058, pages 7–16, 2004.

[26] K. Warwick, M. Gasson, B. Hutt, I. Goodhew, P. Kyberd, B. Andrews, P. Teddy, and A. Shad. The application of implant technology for cybernetic systems. *Archives of Neurology*, 60(10):1369–1373, 2003.

[27] K. Warwick, M. Gasson, B. Hutt, I. Goodhew, P. Kyberd, H. Schulzrinne, and X. Wu. Thought communication and control: a first step using radiotelegraphy. *IEE Proceedings on Communications*, 151(3):185–189, 2004.

 DOI: 10.2420/AF06.2013.25

[28] K. Warwick, S. Nasuto, V. Becerra, and B. Whalley. Experiments with an in-vitro robot brain. In Y. Cai, editor, *"Instinctive Computing", Lecture Notes in Artificial Intelligence*, volume 5987, pages 1–15, 2010.

[29] D. Wu, K. Warwick, Z. Ma, J. G. Burgess, S. Pan, and T. Z. Aziz. Prediction of Parkinson's disease tremor onset using radial basis function neural networks. *Expert Systems with Applications*, 37(4):2923–2928, 2010.

[30] D. Wu, K. Warwick, Z. Ma, M. N. Gasson, J. G. Burgess, S. Pan, and T. Z. Aziz. Prediction of Parkinson's disease tremor onset using a radial basis function neural network based on particle swarm optimization. *International journal of neural systems*, 20(2):109–118, 2010.

DOI: 10.2420/AF06.2013.25

Acta Futura 6 (2013) 37-42
DOI: 10.2420/AF06.2013.37

Acta Futura

Nacre: An Ancient Nanostructured Biomaterial

C. M. Pina*
Departamento de Cristalografía y Mineralogía, Universidad Complutense de Madrid, E-28040 Madrid, Spain
Instituto de Geociencias IGEO (UCM-CSIC). C/ José Antonio Novais, 2. E-28040 Madrid, Spain
A. G. Checa
Departamento de Estratigrafía y Paleontología, Universidad de Granada, E-18071 Granada, Spain
C. I. Sainz-Díaz and J. H. E. Cartwright
Instituto Andaluz de Ciencias de la Tierra, CSIC-Universidad de Granada, E-18071 Granada, Spain

Abstract. Nacre is a much appreciated natural material which forms in the interior of numerous mollusc shells. Its remarkable optical and mechanical properties are due to a highly nanostructured combination of inorganic and organic components, which has not been reproduced by any industrial process to date. In this paper we briefly review the current knowledge on the composition, structure, properties and mechanisms of formation of this iconic biomaterial.

1 Introduction

Nacre, most commonly known as mother-of-pearl, is a material exclusively secreted by molluscs which appeared on the Earth during the Paleozoic Era. First clear evidence of fossil nacre has been found in rocks formed in the late Ordovician, *i.e.* about 450 million years ago [6]. However, nacre might have an even earlier origin, since well-preserved fossils from the late Cambrian to the middle Ordovician are rare [18, 17]. The outstanding mechanical resistance of nacre suggests that this biomaterial evolved as a response to the increasing abilities and diversity of predators after the so-called Cambrian explosion, a unique event of animal diversification in the history of life. The development of claws, jaws and other novel tools of predation led to an arms race between predators and preys, which produced defensive adaptations such as toxicity, new escape methods (burrowing), camouflage, counter-offense, and armour. As a result of this ancient arms race, molluscs developed new crush-resistant shell microstructures, among which nacre is one of the most sophisticated and efficient. Recent paleontological studies indicate that molluscs "invented" nacre several times, *i.e.* nacre convergently evolved in at least four different classes of molluscs [18]. The significant differences in the microstructure and growth process of nacre between molluscan classes and the variation in both the genes and proteins associated with nacre in modern molluscs provide additional evidence that supports the independent origin of nacre within the Mollusca.

Numerous modern molluscs still produce different kinds of nacre. This natural product is a biocomposite, whose highly hierarchical structure and combination of inorganic and organic components, results in a material with unusual mechanical and optical properties [15, 13]. Until the industrial production of plastics, nacre was widely used in button-making, as construction material, and for decoration purposes (e.g. special

*Corresponding author. E-mail: cmpina@geo.ucm.es

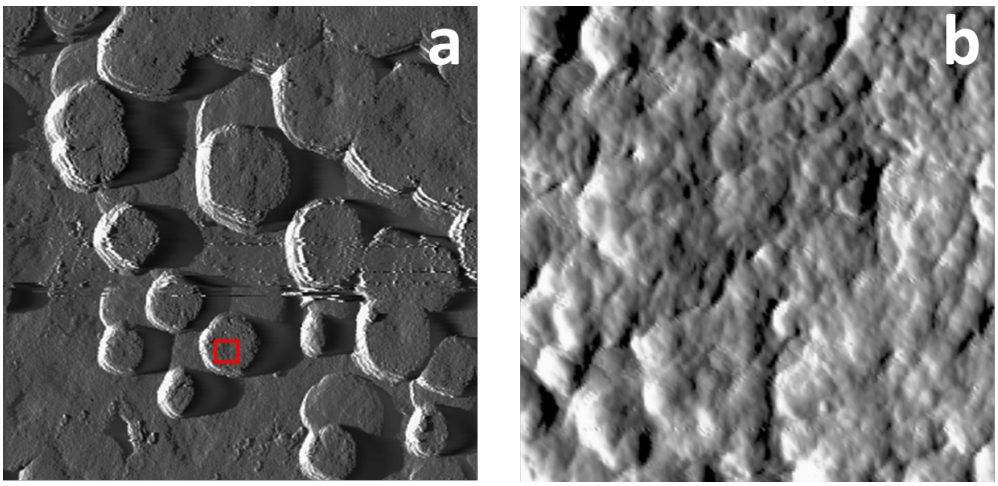

FIGURE 1. *AFM images taken in tapping mode while displaying the amplitude signal. (a) Aragonitic tablets that form the nacre of the mollusc Pteria hirundo. Note that the coalescence of tablets at the upper right results in a homogeneous mineralised layer. (Size of the image: 14.8×14.8 μm^2). (b) Detail of the surface of an aragonitic tablet (red square marked in (a)) showing the agglomerate of nanounits that form it. (Size of the image: 773×773 nm^2).*

tiles and glossy coatings of walls, doors and ceilings). When nacre is deposited in concentric layers around a foreign body in the interior of a mollusc, a pearl is produced. Pearls are appreciated objects in jewellery, whose commercial value depends on their size, perfection and roundness.

In the last few decades, nacre has attracted much attention in material science. Scientists and engineers have realized that nacre is a model material for a new generation of composite ceramics [1]. However, the development of nacre-bioinspired ceramics requires a profound knowledge of the relationships between composition, structure and properties of this ancient natural material.

2 The composition and structure of nacre

Nacre is composed of ≈ 95% of aragonite (orthorhombic $CaCO_3$) and ≈ 5% of a mixture of proteins and the polysaccharide chitin [10, 3]. In nacre, aragonite is in the form of polygonal tablets with a size ranging from 5 to 15 μm and a thickness of about 0.5 μm. Although the shape of the polygonal tablets varies from one species to another, in all the cases their surfaces are rough and formed by numerous mineral subunits of a few nanometres in diameter each (Fig. 1). In mollusc shells, aragonite tablets are arranged forming brickwall-like microstructures in which the organic matter (*i.e.* proteins and chitin) is the "mortar". The arrangement of aragonite tablets varies with the mollusc species and two main patterns can be recognised. While nacre secreted by gastropods is made of columns of tablets, in bivalves, layers of tablets are offset in successive step-like layers (Fig. 2).

3 Formation of nacre

The mechanism of nacre formation is not completely understood yet. Nacre is an extracellular material which forms between the external layer of the shell and the soft living body of the organism, *i.e.*, between a thick layer of calcite or aragonite crystals with a prismatic habit and the so-called mantle. There, one can find the extrapallial cavity, a micro-sized liquid-filled space where the self-assembly of aragonite tablets and organic matter occurs (Fig. 3). Recent authors have proposed a multi-step hierarchic mechanism of nacre formation [3, 4, 5]. Such a complex mechanism begins with the secretion of chitin molecules from the cells of the organism into the extrapallial cavity. These molecules polymerise forming rods of several microns in length which self-organise into a liquid crystal structure. Subsequently the chitin liquid crystal layer is coated by proteins resulting in the formation of an interlamellar membrane. This mem-

 DOI: 10.2420/AF06.2013.37

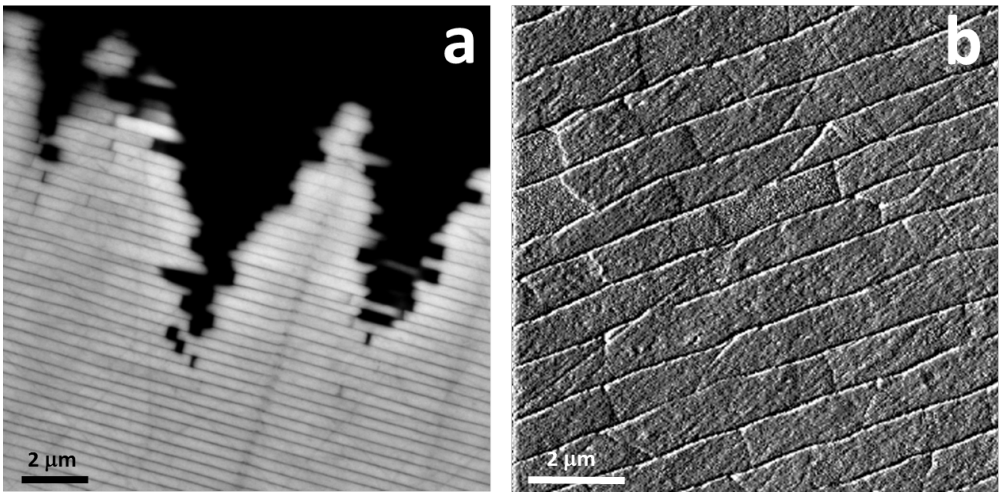

Figure 2. *Examples of the two nacre microstructures found in molluscs. (a) Columnar arrangement of aragonite tablets in the gasteropod Glibula umbilicalis (transmission electron microscopy image). (b) Sheet arrangement of aragonite tablets in the bivalve Neotrigonia margaritacea after the coalescence of tablets (amplitude atomic force microscopy image).*

brane is immersed in the extrapallial fluid which is supersaturated with respect to calcium carbonate. Then the growth of aragonite tablets occurs and the space between interlamellar membranes is progressively mineralised. However, the process leading to the growth and coalescence of aragonite tablets is not well known. Although numerous X-ray diffraction and transmission electron microscopy studies have confirmed the aragonitic nature of the tablets, the formation of amorphous calcium carbonate as a precursor phase of aragonite is still under investigation [19]. The high roughness of the aragonite tablets together with the observation of thin films coating them, suggest that the formation of the tablets takes place by accretion of aragonite nanounits covered by organic membranes. However, thin films might also appear as the result of the "exsolution" of organic molecules during the conversion of amorphous calcium carbonate into aragonite. The fact that the aragonite of nacre frequently incorporates fibrous proteins that previously were found in the interlamelar liquid seems to support both mechanism of tablet formation.

4 The properties of nacre

4.1 Mechanical properties

Nacre shows outstanding mechanical properties, which are superior to those of most common construction materials. As can be seen in Fig. 4, both types of nacre, columnar and sheet nacre, are much more resistant to tensile and compression stress than bricks, cement and concrete. In addition, nacre is significantly stiffer than these materials (*i.e.* it has a higher Young's modulus). Interestingly, nacre has a higher mechanical resistance than pure aragonite. It has been found that while the fracture toughness of nacre ranges from 3.3 to 9.0 $MPam^{1/2}$, the fracture toughness of inorganic aragonite crystals is approximately 1 $MPam^{1/2}$ [9, 14, 20, 8, 16]. The high toughness of nacre is comparable to advanced engineering materials and ceramic metal composites (cermets). This is remarkable considering that the 95% of nacre is made of the brittle mineral aragonite [1].

The mechanical properties of nacre also change with the degree of hydration. Thus, dry nacre behaves under tension elastically up to brittle failure, in a similar way as an aragonite single crystal does. In contrast, hydrated nacre, has an almost ductile response to tension. Such a response of nacre begins at tensile stresses of about 60-

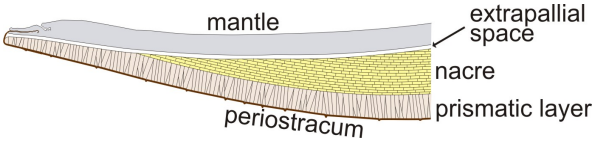

Figure 3. *Schematic drawing of the structure of a mollusc shell.*

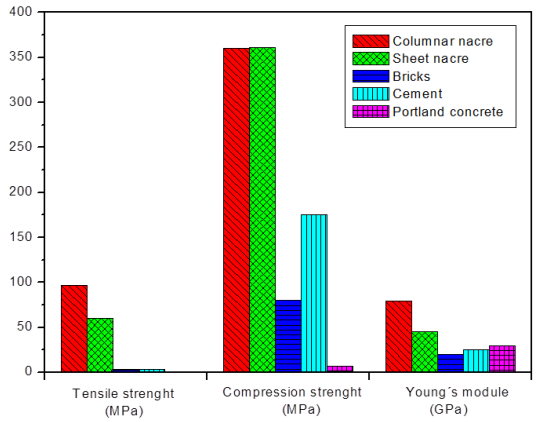

FIGURE 4. *Comparison between main mechanical properties of nacre and construction materials. Data for nacre are averaged from those in [7]. Data for construction materials are typical values found in the literature and internet sources.*

70 MPa, the deformation of the material at the brittle failure being of almost 1% [1]. This strain at the failure is low compared to many engineering materials but it is ten times higher than the strain at failure of aragonite. The ductile behaviour of wet nacre can be explained in terms of a collective sliding of aragonite tables at the microscale [16].

4.2 Optical properties

Undoubtedly, the most remarkable optical property of nacre is its iridescent shine. This shine is due to the fact that the thickness of the aragonite tablets is within the range of wavelengths of visible light (*i.e.* from 400 nm to 700 nm, approximately). As a consequence, light rays interfere constructively and destructively within the aragonite platelets depending on their incident angle. This angle-dependent interference generates different pale colours whose intensity varies with the position of the observer. The resulting effect is called structural coloration, since it is not related to any pigment but to a nanostructured reflective and refractive surface.

When nacre is arranged more or less concentrically, as is the case with pearls, propagation of light becomes more complex and diffraction, birefringence and scattering phenomena modify the iridescent shine [13]. These phenomena, combined with the presence of organic and inorganic impurities, play a major role in determining the variety and quality of the natural and cultivated pearls used in jewellery.

5 Synthetic analogues of nacre

The production of materials with similar properties to those of nacre is not an easy task. Even though complex fabrication methods have been used to obtain composites with the stiffness and toughness of nacre, none of them entirely reproduce all the mechanical properties of the natural material [1]. In all the cases, these synthetic composites are made of hard particles glued together with a much softer and ductile component. The key to achieving all the characteristic mechanical properties of nacre is the control of: (i) the size, thickness and orientation of the hard particles, (ii) the interfacial properties between hard and ductile components, and (iii) the formation of a self-assembled hierarchical microstructure. To this end, various fabrication techniques, which include layer-by-layer deposition, colloidal assembly and sintering, have been explored.

By using a layer-by-layer assembly technique, a "nacre-like" nanocomposite has been recently prepared from vinyl alcohol and Na^{+-} montmorillonite clay nanosheets [12]. The obtained material shows a laminar microstructure which is strong and flexible. Interestingly, the surfaces of this laminated nanocomposite are highly transparent, resembling those of nacre.

Colloidal assembly also resulted in an interesting way of fabricating materials inspired by nacre. Based on this technique, an alumina/chitosan polymer was synthesised to have a low ceramic content but with a structure and mechanical properties similar to nacre [2]. In this case, the aspect ratio of the alumina embedded in the chitosan matrix was essential to ensure an adequate tablet sliding when fracture occurs.

To date, the synthetic material closest to natural nacre is a composite made of alumina and polymethyl methacrylate (PMMA) [11]. To produce such a material a complex protocol is required. Firstly, microscopic particles with a specific size have to be produced from alumina powder and using ice platelets as a template. Only then a sintering process and the infiltration of PMMA are conducted. The result is a highly deformable composite with a remarkable toughness but still not as fracture resistant as that of nacre.

6 Conclusion

Although nacre has been intensively investigated during the last few decades, the origin of its valuable features, as well as the mechanisms of its formation, still remain incompletely understood. Further investigations

 DOI: 10.2420/AF06.2013.37

are needed to elucidate the complex relationships between microstructure, composition and mechanical and optical properties of nacre. In addition, the sequence of processes which lead to a hierarchical self-assembly of organic and inorganic components still requires more material characterisations, experimental work and modelling. The acquisition of this knowledge is fundamental for mimicking all the properties of nacre. Only then, the microstructures and construction principles of nacre will be successfully transferred from nature to technology.

References

[1] F. Barthelat. Nacre from mollusk shells: a model for high-performance structural materials. *Bioinspiration & Biomimetics*, 5(3):035001, 2010.

[2] L. J. Bonderer, A. R. Studart, and L. J. Gauckler. Bioinspired design and assembly of platelet reinforced polymer films. *Science*, 319(5866):1069–1073, 2008.

[3] J. H. E. Cartwright and A. G. Checa. The dynamics of nacre self-assembly. *Journal of The Royal Society Interface*, 4(14):491–504, 2007.

[4] J. H. E. Cartwright, A. G. Checa, B. Escribano, and C. I. Sainz-Díaz. Spiral and target patterns in bivalve nacre manifest a natural excitable medium from layer growth of a biological liquid crystal. *Proceedings of the National Academy of Sciences*, 106(26):10499–10504, 2009.

[5] A. G. Checa, J. H. E. Cartwright, and M.-G. Willinger. The key role of the surface membrane in why gastropod nacre grows in towers. *Proceedings of the National Academy of Sciences*, 106(1):38–43, 2009.

[6] V. V. Druschits, L. Doguzhaeva, and V. G. Korinevskiy. Shell microstructure of the Ordovician monoplacophoran Romaniella Doguzhaeva, 1972. *Dokl. Akad. Nauk SSR*, 245:458–461, 1979.

[7] T. Furuhashi, C. Schwarzinger, I. Miksik, M. Smrz, and A. Beran. Molluscan shell evolution with review of shell calcification hypothesis. *Comparative Biochemistry and Physiology Part B: Biochemistry and Molecular Biology*, 154(3):351–371, 2009.

[8] K. E. Gunnison, M. Sarikaya, J. Liu, and I. A. Aksay. Structure-mechanical property relationships in a biological ceramic-polymer composite: Nacre. *MRS Online Proceedings Library*, 255, 0 1991.

[9] A. P. Jackson, J. F. V. Vincent, and R. M. Turner. The mechanical design of nacre. *Proceedings of the Royal Society of London. Series B. Biological Sciences*, 234(1277):415–440, 1988.

[10] Y. Levi-Kalisman, G. Falini, L. Addadi, and S. Weiner. Structure of the nacreous organic matrix of a bivalve mollusk shell examined in the hydrated state using Cryo-TEM. *Journal of Structural Biology*, 135(1):8–17, 2001.

[11] E. Munch, M. E. Launey, D. H. Alsem, E. Saiz, A. P. Tomsia, and R. O. Ritchie. Tough, bio-inspired hybrid materials. *Science*, 322(5907):1516–1520, 2008.

[12] P. Podsiadlo, A. K. Kaushik, B. S. Shim, A. Agarwal, Z. Tang, A. M. Waas, E. M. Arruda, and N. A. Kotov. Can nature's design be improved upon? high strength, transparent nacre-like nanocomposites with double network of sacrificial cross links. *The Journal of Physical Chemistry B*, 112(46):14359–14363, 2008.

[13] C. Raman and D. Krishnamurti. The structure and optical behaviour of iridescent shells. *Proceedings of the Indian Academy of Sciences - Section A*, 39(1):1–13, 1954.

[14] M. Sarikaya, K. E. Gunnison, M. Yasrebi, and I. A. Aksay. Mechanical property-microstructural relationships in abalone shell. *MRS Online Proceedings Library*, 174, 0 1989.

[15] J. Sun and B. Bhushan. Hierarchical structure and mechanical properties of nacre: a review. *RSC Adv.*, 2:7617–7632, 2012.

[16] J. Sun and J. Tong. Fracture toughness properties of three different biomaterials measured by nanoindentation. *Journal of Bionic Engineering*, 4(1):11–17, 2007.

[17] M. J. Vendrasco, A. Checa, W. P. Heimbrock, and S. D. Baumann. Nacre in molluscs from the ordovician of the midwestern united states. *Geosciences*, 3(1):1–29, 2013.

[18] M. J. Vendrasco, A. G. Checa, and A. V. Kouchinsky. Shell microstructure of the early bivalve pojetaia and the independent origin of nacre within the mollusca. *Palaeontology*, 54(4):825–850, 2011.

[19] S. Weiner, Y. Levi-Kalisman, S. Raz, and L. Addadi. Biologically formed amorphous calcium carbonate. *Connective Tissue Research*, 44(1):214–218, 2003.

[20] M. Yasrebi, G. H. Kim, K. E. Gunnison, D. L. Milius, M. Sarikaya, and I. A. Aksay. Biomimetic processing of ceramics and ceramic-metal composites. *MRS Online Proceedings Library*, 180, 0 1990.

 DOI: 10.2420/AF06.2013.37

Acta Futura 6 (2013) 43-52
DOI: 10.2420/AF06.2013.43

Acta Futura

Forisomes-based Smart Biomaterials: A Boon in Disguise for Space Science Application

Vineet Kumar Srivastava, Renu Tuteja and Narendra Tuteja*
International Center for Genetic Engineering and Biotechnology (ICGEB), Aruna Asaf Ali Marg 110 067, New Delhi, India
Dhruva Tuteja
University of Michigan, Department of Mechanical Engineering (Alumni), GG Brown Laboratory, 2350 Hayward, Ann Arbor, MI 48109, USA

Abstract. This review gives a brief overview of the possible applications of novel forisome protein found in sieve tubes of legumes, which are ATP-independent mechanically active protein as biomimetic smart materials. It also focuses on the potential applications of forisome as actuators in micro fluidics system. Technology enabling improvement in micro instrument has been identified as a key technology by European Space Agency (ESA) and National Aeronautics and Space Administration (NASA) in future space exploration missions. Forisome as smart materials have a dual function both as sensors and actuators, thus reducing the complexity of the system. Potentially, forisome are ideal biomimetic materials for micro fluidic system because the conformational shifts can be replicated in vitro and are fully reversible over large number of cycles. It can be produced on demand and also tailored in the form of recombinant protein by genetic engineering. Recently, forisome has received attention because of its unique ability to convert chemical energy into mechanical energy. For handling biomolecules such as DNA, RNA, protein and cell as a whole microfluidic system will be the most powerful technology. The field of microfludic, particularly in terms of development of its components along with identification of new biomimetic smart materials, deserves more attention. The discovery of new biomimetic smart materials has been a key factor in development of space science and its requirements in such a challenging environment. More biophysical investigation is required to characterize it to make it more amenable through genetic engineering in general and protein engineering in particular to make it more suitable under parameters of performance.

*Corresponding author. E-mail: narendra@icgeb.res.in

1 Introduction

Proteins are biopolymers, with their monomer unit composed of 20 different amino acids and given their nature of composition; they can serve as very good smart materials. Forisome, a plant protein specific to legume family, is located in plant phloem tissue specifically known as sieve elements [18]. The term forisome is coined by Knoblauch [18], meaning gate-bodies (latin *foris*: wing of a gate; greek *soma*: body). The sieve tubes in legume contain forisome, which are spindle-like bodies that are composed of ATP-independent, mechanically active proteins. The motility in both animal and plant cells is linked both with the movement of motor proteins and with the hydrolysis of ATP, the energy currency of cell. Motor proteins are defined as nucleoside triphosphate-dependent actuators [1]. These proteins

are found in vascular system of leguminous plants and often defined as 'stopcocks' [20]. The basic requirement in designing of smart molecules lies in the understanding of the structure and functioning of smart materials in their natural environment. In the past, a lot of research has been done in the field of motor proteins linked with ATP hydrolysis like kinesin involved in cell dynamics and organization of living cells [27], and helicases involved in DNA/RNA unwinding [43, 42]. Forisome is particularly attractive as a biomimetic-based smart material because unlike most motor proteins, it is independent of ATP for its activation, making it more flexible, which can be used to produce self powered monitoring and diagnostic systems [44]. The anisotropic contractility in forisome in in vitro study is triggered by an increase in free calcium ion concentration or by pH changes [18, 35]. Thus, forisomes are a class of protein complex which have unique properties that could be exploited in nanotechnological and biomimetics applications. The possible applications include microvalves, microactuators and self powered smart biosensors [18, 19, 26, 45]. These future applications provide the basis for potential applications in biomimetic devices in mechanical nanosystems. Forisome is a smart material with large strain, stiff (forisome-based composites) with quick response, and strong anisotropic deformation. Such smart systems can be integrated with the functions of sensing, actuation, logic, and control to respond repetitively to external stimuli. The forisome-based smart materials can also be developed for use in health monitoring of structural integrity in civil infrastructure and for aerospace hardware. Sensory nervous system for civil structures by using forisomes as the mechanoreceptor has been designed. This can mitigate the damage and prevent the catastrophe with built-in actuators and multi-functional materials.

2 Microfluidics System in Plants-Sieve Element Architecture-Forisome Environment

In nature, the vascular system (microfluidic system) in higher plants consists of two different kinds of microfluidic systems composed of xylem and phloem. Xylem is composed of dead lignified cells and is involved in transport of soluble mineral nutrients from the roots throughout the plant apoplastically. On the other hand phloem is composed of sieve element (SE) and companion cells (CC) (Fig. 1A). The SE are highly specialized cells that loses nucleus, microfilament [31], and dictyosomes. Phloem conducts photoassimilates from source to sink symplastically (Fig. 1 A) [3]. The intimate association between SEs and CCs is necessary because SEs depends on CCs for most of their vital functions as they lose their nucleus and important cell organelles (Fig. 1 A) [46]. Sieve plate is characteristic feature of SE, which is developed due to numerous pores present in the cell wall of the adjacent SE. These sieve plates ensure continuity between adjacent SE (Fig1 B) [11, 22]. Forisome protein are located in SE and prevent loss of photoassimilate upon mechanical injury provided they can be repaired (Fig. 1A) [21, 18] by plugging the point of injury by changing its dimension in relation to elevated level of free calcium ions (Fig. 2 A and B). They function as actuators by changing their geometrical parameters (Fig. 2 B) in response to increased Ca^{2+} concentration above a threshold level (10 mM) (Fig. 2 A) [35, 34]. Geometrically forisome shape changes with an increase in diameter to 100% from 300% whereas its length is reduced by 30% (Fig.2 A).

3 Biological Function of Forisome: Natural Wattless Actuators and Signaling Cascade

Unique natural crystalline protein bodies that undergo reversible dimensional shifts and are not driven by ATP are specific to SE of legume [21] family of plants. The architecture and degree of expansion of forisomes differ between legume species [44]. When plants phloem tissue undergoes injury like mechanical damage, wounding, osmotic shock which generates electro-potential wave's (EPWs) [47] the level of free calcium ion tends to increase. Increased concentration of calcium ion is mediated by voltage, mechano and ligand sensitive calcium channels [47]. The role of EPWs propagation and their origin is of prime importance as they are involved in calcium influx and play pivotal role in signaling and physiological process [47]. Principle forms of EPWs the action potential [12] are mainly propagated in phloem and are initiated by voltage activated calcium channels [47]. Variation potential is electrical message which originates due to relaxation of negative hydrostatic pressure in xylem vessels (microfluidic channels). Variation potential originates in xylem and travels towards phloem, initiated by mechano-sensitive calcium channels [47]. Variation potential leads to increase in calcium ion concentration. Both these forms of waves

 DOI: 10.2420/AF06.2013.43

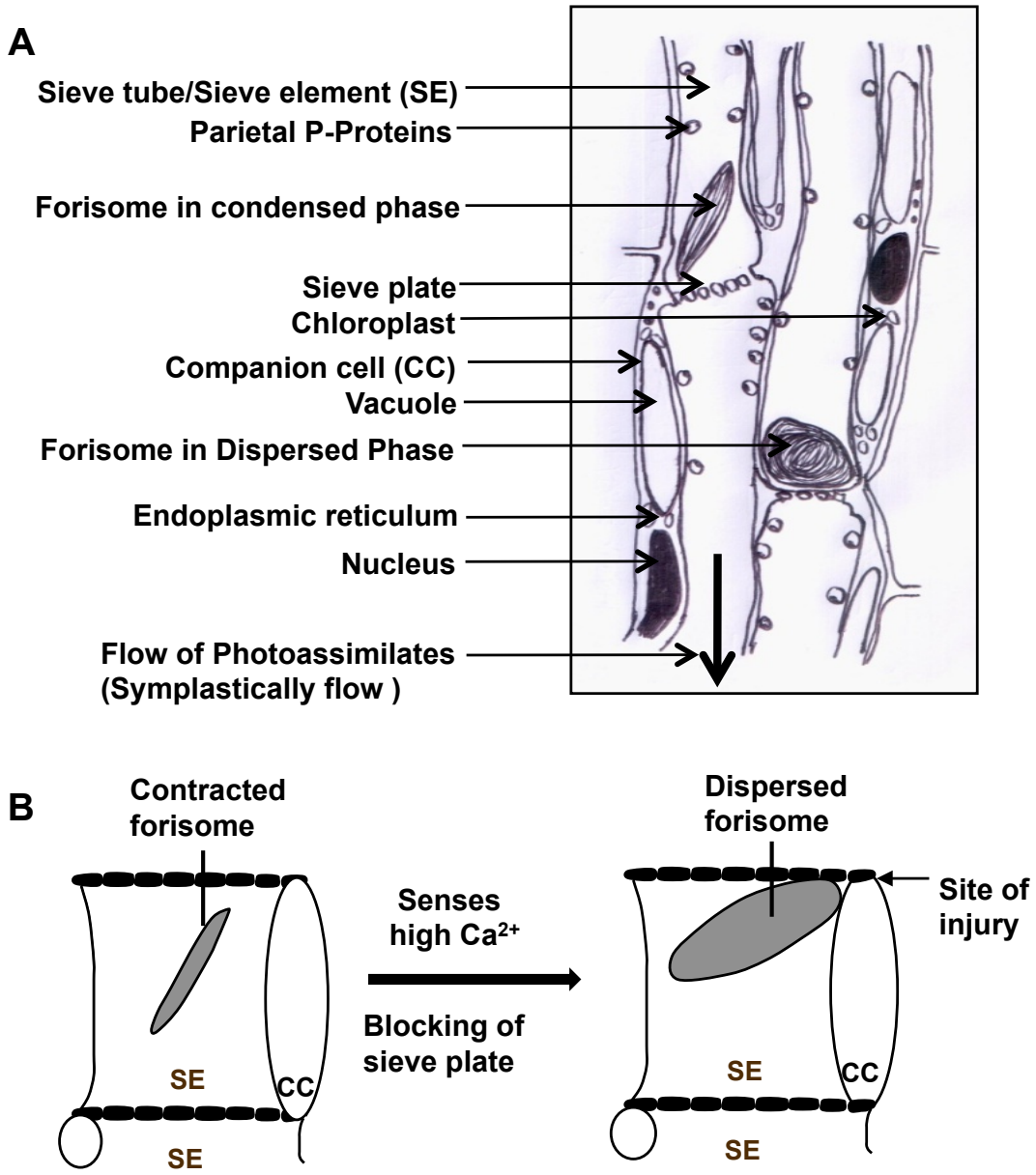

Figure 1. *(A) Labeled diagram showing longitudinal section of Sieve element (SE) and Companion cells (CC) of plant phloem tissue (Architecture of SE). Forisomes are located in SE in condensed phase (absence of* Ca^{2+}*) and in dispersed phase (in presence of* Ca^{2+}*) it plugs the pores in case of injury to plants phloem tissue. Sieve plates are characteristic feature of SE. CC, which contain nucleus are located adjacent to the SE to support the SE. SE contains other components; parietal P proteins, endoplasmic reticulum (source of transient increase in level of* Ca^{2+} *concentration). Bold arrow at the bottom indicates direction of flow of photoassimilates (symplastically flow i.e. through cells). (B) Cartoon showing structural architecture of SE and CC, in phloem tissue of plants. Forisomes are shown in longitudinally expanded (below threshold level of* Ca^{2+} *(10 mM)) and longitudinally contracted state (*Ca^{2+} *above threshold level).*

DOI: 10.2420/AF06.2013.43

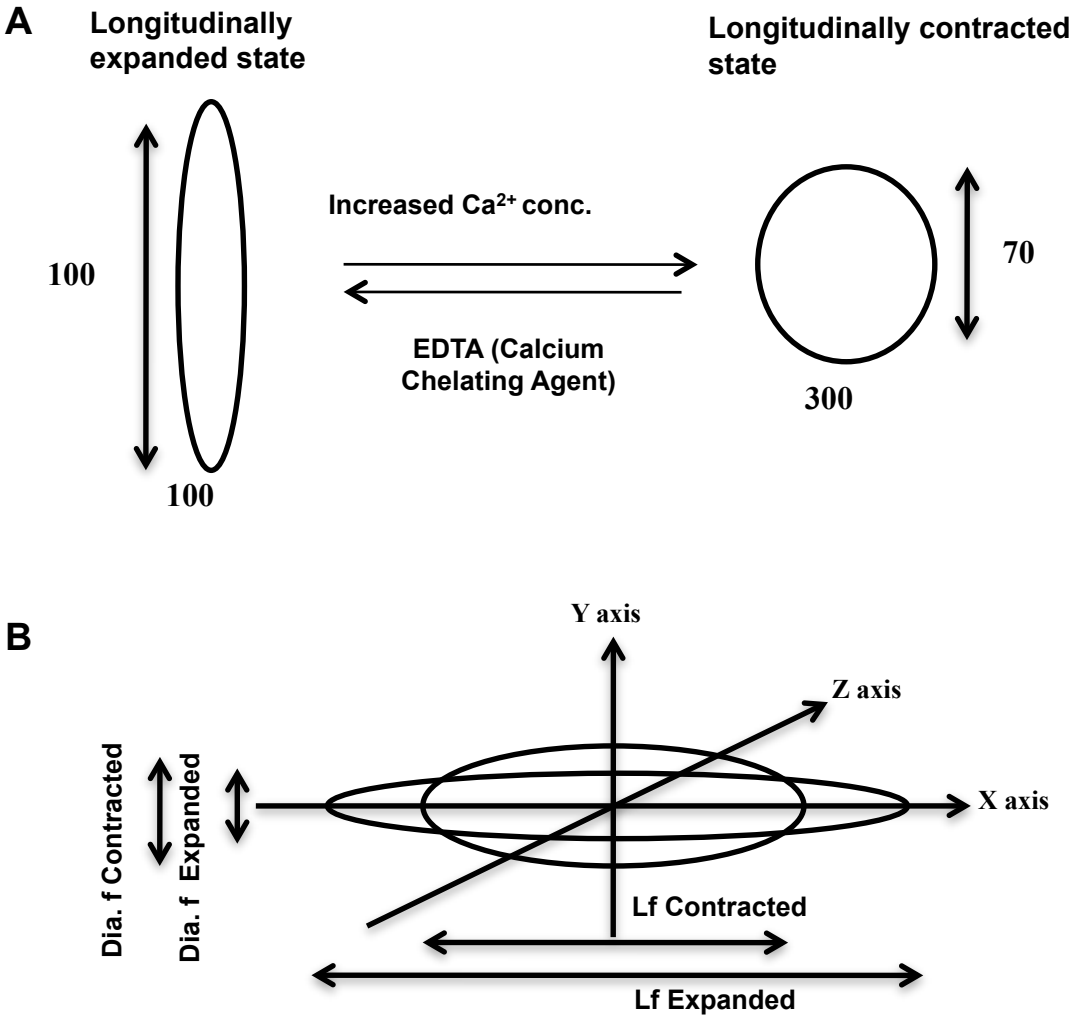

Figure 2. *(A) Cartoon showing forisome working in presence of increased Ca2+ concentration, forisome volume increases three fold (Dia. increases from 100 % to 300 %), whereas the forisome length is reduced by 30%. Volume contraction thus occurs with an increase in length, whereas length contraction occurs with forisome expansion. The dimensional shift of a forisome from the longitudinally expanded to longitudinally contracted state. In presence of calcium chelating agent like EDTA forisomes conformation shifts back to its original confirmation (conformationals shifts is reversible for forisome proteins, which is its unique characteristics). (B) Cartoon showing geometric construction of forisomes and change in geometric values along x, y, z axis. Dia.f Contracted is the Diameter of forisome in longitudinally contracted state, Dia.f expanded is the Diameter of forisome in longitudinally expanded state. Lf contracted is length of forisome in longitudinally contracted state, Lf expanded is length of forisome in longitudinally expanded state.*

 DOI: 10.2420/AF06.2013.43

result in calcium influx through activated calcium channels at plasma membrane and the endoplasmic reticulum membrane. This increased level of calcium by various signaling cascade is sensed by forisome followed by dimensional shift [13, 34] that plugs the point of injury. SE is very much prone to be attacked by insect for photoassimilate .The development of efficient and instant sealing mechanism is of prime importance. CLSM (Confocal Laser Scanning Microscopy) studies have shown that structural phloem specific proteins forisome functions as stopcock blockade under pressure driven mass flow and play a prominent role in sieve tube sealing [11].

4 Biosensor in Plant: A Prime Candidate for Smart Material

Sensitivity towards changes in level of free calcium in relation to forisome protein is known and have been used readily as biosensors to monitor Ca^{2+} changes in various systems. Forisome as smart materials when integrated in monitoring device are capable of converting input signals into appropriate output [19]. Biological compound are gaining more importance as these novel materials have the capacity to sense and process the information resulting in appropriate action and have given rise to the new field of biomimetics [40]. Forisome conformation is controlled by Ca^{2+} level which are in micromolar range [13, 15, 35]. The manipulation of Ca^{2+} concentrations in this range is difficult, so electrical and pH control is more practical alternative under a given set of conditions [44]. The most striking feature of forisome as smart material is their ability to undergo reversible ATP independent conformational change in vitro under non physiological pH [13, 35]. Forisome acts as "stopcocks" to control the loss of photoassimilate [21] and their ability to contract/expand in a pH dependent manner makes it ideal for its application in microfluidic systems. The flow can be controlled by changing pH and manipulating the level of Ca^{2+} (Fig. 2 A). The list of various smart materials along with their working principle has been described in Table 1.

Forisome conformational shifts generate considerable mechanical forces upon contraction and expansion of about 0.1 μN [18]. They are able to push and pull flexible glass fiber and addition of EDTA i.e. removal of Ca^{2+} pushes the glass fiber away. The closest alternative with regard to their use as fluidic actuators are poly(N-isopropylacrylamide) (PNIPAAm) known as artificial gels, which have an elasticity of 3 and 183 kPa in their swollen and unswollen state, respectively (Table 1) [4, 25]. PNIPAAm is of special interest because it can be considered as the closest alternative to forisomes when their use as fluidic actuators is concerned. The measured values of different physical properties of forisomes are shown in Table 2. The Young's Modulus in expanded and contracted state of forisome is measured to be 32.7 and 2.748 kPa respectively (Table 2) [17]. These unique characteristic parameters and geometrical construction make forisome ideal for the development of microscale and nanoscale machines. Forisome smart materials are also suitable for application in medical science as scaffold [29] for tissue engineering because they do not elicit immune response as they are biocompatible and biodegradable [16, 48, 50]. The efforts are going on towards the development of novel materials that can be used as scaffolds for cell attachment, cell-cell adhesion and differentiation [14, 32]. Forisome smart materials are known to be capable of self assembly consisting of fibers of nanometer range [28]. Studies show that forisme protein can self assemble even in in-vitro condition which is required for its mechanical and biological functions [11, 18].

5 Space Science: Forisome based actuators in microfluidic devices

Microfluidics is a recent developing technology with increasingly diverse applications. The development in the field of micro fluidic systems with the advent of nanotechnology has a potential impact on space science applications [5]. The identification of novel smart materials suitable for actuators has a significant impact on future space exploration missions. Forisome can be used as actuators with list of modifications which can be applied to modify its materialistic properties like cohesion, adhesion and identification of critical amino acid residue important in bringing conformational change. Studying these aspects will enhance our understanding to design microfludic devices. A list of several smart materials and their details are shown in Table 1. New smart materials qualified as regulator micro valves for improvement in micro instruments on future space exploration, has been identified as key technology by ESA and NASA [5]. Micro valves have a number of applications which include - miniature vacuum system, micro propulsion, micro instruments for in situ analysis, microbiology and

Table 1. *List of Smart Materials*

Smart Materials	Operating Principle	Input Signal	Output signal	Example
Piezoelectric	Develop a mechanical strain when an electric field was applied.	Electric Field.	Mechanical Strain	PZT (Alloy of Lead Zirconate Titanate).
Shape Memory Alloys	Changes Shape in response to heat and cold (linked to transformation temperature).	Thermal.	Mechanical Stress.	Nitinol (Alloy of Nickel and Titanium).
Electrorestrictive	Changes shape in response to applied electric field/ Conversely can produce voltage when stretched.	Electric Field.	Mechanical Strain.	PMN-PT (Alloy of Lead magnesium niobate-lead titanate),PLZT(Lead Lanthanum Zirconate Titanate.
Carbon Nanotubes	Geometric expansion of carbon-carbon covalent bonds.	Applied voltage in electrolyte.	Mechanical Stress.	Bucky Paper.
Magnetorestrictive	Expand in presence of Magnetic field	Magnetic Field.	Mechanical deformation.	Terfenol-D(Alloy of Terbium,Dysprosium,Iron)
Electrorheological	Change their rheological properties (Viscosity) instantly through the application of an electric field. (Semiconducting particles suspended in dielectric oil)	Electric Field	Orientation of particles along the direction of applied field.	MBPZT microspheres dispersed in a silicon oil.
Magnetorheological	Change their rheological properties(Viscosity) instantly through the application of an electric field.	Magnetic Field.	Alignment of particles along magnetic flux.	Magnetically polarisable colloidal particles suspended in some functional suspension.
Hydrogels (Crosslnked polymer)	Phase transition- giving distinct volumetric changes.	pH, Temperature, Electric field.	Volumetric changes.	pH sensitive poly(HEMA-co-AA) poly(2-hydroxyethyl methylacrylate-co-acrylic acid,Temperature sensitive poly(NIPAAM) poly(N-isopropylacrylamide)
Biomimetic Protein Actuators (ATP independent mechanically active protein) isolated from living organism.	Confirmational shift in response to free calcium ion and pH changes.	pH, Free calcium ion concentration.	Fold increase in volume with generation of mechanical forces.	Foriosme from Sieve element of Phloem tissue.

medicine in space [5]. The micro fluidic devices use arrangement of micro channels to mix, transport, and separate fluids in a specific order [10]. Working at micro scale has several advantages such as reduction in reagents required, power consumed, time and cost [39]. Micro fluidics system is significant for space exploration missions as it reduces space and resource requirement. In micro fluidics system many characteristics like surface tension, fluid resistance, Reynolds number that are unfavorable to work can be dealt with [24]. Micro valve consists of several parts-seat, the diaphragm and the actuators [5]. The actuators consist of novel smart materials which generate force and are housed in a rigid compartment. The central portion of the valve consists of a diaphragm wafer and the base of the valve consists of a seat which contains an inlet and an outlet [5]. Micro fluidics devices in general are similar in scale of semiconductor integrated circuits and are planar in structure [9]. This further opens up the possibilities that they can be integrated with electrical, optical and mechanical elements [9].

6 Forisome in Relation to other Smart Materials

Microfluidics is rapidly growing field with diverse array of applications ranging from microinstrument for in situ analysis, miniature vacuum system, microbiology and medicine in space. The discoveries of novel smart materials with unique characteristics which can be controlled by electrical stimuli [20] under non physiological environment are fulfilling the requirement for space science technology. In vitro studies have shown that forisome smart material can be repeatedly stimulated to contract and expand anisotropically [18]. It can function under non physiological pH values [44]. Its functioning does not require any metabolic apparatus and thus makes it prime candidate [37] for biomimetics actuators (Table 1). ATP driven motors have limitation that they have to maintain a proper ratio of ATP and ADP under metabolic condition which is difficult as they rely heavily on well defined chemical environment which is a disadvantage [19]. Whereas forisome smart materials do not have this limitation of well defined chemical environment. One of the attractive av-

 DOI: 10.2420/AF06.2013.43

Table 2. *Measured Values of different physical properties of Forisomes*

Physical Parameters	Values	References
Young's modulus (kPa) Expanded state	32.7	[17]
Young's modulus (kPa) Contracted state	2.748	[17]
Max Strain (%)	30-200	[37]
Force generated in longitudinal direction (nN) in response to Ca^{2+}	120 ± 20	[34]
Force generated in radial direction (nN) in response to Ca^{2+}	40 ± 10	[34]
Energy Density (J/m-3)	230-800	[34]

enues with forisome smart materials are that their size can be tailored by genetic engineering [44] therefore further studies are required to characterize the gene. It offers further advantage that it can be isolated easily from living plant tissue. The experiment to test the forisome smart materials as micro-valves such as nanomotors and micro-stopcock in microfluidity system have been conducted [18, 19, 26, 45]. Prototypes have indicated that dispersed forisome are able to occlude artificial micro channels [45]. In comparison to other smart materials forisomes differ significantly in relation to the input and output signals (Table 1). Earlier studies show that there is an insufficient adhesion at the forisome edges and wall material has been noticed [44, 45]. Thus, further research for more adhesive wall material is required. Self powered forisome based model system that is based on transmission of neuronal signals in humans for sensing and information transfer has been designed to provide information about the fault location within the structure [38]. Basically smart materials function as sensing the stimuli and function as actuator to logically control the fluid flow [8]. Forisomes have several advantages over other smart materials in terms of its production, availability and manipulation of its property of generating mechanical force by changing confirmation, through protein engineering. Other smart materials which can function as actuators are piezoelectric materials, shape memory alloys (SMA), and stimuli sensitive materials (SSM) (Table 1). The piezoelectric materials exhibit linear shape changes in response to applied electric field, and require high voltage to function as actuators (Table 1). PVF (polyvinylidiene fluoride) is a well known piezoelectric polymer for its properties like low cost, light weight and fabrication on different types of sensor. Forisome smart material can be used in combination with other smart materials for example forisome smart materials together with piezoelectric element have been used to mimic the transmission of neuronal signals in humans [38]. Other smart materials like SMA which can change shape in response to heat and cold. It generates large forces when encounters any resistance during transformation. SMA can be deformed easily into new shape when it is below its transformation temperature [41]. SMA provides unique mechanism for remote actuation; however the disadvantage of using SMA is the difficulty in controlling precise shape due to non-linear changes but forisomes do not suffer from this limitation.(Table 1) [37]. Another smart material SSM responds to number of parameters such as pH, temperature and electro-magnetic fields. They can be used in a number of applications listing from valves, pumps, and shock tube instruments [6, 7, 23, 36, 33]. SSM are electroactive polymers (EAPs) and can be deformed repetitively by applying external voltage (Table 1) [33]. In space science where every action has to be performed in most demanding and harsh condition with robustness and durability, these extraordinary demands can be met with smart materials [6]. The characteristics feature and the parameters under which forisome smart material exhibit and performs are unique. It can be applied in designing micofluidics system in which precise flow regulation is needed. The use of microfluidic devices to probe forisome materials properties has large number of significant advantages.

7 Conclusions

Nature has always inspired the researcher to take lessons from nature's mechanism and has huge impact on the development and improvement of biomimetics tools [7]. Scientist and engineers at ESA and NASA are very much interested in reducing the mass and size of its microfludics devices, which is a challenging problem to deal with [5]. It is well known that a reduction in these two parameters i.e. mass and size results in exponential reduction in cost and significant increase in mission duration [5]. Field of space science and technology has been benefitted by mimicking biological method and system particularly in the field of microctuators. Forisome as smart materials had a dual advantage i.e. acts as

sensor and as actuators which in turn reduce the complexity of the system in terms of control. Artificial gels do serve the purpose of sensor and actuators but have a disappointing time scale for many practical applications [9]. Forisome can serve as an alternative to artificial gels [2] in microfluidic systems as actuators in response to various stimuli. In other systems there are limitations like power consumption in case of solenoid valves. To generate large actuation force, number of turns of copper wire increases thus making the size of actuators larger than suitable for a particular application [49]. Further it requires continuous power supply to keep it open in case of normally closed and vice versa [30]. On the other hand forisome as smart materials in aqueous environment senses the change in pH or free calcium concentration. The piezoelectric micro valve also suffers from the risk of getting exposed to ambient heating and cooling resulting in uncontrolled initiation of the actuation [49]. The availability of forisome as a smart materials for micro fluidic system open new avenues to tackle the challenges in development of micro valves like size, volume, mass, power consumption, robustness, durability, leak rate, temperature and particulates. Miniaturization concept of the microfludics system with the identification of new smart materials like forisome is of great interest in space science community as they are heading towards micro spacecraft concept. In future the ongoing effort will lead to successful fabrication of actuators on chips like we have large integrated circuits today.

8 Acknowledgments

Work on motor proteins, signal transduction and plant stress tolerance in NT's laboratory is partially supported by Department of Science and Technology (DST) and Department of Biotechnology (DBT), Government of India. VKS is a recipient senior research fellowship from Council for Scientific and Industrial Research (CSIR), Government of India.

References

[1] B. Alberts, A. Johnson, J. Lewis, M. Raff, K. Roberts, and P. Walter. *Molecular biology of the cell*. Garland Science, 2002.

[2] D. J. Beebe, J. S. Moore, J. M. Bauer, Q. Yu, R. H. Liu, C. Devadoss, and B.-H. Jo. Functional hydrogel structures for autonomous flow control inside microfluidic channels. *Nature*, 404(6778):588–590, 2000.

[3] H. D. Behnke and R. D. Sjolund. *Sieve elements. Comparative structure, induction and development*. Springer Verlag, 1990.

[4] P. Calvert. Hydrogels for soft machines. *Advanced Materials*, 21(7):743–756, 2009.

[5] I. Chakraborty, W. C. Tang, D. P. Bame, and T. K. Tang. Mems micro-valve for space applications. *Sensors and Actuators A: Physical*, 83(1):188–193, 2000.

[6] Y. B. Cohen. *Biomimetics: biologically inspired technologies*. CRC, 2005.

[7] Y. B. Cohen. Biomimetics using nature to inspire human innovation. *Bioinspiration & Biomimetics*, 1(1):1–12, 2006.

[8] B. Culshaw. *Smart structure and material*. Artech House, Boston, London, 1995.

[9] L. Dong and H. Jiang. Autonomous microfluidics with stimuli-responsive hydrogels. *Soft Matter*, 3(10):1223–1230, 2007.

[10] D. Erickson and D. Li. Integrated microfluidic devices. *Analytica Chimica Acta*, 507(1):11–26, 2004.

[11] A. M. Ernst, S. B. Jekat, S. Zielonka, B. Müller, U. Neumann, B. Rüping, R. M. Twyman, V. Krzyzanek, D. Prüfer, and G. A. Noll. Sieve element occlusion (seo) genes encode structural phloem proteins involved in wound sealing of the phloem. *Proceedings of the National Academy of Sciences*, 109(28):E1980–E1989, 2012.

[12] J. Fromm and S. Lautner. Electrical signals and their physiological significance in plants. *Plant, cell & environment*, 30(3):249–257, 2006.

[13] A. C. U. Furch, A. J. E. van Bel, M. D. Fricker, H. H. Felle, M. Fuchs, and J. B. Hafke. Sieve element ca2+ channels as relay stations between remote stimuli and sieve tube occlusion in vicia faba. *The Plant Cell Online*, 21(7):2118–2132, 2009.

[14] J. Glowacki and S. Mizuno. Collagen scaffolds for tissue engineering. *Biopolymers*, 89(5):338–344, 2007.

 DOI: 10.2420/AF06.2013.43

[15] J. B. Hafke, A. C. Furch, M. D. Fricker, and A. J. Van Bel. Forisome dispersion in vicia faba is triggered by ca2+ hotspots created by concerted action of diverse ca2+ channels in sieve element. *Plant signaling & behavior*, 4(10):968–972, 2009.

[16] J. D. Hartgerink, E. Beniash, and S. I. Stupp. Peptide-amphiphile nanofibers: a versatile scaffold for the preparation of self-assembling materials. *Proceedings of the National Academy of Sciences USA*, 99(8):5133–5138, 2002.

[17] M. S. Jaeger, K. Uhlig, H. Clausen-Schaumann, and C. Duschl. The structure and functionality of contractile forisome protein aggregates. *Biomaterials*, 29(2):247–256, 2008.

[18] M. Knoblauch, G. A. Noll, T. Müller, D. Prüfer, I. Schneider-Hüther, D. Scharner, A. J. van Bel, and W. S. Peters. Atp-independent contractile proteins from plants. *Nature materials*, 2(9):600–603, 2003.

[19] M. Knoblauch and W. S. Peters. Biomimetic actuators: where technology and cell biology merge. *Cellular and molecular life sciences*, 61(19):2497–2509, 2004.

[20] M. Knoblauch and W. S. Peters. Forisomes, a novel type of ca2+-dependent contractile protein motor. *Cell motility and the cytoskeleton*, 58(3):137–142, 2004.

[21] M. Knoblauch, W. S. Peters, K. Ehlers, and A. J. van Bel. Reversible calcium-regulated stopcocks in legume sieve tubes. *The Plant Cell Online*, 13(5):1221–1230, 2001.

[22] M. Knoblauch and A. J. van Bel. Sieve tubes in action. *The Plant Cell*, 10(1):35–50, 1998.

[23] W. Kuhn, B. Hargitay, A. Katchalsky, and H. Eisenberg. Reversible dilation and contraction by changing the state of ionization of high-polymer acid networks. *Nature*, 165:514–516, 1950.

[24] R. H. Liu, M. A. Stremler, K. V. Sharp, M. G. Olsen, J. G. Santiago, R. J. Adrian, H. Aref, and D. J. Beebe. Passive mixing in a three-dimensional serpentine microchannel. *Microelectromechanical Systems, Journal of*, 9(2):190–197, 2000.

[25] Z. Liu and P. Calvert. Multilayer hydrogels as muscle-like actuators. *Advanced Materials*, 12(4):288–291, 2000.

[26] C. Mavroidis and A. Dubey. From pulses to motors. *Nature materials*, 2(9):573–574, 2003.

[27] H. Miki, Y. Okada, and N. Hirokawa. Analysis of the kinesin superfamily: insights into structure and function. *Trends in cell biology*, 15(9):467–476, 2005.

[28] B. Müller, G. A. Noll, A. M. Ernst, B. Rüping, S. Groscurth, R. M. Twyman, L. M. Kawchuk, and D. Prüfer. Recombinant artificial forisomes provide ample quantities of smart biomaterials for use in technical devices. *Applied microbiology and biotechnology*, 88(3):689–698, 2010.

[29] G. A. Noll, B. Müller, A. M. Ernst, B. Rüping, R. M. Twyman, and D. Prüfer. Native and artificial forisomes: functions and applications. *Applied microbiology and biotechnology*, 89(6):1675–1682, 2011.

[30] K. W. Oh and C. H. Ahn. A review of microvalves. *Journal of Micromechanics and Microengineering*, 16(5):R13, 2006.

[31] M. Parthasarathy and T. Pesacreta. Microfilaments in plant vascular cells. *Canadian Journal of Botany*, 58(7):807–815, 1980.

[32] D. E. Przybyla and J. Chmielewski. Higher-order assembly of collagen peptides into nano-and microscale materials. *Biochemistry*, 49(21):4411–4419, 2010.

[33] D. J. B. Q Yu, J M Bauer and J. S. Moore. A responsive bio-mimetic hydrogel valve for microfluidics. *Applied Physics Letters*, 78(17):2589–2591, 2001.

[34] S. Schwan, N. Ferrell, D. Hansford, U. Spohn, and A. Heilmann. Measurement of mechanical forces generated by plant P-protein aggregates (forisomes). *European biophysics journal*, 38(4):533–536, 2009.

[35] S. Schwan, M. Fritzsche, A. Cismak, A. Heilmann, and U. Spohn. In vitro investigation of the geometric contraction behavior of chemomechanical P-protein aggregates (forisomes). *Biophysical chemistry*, 125(2):444–452, 2007.

[36] M. Shahinpoor. Ionic polymer–conductor composites as biomimetic sensors, robotic actuators and artificial muscles: a review. *Electrochimica Acta*, 48(14):2343–2353, 2003.

[37] A. Q. Shen, B. Hamlington, M. Knoblauch, W. S. Peters, and W. F. Pickard. Forisome based biomimetic smart materials. *Smart Structures and Systems*, 2(3):225–236, 2006.

[38] R. A. Shoureshi and A. Q. Shen. Design of a biomimetic-based monitoring and diagnostic system for civil structures. *International journal of nanotechnology*, 4(3):309–324, 2007.

[39] S. K. Sia and G. M. Whitesides. Microfluidic devices fabricated in poly (dimethylsiloxane) for biological studies. *Electrophoresis*, 24(21):3563–3576, 2003.

[40] R. Stahlberg. The phytomimetic potential of three types of hydration motors that drive nastic plant movements. *Mechanics of Materials*, 41(10):1162–1171, 2009.

[41] T. Tadaki, K. Otsuka, and K. Shimizu. Shape memory alloys. *Annual Review of Materials Science*, 18(1):25–45, 1988.

[42] N. Tuteja. Unraveling DNA helicases from plant cells. *Plant molecular biology*, 33(6):947–952, 1997.

[43] N. Tuteja and R. Tuteja. DNA helicases: the long unwinding road. *Nature genetics*, 13:11–12, 1996.

[44] N. Tuteja, P. Umate, and A. J. E. van Bel. Forisomes: calcium-powered protein complexes with potential as smart biomaterials. *Trends in biotechnology*, 28(2):102–110, 2010.

[45] K. Uhlig, M. S. Jaeger, F. Lisdat, and C. Duschl. A biohybrid microfluidic valve based on forisome protein complexes. *Microelectromechanical Systems, Journal of*, 17(6):1322–1328, 2008.

[46] A. J. van Bel. The phloem, a miracle of ingenuity. *Plant, Cell & Environment*, 26(1):125–149, 2003.

[47] A. J. E. van Bel, M. Knoblauch, A. C. U. Furch, and J. B. Hafke. (Questions)n on phloem biology. 1. Electropotential waves, Ca2+ fluxes and cellular cascades along the propagation pathway. *Plant Science*, 181(3):210–218, 2011.

[48] D. N. Woolfson. Building fibrous biomaterials from α-helical and collagen-like coiled-coil peptides. *Peptide Science*, 94(1):118–127, 2010.

[49] E. H. Yang, C. Lee, and J. Khodadadi. Development of MEMS-based piezoelectric microvalve technologies – fabrication, characterization and modeling. *Journal of Sensors and Materials*, 19:1–18, 2007.

[50] L. Zhang and T. J. Webster. Nanotechnology and nanomaterials: promises for improved tissue regeneration. *Nano Today*, 4(1):66–80, 2009.

 DOI: 10.2420/AF06.2013.43

Acta Futura 6 (2013) 53-67
DOI: 10.2420/AF06.2013.53

Acta Futura

Physarum machines for space missions

Andrew Adamatzky*
Unconventional Computing Center, University of the West of England, Bristol, UK

Abstract. A Physarum machine is a programmable amorphous biological computer experimentally implemented in plasmodium of *Physarum polycephalum*. We overview a range of tasks solvable by Physarum machines and speculate on how the Physarum machines could be used in future space missions.

1 Prototypes of unconventional computers

An unconventional computing applies principles of informations processing in physical, chemical and biological systems in design of future and emergent computing paradigms, architectures and implementations [21, 2, 62]. The field is proud with its theoretical achievements, e.g. membrane computing, quantum computing, hyper-computation and artificial immune systems, yet can boast about only a few experimental laboratory prototypes of unconventional computers. They include chemical reaction–diffusion processors [1], extended analog computers [41], micro-fluidic circuits [28], gas-discharge systems [49], chemo-tactic droplets [35], enzyme-based logical circuits [33, 48], crystallization computers [9] (Fig. 1), geometrically constrained chemical computers [50, 42, 31, 64, 30], molecular logical gates and circuits [60, 39]. Slime mould *Physarum polycephalum* (Fig. 2) is one of the most recent candidates for a role of general-purpose amorphous living computer [13].

*Corresponding author. E-mail: andrew.adamatzky@uwe.ac.uk

2 *Physarum polycephalum*

P. polycephalum belongs to the species of order *Physarales*, subclass *Myxogastromycetidae*, class *Myxomycetes*, division *Myxostelida*. It is commonly known as a true, acellular or multi-headed slime mould. Plasmodium is a 'vegetative' phase, a single cell with a myriad of diploid nuclei. The plasmodium is visible to the naked eye (Fig. 3). The plasmodium looks like an amorphous yellowish mass with networks of protoplasmic tubes. The plasmodium behaves and moves as a giant amoeba (Fig. 5). It feeds on bacteria, spores and other microbial creatures and micro-particles [59].

Acellular slime mould *P. polycephalum* has a rich life cycle [59]: fruit bodies, spores, single-cell amoebas, and syncytium. In its plasmodium stage, *P. polycephalum* consumes microscopic particles, and during its foraging behaviour the plasmodium spans scattered sources of nutrients with a network of protoplasmic tubes (Fig. 8). The plasmodium optimises its protoplasmic network that covers all sources of nutrients and guarantees robust and quick distribution of nutrients in the plasmodium's body. Plasmodium's foraging behaviour can be interpreted as a computation [43, 44, 45, 46]: data are represented by spatial of attractants and repellents, and results are represented by structure of protoplasmic network [13]. Plasmodium can solve computational problems with natural parallelism, e.g. related to shortest path [44] and hierarchies of planar proximity graphs [3], computation of plane tessellations [53], execution of

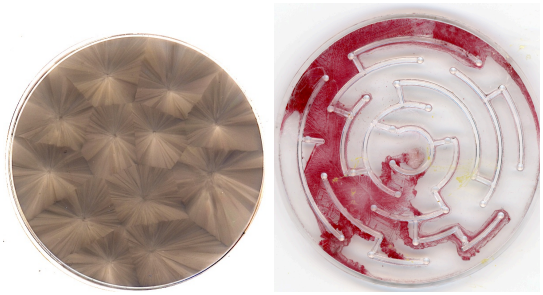

Figure 1. *Crystallisation based unconventional computer. (a) Hot ice computer approximates Voronoi diagram of a planar data set. Crystallisation was inoculated in several sites of planar data set. Edges of Voronoi diagram are represented by boundaries of crystallisation domains. (b) Potassium ferricyanide crystallisation computer approximates paths out of a labyrinth. Crystallisation was initiated in a central chamber of the labyrinth. Path between outside channel and the central chamber is represented by crystal needles. See deails in [9].*

logical computing schemes [63, 11], and natural implementation of spatial logic and process algebra [56].

Plasmodium can be cultivated on a non-nutrient or a nutrient agar. While grown on a nutrient agar the plasmodium propagates as an omnidirectional wave. On a non-nutrient agar plasmodium propagates as a travelling localisation (Fig. 5), and behaves like a wave-fragment in a sub-excitable medium [4, 5]. While presented with a configuration of attractants, e.g. oat flakes (Fig. 8), on a non-nutrient substrate, the plasmodium develops active zones that explore the substrate and propagate towards the oat flakes. Neighbouring oat flakes colonised by plasmodium are usually connected by protoplasmic tubes. Distribution of chemo-attractants and position of initial inoculation of plasmodium are input data for Physarum machines. Structure of the protoplasmic networks and/or domains occupied by plasmodium are results of computation in Physarum machines. Propagating active zones can be considered as elementary processors of Physarum machines.

3 Physarum machines

A Physarum machine is a programmable amorphous biological computing device experimentally implemented in plasmodium of *P. polycephalum* [13]. A Physarum machine is programmed by configurations of repelling and attracting gradients. A mechanics of Physarum machines is based on the following unique features of *P. polycephalum*:

- Physarum is a living, dynamical reaction-diffusion pattern formation mechanism.
- Physarum may be considered as equivalent to a membrane bound sub excitable system: excitation stimuli provided by chemo-attractants and chemo-repellents (Fig. 6).
- Physarum may be regarded as a highly efficient and living micro-manipulation and micro-fluidic transport device.
- Physarum is sensitive to illumination and AC electric fields and therefore allows for parallel and non-destructive input of information.
- Physarum represents results of computation by configuration of its body (Fig. 2).

Physarum is thus a computing substrate which transforms data represented in spatially extended chemical and physical stimuli to results represented in a topology of protoplasmic networks.

Plasmodium can be cultivated on a non-nutrient (e.g. Select agar, Sigma Aldrich) or a nutrient agar (e.g. Corn Meal Agar). While grown on a nutrient agar the plasmodium propagates as an omnidirectional wave. On a non-nutrient agar plasmodium propagates as a travelling finite localisation, and behaves like a wave-fragment in a sub-excitable medium [4, 5]; most implementations discussed in the paper are done on a non-nutrient agar. Thus by *active zone* we mean either omnidirectional growing pattern (on nutrient substrate) or — in majority of examples — a localised growing pattern (on non-nutrient substrate). While presented with a configuration of attractants, e.g. oat flakes (Fig. 8a), on a non-nutrient substrate, the plasmodium develops active zones (Fig. 8d) that explore the substrate and propagate towards the oat flakes. Neighbouring oat flakes colonised by plasmodium (Fig. 8b) are usually connected by protoplasmic tubes (Fig. 8c). Distribution of chemo-attractants and position of initial inoculation of plasmodium are input data for Physarum machines. Structure of the protoplasmic networks and/or domains occupied by plasmodium are results of computation in Physarum machines. Propagating active zones can be considered as elementary processors of Physarum machines.

We illustrate mechanics of computation in Physarum on an approximation of Voronoi diagram of a planar set.

 DOI: 10.2420/AF06.2013.53

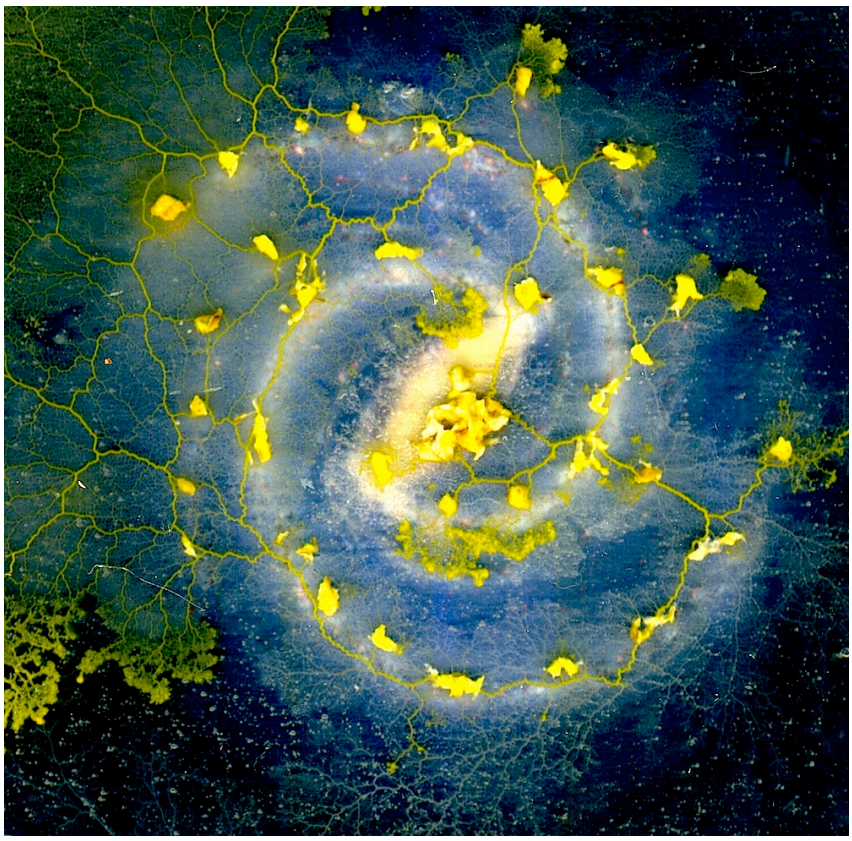

Figure 2. *Physarum propagating on an artistic impression of galaxy. See original picture in public domain NASA/JPL-Caltech [47].*

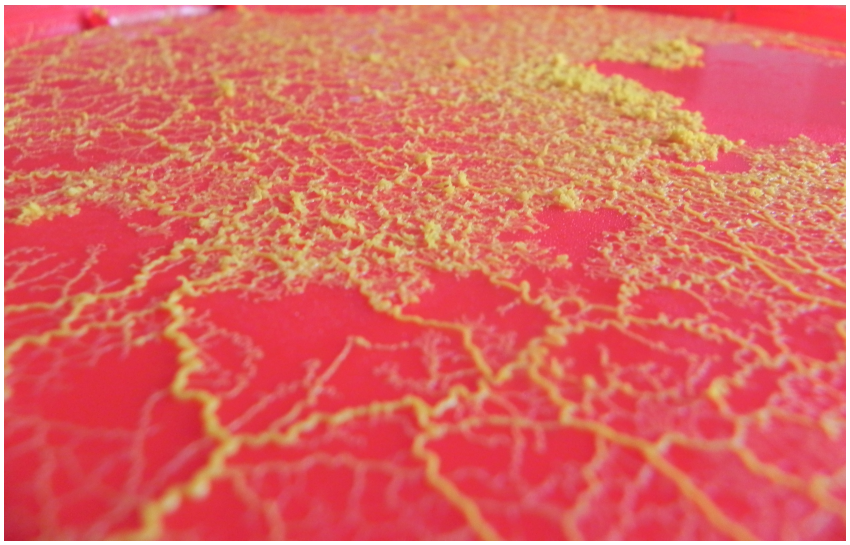

Figure 3. *Physarum propagates on a bare plastic surface.*

DOI: 10.2420/AF06.2013.53

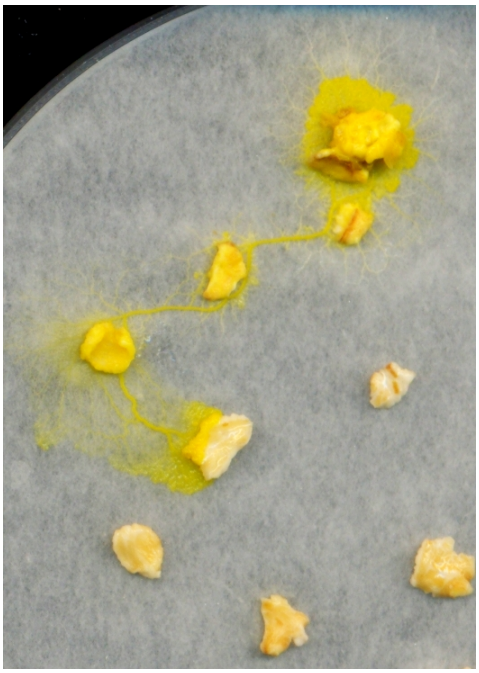

Figure 4. *Physarum spanning sources of nutrients with its protoplasmic network. Physarum was inoculated on the northmost flake. Physarum propagates source. Oat flakes not yet colonised by Physarum are in the south-east part.*

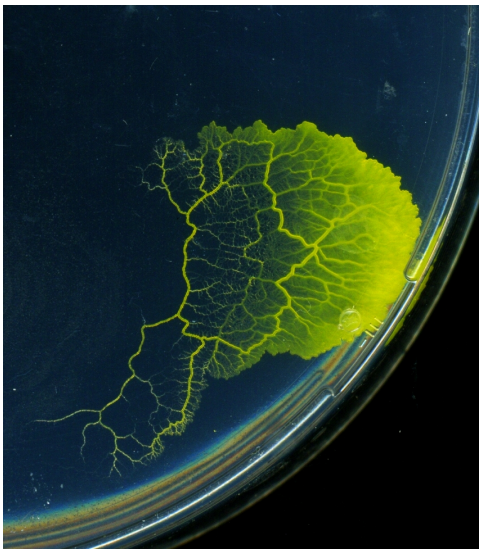

Figure 5. *Localised Physarum propagates on agar gel. This is example of how Physarum forms a dissipative soliton like structures. Slime mould active zone exhibits characteristic wave-front with tail of protoplasmic tubes trailed behind. The active zone resembles wave-fragments (dissipative solitons) in Belousov-Zhabotinsky medium [4, 13]. The active zone is an elementary processor of a multi-processor Physarum machine.*

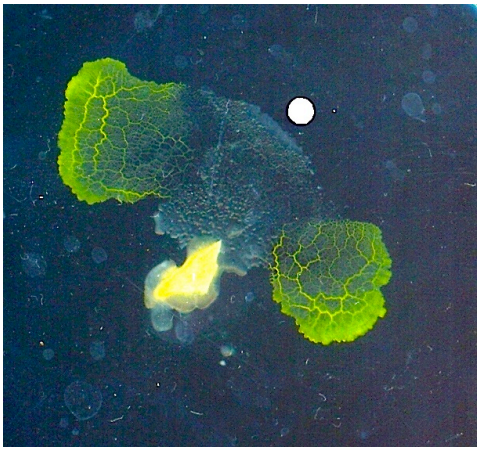

Figure 6. *Controlling Physarum with repellents. Physarum wave-fragment travelling north-east 'collides' with a grain of salt (white disc) and splits into two independent fragments; one fragments travels north-west another south-east.*

A planar Voronoi diagram (VD) of the set **P** is a partition of the plane into such regions that, for any element of **P**, a region corresponding to a unique point $p \in \mathbf{P}$ contains all those points of the plane which are closer to p than to any other node of **P**. Delaunay triangulation (DT) is a dual graph of VD [51].

On a nutrient substrate P. polycephalum approximates VD. On a non-nutrient substrate the plasmodium approximates DT. Plasmodium growing on a nutrient substrate from a single site of inoculation expands circularly as a typical diffusive or excitation wave. When two plasmodium waves encounter each other, they stop propagating. To approximate a VD with Physarum, we physically map a configuration of planar data points by inoculating plasmodia on a substrate (Fig. 9a). Plasmodium waves propagate circularly from each data point (Fig. 9bc) and stop when they collide with each other (Fig. 9d). Thus, the plasmodium waves approximate a VD, whose edges are the substrate's loci not occupied by plasmodia (Figs. 9d). The situation becomes different when Physarum machine is given the same set of data (planar points represented by oat flakes colonised by plasmodium) but placed on a non-nutrient substrate. Being driven by chemo-attractants the plasmodium in each planar point develops just few localised active zones, which grow towards geographically neigh-

 DOI: 10.2420/AF06.2013.53

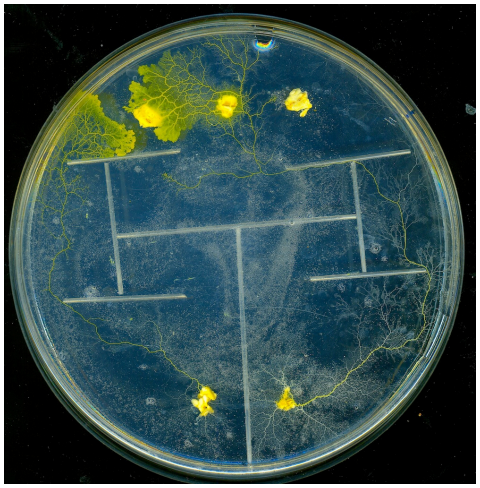

Figure 7. *Decentralised decision making by Physarum. Oat flakes with plasmodium were placed in south part of Petri dish. Virgin oat flakes were placed in the north part. Obstacles were represented by capillary tubes placed on an sagar surface. Optimal — from Physarum machine point of view — paths connected source and destination sites are seen as pronounced protoplasmic tubes.*

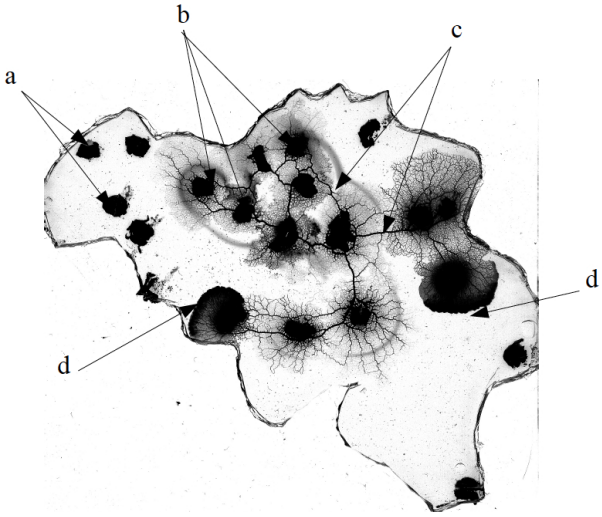

Figure 8. *Plasmodium of* P. polycephalum *on a data set on an agar gel. (a) Virgin oat flakes. (b) Oat flakes colonised by the plasmodium. (c) Protoplasmic tubes. (d) Active zones, growing parts of the plasmodium.*

bouring oat flakes (planar points). Thus the flakes become connected by enhanced protoplasmic tubes, which — up to some degree of accuracy — represent edges of the DT (Figs. 9e) [3].

4 Application domains of Physarum machines

Future space missions could benefit from Physarum machines because living and hybrid functional materials made of *P. polycephalum* will play a role of specialised processors solving tasks of

- computational geometry (approximation of Voronoi diagram of arbitrary geometrical shape, concave and convex hulls),
- image processing (dilation, erosion, opening and closing, image expansion and shrinking, computing connected components of image, and image translation, edge detection, edge completion, boundary detection, feature tracking; and, image recognition),
- graph-theoretic computing (approximation of proximity graphs. Graph restructuring, transformation between cyclic graphs as Delaunay triangulation and Gabriel graph and acyclic graphs as minimum spanning tree and Steiner tree,
- optimisation (computation of spanning trees and

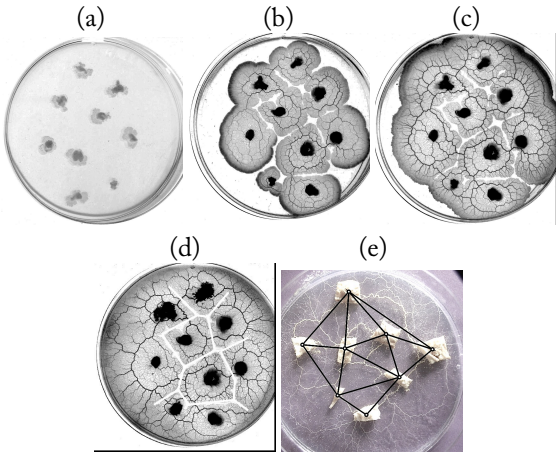

Figure 9. *Voronoi diagram and Delaunay triangulation computer by Physarum machines. (a–d) Approximation of VD by slime mould on nutrient agar gel. (a) Sites of plasmodium inoculation represent planar data points to be sub-divided by edges of VD. (bc) Experimental snapshots of growing plasmodia. (d) Bisectors of VD are represented by loci of substrate not occupied by plasmodium, bisectors computed by classical technique are shown by straight lines. (e) DT approximated by Physarum on a non-nutrient substrate.*

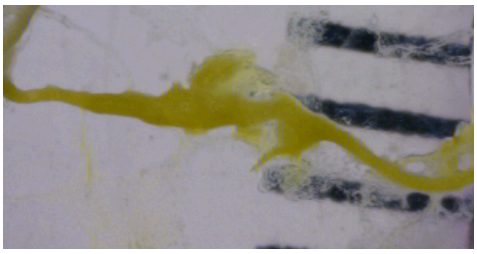

Figure 10. *Protoplasmic tube self-repaired after being ruptured by applying load of 0.2 g.*

obstacle free shortest paths),

- neuro-morphic processors (information processing and sensorial fusion on plasmodial trees), and
- general purpose computing devices with architecture of Kolmogorov-Uspensky storage modification machines.

The slime mould's computing potential and resistance to environmental factors can be increased by hybridising protoplasmic networks with new functional materials, biomorphic mineralisation, bio-synthesis of metal nano-particles, production of bio-wires, and coating protoplasmic networks with with conductive polymers.

Combined with conventional electronic components in a hybrid chip, Physarum networks will radically improve the performance of digital and analog circuits. Physarum machines are analogous to reaction-diffusion chemical systems encapsulated in a growing elastic membrane. The machines can be made hybrid, i.e. combining dead (but coated with conductors) and living parts of slime mould in communication channels. Physarum machines can be powered directly and efficiently by bio-chemical power, fabricated using self-growth and self-organisation, and controllably shaped into two- and three-dimensional structures. Physarum machines are robust to physical damage and exhibit a substantial degree of self-repair (Fig. 10).

Hybrid (live and coated with conductors) Physarum machines can perform computation by classical means of electrical charge propagation, by travelling waves of contraction, and by a physical propagation of the slime mould's body.

In terms of classical computing architectures, the following characteristics can be attributed to hybrid Physarum machine [6]:

- Massive parallelism: there are thousands of elementary processing units, oscillatory bodies, in a slime mould colonised in a Petri dish;
- Massive signal integration: Membrane of plasmodium is able to integrate massive amounts of complex spatial and time-varying stimuli to effect local changes in contraction rhythm and, ultimately, global behaviour of the plasmodium;
- Local connections: micro-volumes and oscillatory bodies of cytoplasm change their states, due to diffusion and reaction, depending on states of, or concentrations of, reactants, shape and electrical charges in their closest neighbours;
- Parallel input and output: Physarum computes by changing its shape, can record computation optically; Physarum is light sensitive, data can be inputted by localised illumination;
- Fault tolerance: being constantly in a shape changing state, Physarum machine restores its architecture even after a substantial part of its protoplasmic network is removed.

Development of Physarum machines bring benefits to several fields of science, technology and engineering, few are exemplified below.

Future electronic designs will be integrated at a cellular scale, where growing Physarum networks will be forming a skeleton of conductive and information processing elements of the circuits. Future bio-electronic designs require novel computational approaches: Physarum machines offer robust and reliable methods for controlled development of novel hardware components and systems, including high density of computing elements and very low power consumption.

Novel and emergent computing paradigms and architectures — laboratory prototypes and models of novel computing substrates will be based on prototypes of Physarum machines, thus enabling those working in nature-inspired computing to access original computing algorithms and experimental procedures. A bio-network based computers employing Physarum machines can be built on in broad variety of ways: change of interface (optical, electrical, chemical, mechanical); change of internal structure of growing networks for information transmission and processing; units can be mass-produced cheaply and can be shared among labs without incurring additional expenses; hybrid units combining several types of biological substrates and conventional hardware can be made with units shared among labs.

 DOI: 10.2420/AF06.2013.53

The complex systems community will benefits from Physarum computing for the control of the growing architecture and functions of disordered unreliable networks, and computational paradigms of growing, and structurally dynamic, random computing networks.

Theory of computation — logical schemes and computational circuits developed in Physarum machines will belong to a class of hybrid, digital-analog systems, which are a fertile subject of research at the edge of analog, mechanical and discrete computation. Benefits are envisaged also in the fields of self-assembly, self-regenerative systems, survivability and fault-tolerance of novel computing schemes. Physarum is capable of relatively quick recovery after damage and constantly explore space available and competition for resources.

Growing protoplasmic tubes of slime mould could be used as the architectural skeleton to build bio-electronic circuits to provide connections between living tissue and computers, such as brain-machine interfaces. Similar devices made with conventional technology tend to be rigid and must be encapsulated to protect the electrical circuits from the moisture inherent in biology.

Further we illustrate computing abilities of Physarum — which could be useful in future space missions — in few examples of experimental laboratory studies.

5 Physarum logical gates

Given cross-junction of agar channels and plasmodium inoculated in one of the channels, the plasmodium propagates straight through the junction [11]; the speed of propagation may increase if sources of chemoattractants present (however presence of nutrients does not affect direction of propagation). An active zone, or a growing tip, of plasmodium propagates in the initially chosen direction, as if it has some kind of inertia. Based on this phenomenon we designed two Boolean gates with two inputs and two outputs, see Fig. 11ab. Input variables are x and y and outputs are p and q. Presence of a plasmodium in a given channel indicates Truth and absence — False. Each gate implements a transformation from $\langle x, y\rangle \to \langle p, q\rangle$. Experimental examples of the transformations are shown in Fig. 11.

Plasmodium of *P. polycephalum* implements two-input two-output Boolean gate P_1: $\langle x, y\rangle \to \langle xy, x + y\rangle$. Plasmodium inoculated in input y of P_1 propagates along the channel yq and appears in the output q (Fig. 11c). Plasmodium inoculated in input x of P_1 propagates till junction of x and y, 'collides' to the impassable edge of channel yq and appears in output q (Fig. 11d). When plasmodia are inoculated in both inputs x and y of P_1 they collide with each other and the plasmodium originated in x continues along the route xp. Thus the plasmodia appear in both outputs p and q (Fig. 11e).

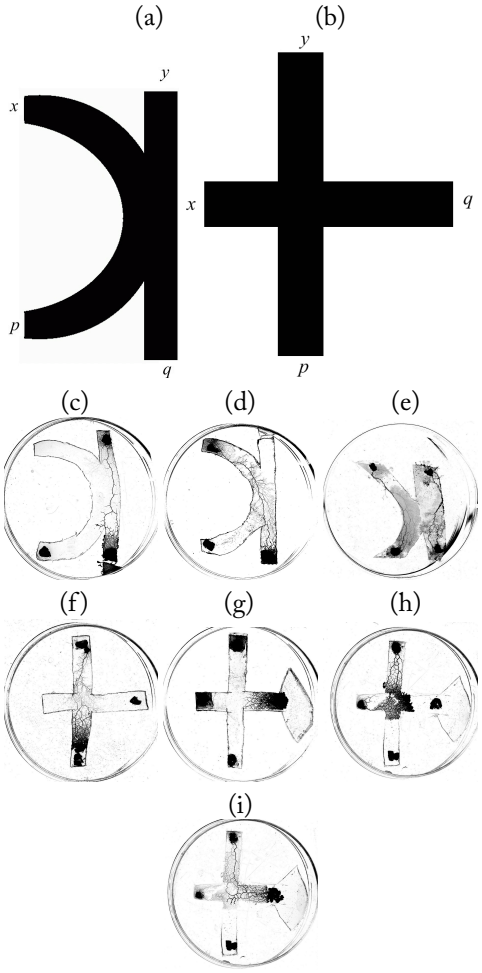

Figure 11. *Physarum logical gates. (ab) Geometrical structure of Physarum gates* P_1 *(a) and* P_2 *(b):* x *and* y *are inputs,* p *and* q *are outputs. (c–e) Experimental examples of transformation* $\langle x, y\rangle \to \langle p, q\rangle$ *implemented by Physarum gate* P_1. *(c)* $\langle 0, 1\rangle \to \langle 0, 1\rangle$. *(d)* $\langle 1, 0\rangle \to \langle 0, 1\rangle$. *(e)* $\langle 1, 1\rangle \to \langle 1, 1\rangle$. *(f–i) Experimental examples of transformation* $\langle x, y\rangle \to \langle p, q\rangle$ *implemented by Physarum gate* P_2. *(f)* $\langle 0, 1\rangle \to \langle 1, 0\rangle$. *(g)* $\langle 1, 0\rangle \to \langle 0, 1\rangle$. *(hi) Two snapshots (taken with 11 h interval) of transformation* $\langle 1, 1\rangle \to \langle 0, 1\rangle$.

Plasmodium of *P. polycephalum* implements two-input two-output gate P_2: $\langle x, y\rangle \to \langle x, \bar{x}y\rangle$. If input

x is empty, plasmodium placed in input y of P_2 propagates directly towards output p (Fig. 11f). Plasmodium inoculated in input x of P_2 (when input y is empty) travels directly towards output q (Fig. 11g). Thus transformations $\langle 0,1\rangle \to \langle 1,0\rangle$ and $\langle 1,0\rangle \to \langle 0,1\rangle$ are implemented. The gate's structure is asymmetric, x-channel is shorter than y-channel. Therefore the plasmodium placed in input x of P_2 usually passes the junction by the time plasmodium originated in input y arrives at the junction (Fig. 11h). The y-plasmodium merges with x-plasmodium and they both propagate towards output q (Fig. 11i). Extension of gel substrate after output q does usually facilitate implementation of the transformation $\langle 1,1\rangle \to \langle 0,1\rangle$.

6 Path finding and routing

Maze-solving is a classical task of bionics, cybernetics and unconventional computing. A typical strategy for a maze-solving with a single device is to explore all possible passages, while marking visited parts, till the exit or a central chamber is found. Several attempts have been to outperform Shannon's electronic mouse Theseus [52] using propagation of disturbances in unusual computing substrates, including excitable chemical systems, gas-discharge, and crystallisation. Most experimental prototypes were successful yet suffered from the computing-substrates specific drawbacks [14]. Below we briefly outline laboratory experiment on path finding with Physarum guided by a diffusion of an attractant placed in the target site.

In laboratory experiments we used plastic mazes [14], 70 mm diameter with 4 mm wide and 3 mm deep channels (Fig. 12a). We filled channels with agar gel as a non-nutrient substrate. An oat flake was placed in the central chamber of the maze and the plasmodium was inoculated in the most peripheral channel of the maze.

A typical experiment is illustrated in Fig. 12. After its inoculation the plasmodium started exploring its vicinity and at first generated two active zones propagating clock- and contra-clockwise (Fig. 12ab). Several active zones are developed to explore the maze (Fig. 12d). By the time diffusing chemo-attractants reached distant channels, one of the active zone already became dominant and suppressed another active zones (Fig. 12c). In example shown active zone travelling contra-clockwise inhibited active zones propagating clockwise. The dominating active zone then followed the gradient of chemo-attractants inside the maze, navigated along intersections of the maze's channels and solved the maze by entering its central chamber (Fig. 12c). Physarum machines do not always fine an optimal solution but they always find some solution, rather optimal for given conditions and efforts, and rarely fail (Fig. 2).

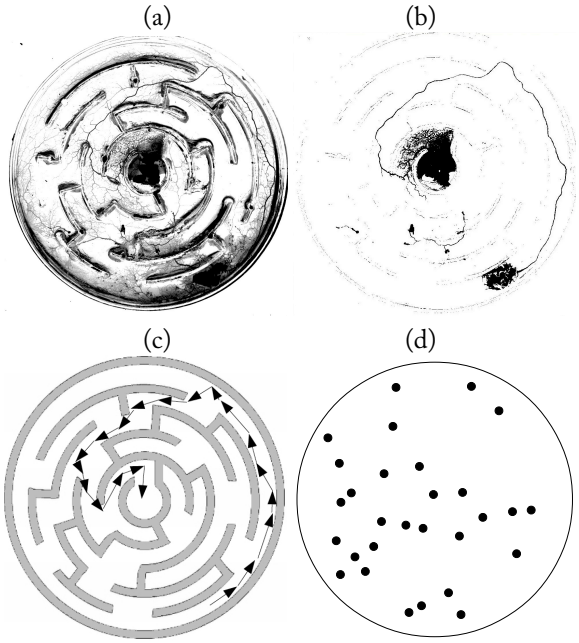

Figure 12. *Experimental maze-solving with plasmodium of* P. polycephalum. *Plasmodium is inoculated in peripheral channel, east part of the maze, and a virgin oat flake is placed in central chamber. (a) Scanned image of the experimental maze, protoplasmic tubes are light-coloured. (b) Binarised image, major protoplasmic tubes are thick black lines. (c) Scheme of plasmodium propagation, arrows symbolise velocity vectors of propagating active zone. (d) Locations of active growing zones, sprouted by plasmodium during exploration of the maze. See details in [14].*

Physarum machines can well act in an open air, proceed to long distances on a non-friendly substrates and yet perform tasks satisfactory. Thus, slime mould path finding on three-dimensional nylon terrains of Germany, Russia, UK and USA is discussed in [18]. Two snapshots of Physarum propagation are shown in Fig. 13.

7 Wires, transportation and building

When inoculated on a substrate with scattered sources of nutrients Physarum propagates towards the sources

 DOI: 10.2420/AF06.2013.53

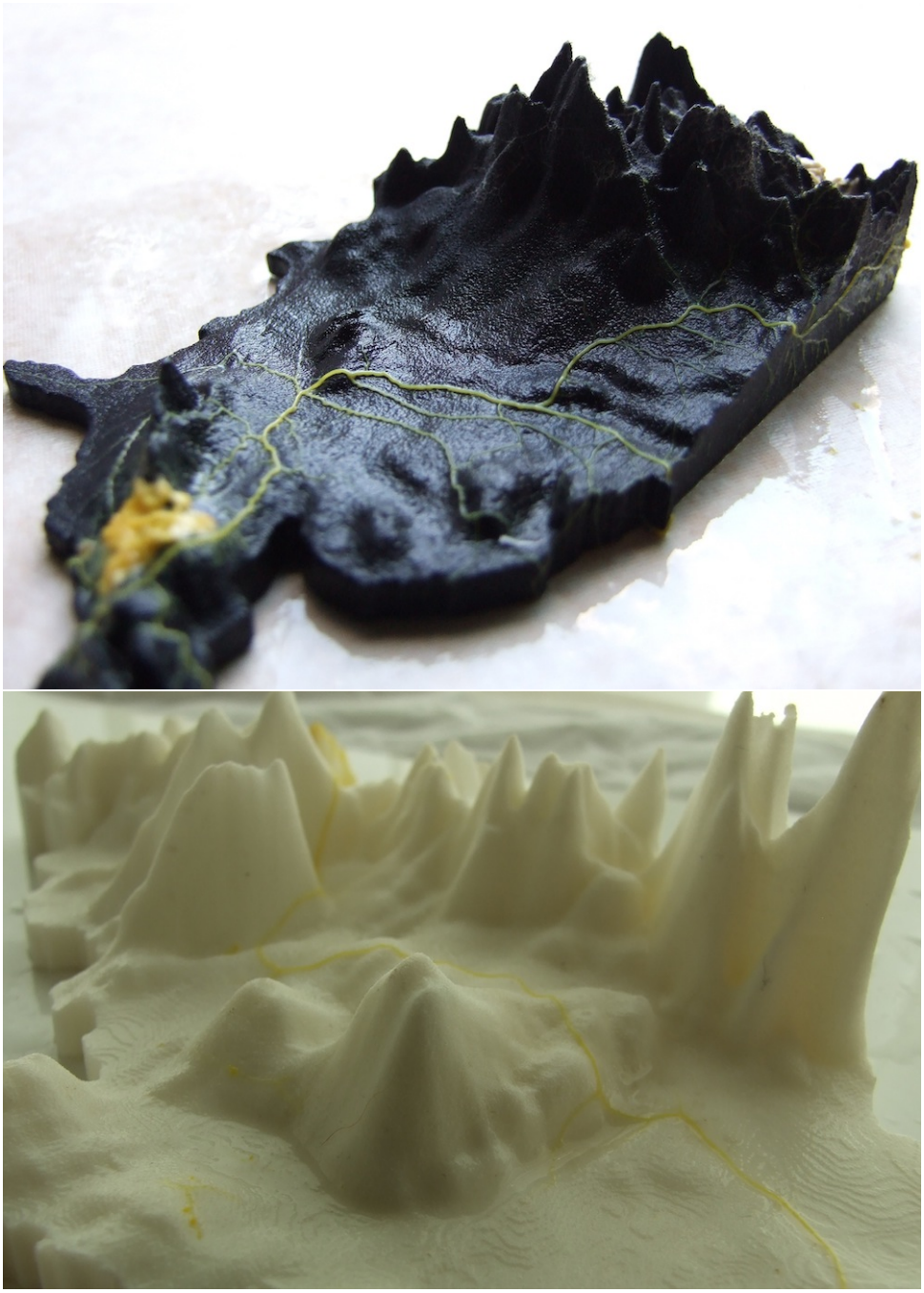

Figure 13. *Physarum machines navigate elevations on three-dimensional nylon models of continents. (a) Slime mould navigate around mountains in USA. (b) Slime mould passes through Central Siberian Plateau north of Enashimsky mountain, in the region of Tura city. See details in [18].*

DOI: 10.2420/AF06.2013.53

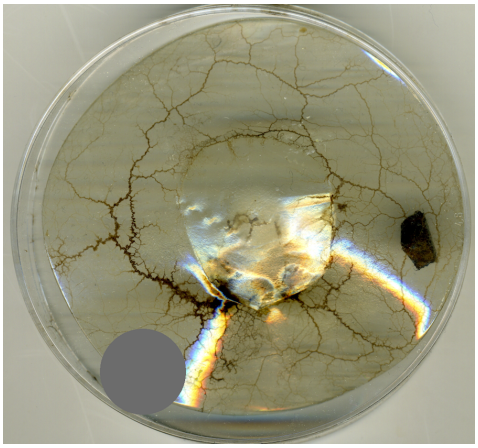

Figure 14. *Towards Physarum wires. Control of magnetic nanoparticles in protoplasmic network. Position of 25×20 mm N52 neodymium magnet is shown by grey disc. Segments of the tubes closest to the magnet exhibit black colour indicating a high concentration of the internalised magnetic material.*

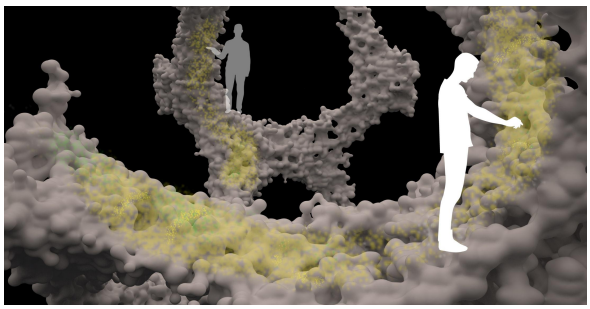

Figure 15. *Bio-inspired architectures designed by Team:Spores. Courtesy of Team:Spores [58].*

and spans them with a network of protoplasmic tubes. Structure of the network may vary between experiments however statistically most common planar graphs approximated are proximity graphs: relative neighbourhood graph, Gabriel graph and β-skeletons [13]. A topological structure of protoplasmic network is always in a flux but a general tendency is that typically an acyclic proximity graph — a spanning tree is built at first. The spanning tree is then transformed into a relative neighbourhood graph or a Gabriel graph. Further development of the protoplasmic network leads to formation of a Delaunay triangulation.

When configuration of nutrients matches a configuration of major urban areas of a country, the plasmodium of *P. polycephalum* approximates a human-

Figure 16. *Physarum derived wearable devices. Drawing by Theresa Schubert, Bauhaus-Universität Weimar, Germany [55].*

made transport network, motorways and highways of the country. In [17] we developed a simple and user-friendly technique for evaluating man-made transport systems using slime mould *P. polycephalum*. The experimental laboratory methods are cost efficient and require little if any specialised equipment. We found that the slime mould *P. polycephalum* approximates best of all motorways in Belgium, Canada and China. The countries studied can be arranged in the following descending order of biorationality: Belgium, Canada, China, Italy, Malaysia, The Netherlands, Brazil, Germany, Mexico, UK, Africa and USA [17].

In [17] we undertook a comparative analysis of the motorway and protoplasmic networks. We found that in terms of absolute matching between slime mould networks and motorway networks the regions studied can be arranged in the following order of decreasing matching: Malaysia, Italy, Canada, Belgium, China, Africa, the Netherlands, Germany, UK, Australia, Iberia, Mexico, Brazil, USA. We compared the Physarum and the motorway graphs using such measures as average and longest shortest paths, average degrees, number of independent cycles, the Harary index, the Π-index and the Randić index. We found that in terms of these measures motorway networks in Belgium, Canada and China are most affine to protoplasmic networks of slime mould

 DOI: 10.2420/AF06.2013.53

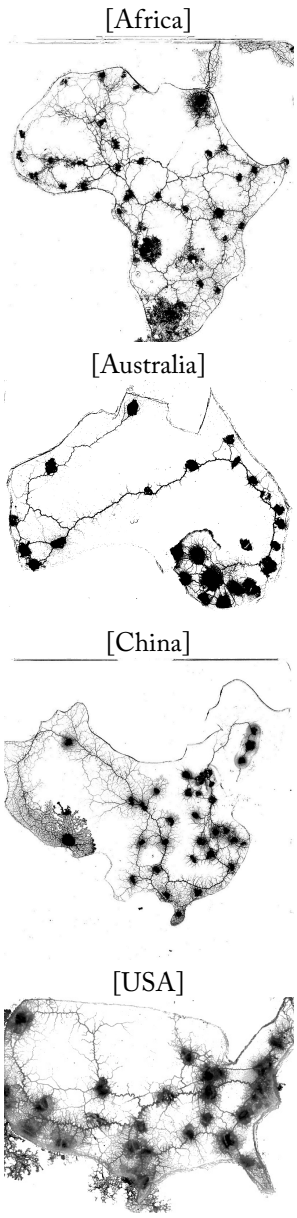

Figure 17. *Exemplar configurations of protoplasmic networks developed by slime mould* P. polycephalum *on major urban areas* **U** *obtained in experimental laboratory studies [17].*

P. polycephalum. With regards to measures and topological indices we demonstrated that the Randić index could be considered as most bio-compatible measure of transport networks, because it matches incredibly well the slime mould and man-made transport networks, yet efficiently discriminates between transport networks of different regions.

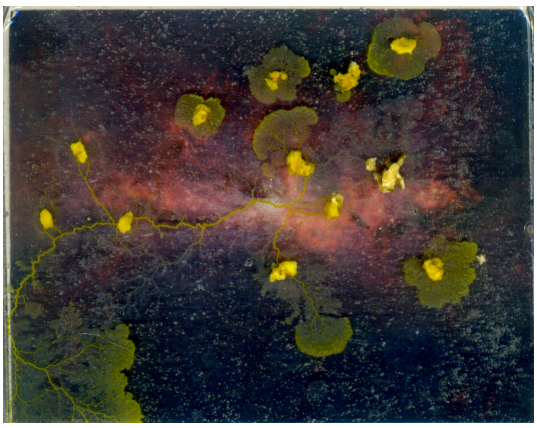

Figure 18. *Physarum spanning oat flakes imitating stars clusters on the infrared image of the Centre of the Milky Way Galaxy. See source at [40].*

The biological mechanisms [17], underlying the optimal network formation in Physarum machines could be employed in design of large scale transportation and communication networks, when e.g. major clusters, stars and matter formations are represented by sources of chemo-attractants and nutrients (Figs. 2 and 18). The Physarum built transportation networks will assist path planning tasks [29, 66, 34, 19] for space ships and space stations, intra-planetary transportation [36]. The dynamical graphs developed by the slime mould may form a basis for future and emergent routing protocols and topology control of communication networks [37, 57] and optimisation of wireless networks [67].

These behavioural trait of Physarum can be used to

- execute bio-inspired routing of conductive pathways in Physarum-built electronic circuits, e.g. by loading the slime mould with conductive nanobeads (Fig. 14), see also [38]
- growing of a large-scale dwellings which architecture can be tuned depending on environmental conditions (Fig. 15), structures build by another single cell organism *Syringammina fragilissima* [61] prove feasibility of the approach, and
- growth of wearable bio-hybrid networks of distributed sensorial, computing and actuating elements (Fig. 16), first attempts of growing functional networks for transportation of substances were successful [13].

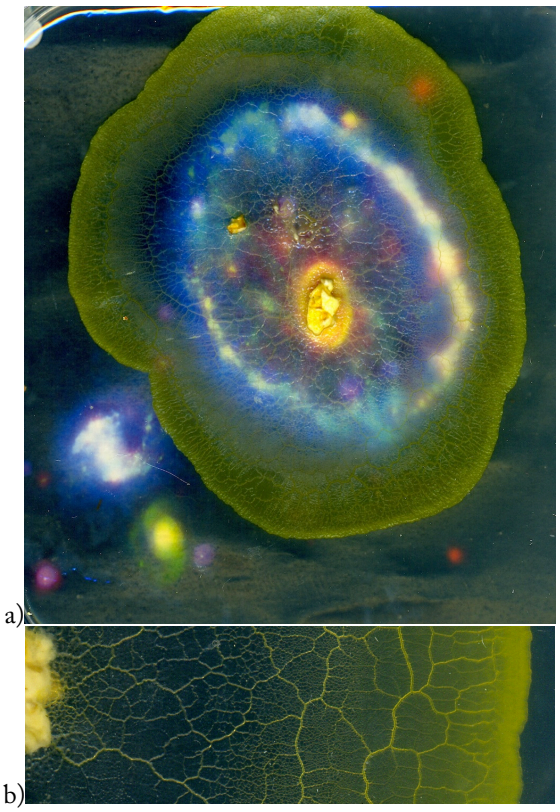

FIGURE 19. *Image of Physarum growing on a nutrient agar superimposed on an false colour composite image of Cartwheel galaxy. PIA03296: A Stellar Ripple. NASA/JPL-Caltech [23]. (a) Image of the whole Physarum expanding pattern. (b) Zoomed segment of Physarum showing changing topology of protoplasmic tubes: inoculation site is on the left and wave front is on the right.*

8 Physarum networks and Cosmic Web

On a nutrient substrate Physarum expands as an omnidirectional wave, e.g. as a classical excitation wave in a two-dimensional excitable medium (Fig. 19a). It shows a pronounced wave front, comprised of a very dense network of protoplasmic tubes. There are several orders of tubes which are seasily differentiable by their width (Fig. 19b). Density of the protoplasmic network decreases towards inoculation site, the epicentre of the wave pattern. Morphological transitions of the slime mould's network s during expansion, colonisation and development bear remarkable resemblance to the Cosmic Web [65, 8, 24]. Weblike spatial arrangement of galaxies and masses into elongated filaments of Cosmic Web [65] are represented by wave-fragment like active growing zones and colonies of Physarum. Morphologies of sheetlike walls and dense compact clusters [65] are typical for the slime mould growing on a nutrient agar. Large near-empty void regions [65] are formed in the protoplasmic networks due to release of metabolites into a substrate surrounding protoplasmic sheets and competition between the protoplasmic tubes. A hierarchical nature of mass distribution in Cosmic Web [65] is represented by hierarchies of protoplasmic tubes and their degrees of branching.

9 Conclusion

Slime mould of *P. polycephalum* is a unique living substrate which implements distributed sensing, massive-parallel information processing, decentralised decision making and concurrent actuation and manipulation. Physarum machines are experimental prototypes of unconventional computing devices implemented in the slime mould of *P. polycephalum*. We briefly introduced Physarum machines and exemplified their functionality on Boolean logic and path finding tasks. We speculated that in future space missions Physarum machines could be used as onboard amorphous computers for route planning and network communication, as well as smart living materials for growing electrical computing circuits, developing dwellings and inhabitable enclosures, and fabrication of wearable sensing, computing and actuating devices. Moreover, the slime mould *per se* can be an ideal analog modelling substrate to study a development of galaxies and evolution of cosmic matter.

10 Acknowledgement

The research was partly supported by European Commission grant "Physarum Chip: Growing Computers from Slime Mould", programme type "Seventh Framework Programme", sub-programme area "Unconventional Computation (UCOMP)', project reference 316366. I thank TEAM:SPORES, especially Grace Chung and Preety Anand for discussions on architectural potential of Physarum, and I am grateful to Theresa Schubert for her impression of 'slimeware'.

References

[1] A. Adamatzky, B. De Lacy Costello, T. Asai, *Reaction-Diffusion Computers*, Elsevier, 2005.

 DOI: 10.2420/AF06.2013.53

[2] A. Adamatzky and C. Teuscher, *From Utopian to Genuine Unconventional Computers*, Luniver Press, 2006.

[3] A. Adamatzky, Developing proximity graphs by Physarum Polycephalum: Does the plasmodium follow Toussaint hierarchy? *Parallel Processing Letters* **19** (2008), 105–127.

[4] A. Adamatzky, B. De Lacy Costello, and T. Shirakawa, Universal computation with limited resources: Belousov–Zhabotinsky and Physarum computers, *Int. J. Bifurcat. Chaos* **18** (2008), 2373–2389.

[5] A. Adamatzky, If BZ medium did spanning trees these would be the same trees as *P*hysarum built, *Physics Letters A* **373** (2009), 952–956.

[6] A. Adamatzky SlimeWare. Artificial Life (2013), in press.

[7] A. Adamatzky. Advances in Physarum machines gates, hulls, mazes and routing with slime mould. K. De Bosschere, E. H. D'Hollander, G. R. Joubert, D. A. Padua, F. J. Peters, M. Sawyer (Eds.): Applications, Tools and Techniques on the Road to Exascale Computing, Proceedings of the conference ParCo 2011, 31 August – 3 September 2011, Ghent, Belgium. IOS Press 2012 Advances in Parallel Computing. 41–54.

[8] B. Beygu, K. Kreckel, R. van de Weygaert, J. M. van der Hulst, J. H. van Gorkom An Interacting Galaxy System Along a Filament in a Void. (2013) arXiv:1303.0538 [astro-ph.CO]

[9] A. Adamatzky, Hot ice computer, *Physics Lett A* **374** (2009), 264–271.

[10] A. Adamatzky, Steering plasmodium with light: Dynamical programming of Physarum machine, arXiv:0908.0850v1 [nlin.PS] (2009).

[11] A. Adamatzky, Slime mould logical gates, arXiv:1005.2301v1 [nlin.PS] (2009).

[12] A. Adamatzky and J. Jones, Programmable reconfiguration of Physarum machines, *J Natural Computation* 9 (2010), 219–237.

[13] A. Adamatzky, Physarum Machines: Making Computers from Slime Mould, World Scientific, 2010.

[14] A. Adamatzky, Slime mould solves maze in one pass ... assisted by gradient of chemo-attractants. IEEE Trans on NanoBioscience Volume: 11 , Issue: 2, 2012, Page(s): 131–134.

[15] A. Adamatzky On attraction of slime mould Physarum polycephalum to plants with sedative properties. *Nature Proc 2011*; `http://dx.doi.org/10.1038/npre.2011.5985.1`

[16] A. Adamatzky, Simulating strange attraction of acellular slime mould *Physarum polycephalum* to herbal tablets. Math Comput Modelling (2011).

[17] A. Adamatzky. *Bioevaluation of World Transport Networks*. World Scientific, 2012.

[18] A. Adamatzky. Route 20, autobahn 7 and Physarum polycephalum: Approximating longest roads in USA and Germany with slime mould on 3D terrains. (2012) arXiv:1211.0519 [nlin.PS]; *IEEE Transactions on Systems, Man, and Cybernetics, Part B:Cybernetics* (in press), 2013.

[19] R. Araujo and A.T. de Almeida Learning sensor-based navigation of a real mobile robot in unknown worlds *IEEE Transactions on Systems, Man, and Cybernetics, Part B: Cybernetics*, 29 (1999) 2, 164–178.

[20] M.A. Bedau and J.S. McCaskill, Packard N. H., Rasmussen S. Living technology: exploiting life's principles in technology. *Artificial Life* 16 (2010) 89–97.

[21] C. S. Calude, J. Casti, M. Dinneen (Eds.). *Unconventional Models of Computation*, Springer-Verlag, Singapore, 1998, 416 pp.

[22] C.S. Calude, M.J. Dinneen, G. Paun, G. Rozenberg, S. Stepney, *Unconventional Computation: 5th International Conference*, Springer, 2006.

[23] Cartwheel galaxy. PIA03296: A Stellar Ripple. `http://photojournal.jpl.nasa.gov/catalog/PIA03296`

[24] M., Cautun M., van de Weygaert R., Jones B. J. T., Frenk C. S., Hellwing W. A. Nexus of the Cosmic Web. *Proceedings of the 13th Marcel Grossman Meeting on General Relativity* (Stockholm, Sweden, July 1–7, 2012). arXiv:1211.3574 [astro-ph.CO

[25] B. De Lacy Costello, A. Adamatzky, I. Jahan, L. Zhang, Towards constructing one-bit binary adder in excitable chemical medium, *Chemical Physics* 381 (2011), 88–99.

[26] H.D. Edelsbrunner, D. Kirkpatrick, R. Seidel, On the shape of a set of points in the plane, *IEEE Trans Inform Theor* 29 (1983), 551–559.

[27] H. Edelsbrunner, E.P. Muke, Three-dimensional alpha shapes. *ACM Trans Graphics* 13 (1994), 43–72.

[28] M.J. Fuerstman, P. Deschatelets, R. Kane, A. Schwartz, P.J.A. Kenis, J.M. Deutch, G.M. Whitesides, Solving mazes using microfluidic networks, *Langmuir* 19 (2003), 4714–4722.

[29] Ge, S.S.; Xuecheng Lai; Mamun, A.A. Boundary following and globally convergent path planning using instant goals *IEEE Transactions on Systems, Man, and Cybernetics, Part B: Cybernetics*, 35 (2005) 2, 240–254.

[30] J. Górecki and J.N. Górecka, . Information processing with chemical excitations — from instant machines to an artificial chemical brain, *Int J Unconv Comput* 2 (2006), 321–336.

[31] J. Górecki, J.N. Górecka, Y. Igarashi, Information processing with structured excitable medium, *Natural Computing* 8 (2009), 473–492.

[32] R. Jarvis, On the identification of the convex hull of a finite set of points in the plane, *Inform Process Lett* 2 (1973), 18–21.

[33] E. Katz and V. Privman, Enzyme-based logic systems for information processing, *Chem. Soc. Rev.* 39 (2010), 1835–1857.

[34] Kurz, A. Constructing maps for mobile robot navigation based on ultrasonic range data *IEEE Transactions on Systems, Man, and Cybernetics, Part B: Cybernetics*, 26 (1996) 2, 233–242

[35] I. Lagzi, S. Soh, P.J. Wesson, K.P. Browne and B.J. Grzybowski, Maze solving by chemotactic droplets, *J Am Chem Soc.* 132 (2010), 1198-9.

[36] J.F. Leng and W. Zeng An Improved Shortest Path Algorithm for Computing One-to-One Shortest Paths on Road Networks *2009 1st International Conference on Information Science and Engineering (ICISE)*, 2009, 1979–1982

[37] L. Liu, Y. Song, H. Ma, X. Zhang Physarum optimization: A biology-inspired algorithm for minimal exposure path problem in wireless sensor networks *INFOCOM, 2012 Proceedings IEEE*, 2012, 1296–1304.

[38] Mayne R., Patton D., De Lacy Costelo B., Patton R., Adamatzky A. Loading slime mould *Physarum polycephalum* with metallic particles. *Submitted* (2013).

[39] J. Macdonald, Y. Li., M. Sutovic, H. Lederman, H. Pendri, W. Lu, B.L. Andrews, D. Stefanovic, M.N. Stojanovic, Medium scale integration of molecular logic gates in an automaton. *Nano Letters* 6 (2006), 2598–2603.

[40] The Centre of the Milky Way Galaxy. *Spitzer Space Telescope. IRAC. NASA JPL Caltech*. S. Stolovy. (2006).

[41] J. Mills, The nature of the Extended Analog Computer, *Physica D* 237 (2008), 1235–1256.

[42] I. N. Motoike and K. Yoshikawa, Information operations with multiple pulses on an excitable field, *Chaos, Solitons & Fractals* 17 (2003), 455–461.

[43] T. Nakagaki, H. Yamada, A. Toth, Maze-solving by an amoeboid organism, *Nature* 407 (2000), 470–470.

[44] T. Nakagaki, H. Yamada, and A. Toth, Path finding by tube morphogenesis in an amoeboid organism, *Biophysical Chemistry* 92 (2001), 47–52.

[45] T. Nakagaki, M. Iima, T. Ueda, Y. Nishiura, T. Saigusa, A. Tero, R. Kobayashi, K. Showalter, Minimum-risk path finding by an adaptive amoeba network, *Physical Review Letters* 99 (2007), 068104.

[46] T. Nakagaki (Ed.) The Birth of Physarum Computing. Special Issue of the *Int J Unconventional Computing* 6 (2010), 1–161.

[47] NASA/JPL-Caltech: Our Milky Way Gets a Makeover. March 2008. `http://www.nasa.gov/mission_pages/spitzer/multimedia/20080603a.html`

[48] V. Privman, V. Pedrosa, D. Melnikov, M. Pita, A. Simonian and E. Katz, Enzymatic AND-gate based on electrode-immobilized glucose-6-phosphate dehydrogenase: Towards digital

 DOI: 10.2420/AF06.2013.53

biosensors and biochemical logic systems with low noise, *Biosens. Bioelectron.* 25 (2009), 695–701.

[49] D. R. Reyes, M. G. Ghanem, M. George, Glow discharge in micro fluidic chips for visible analog computing, *Lab on a Chip* 1 (2002), 113–116.

[50] J. Sielewiesiuk and J. Górecki, Logical functions of a cross junction of excitable chemical media, *J. Phys. Chem.* A105 (2001), 8189.

[51] F. P. Preparata, and M. I. Shamos, *Computational Geometry*, Spinger-Verlag, New York, 1985.

[52] C. Shannon, Presentation of a maze solving machine, *Trans. 8th Conf. Cybernetics: Circular, Causal and Feedback Mechanisms in Biological and Social Systems* (1951), 169–181.

[53] T. Shirakawa, A. Adamatzky, Y.-P. Gunji, Y. Miyake, On simultaneous construction of Voronoi diagram and Delaunay triangulation by *Physarum polycephalum*, *Int. J. Bifurcation Chaos* 9 (2009), 3109–3117.

[54] T. Shirakawa, Y.-P. Gunji, and Y. Miyake, An associative learning experiment using the plasmodium of *Physarum polycephalum*, *Nano Communication Networks* 2 (2011) 99–105.

[55] T. Schubert. `www.theresaschubert.org`

[56] A. Schumann and A. Adamatzky, Physarum spatial logic, *New Mathematics and Natural Computation* 7 (2011), 483–498.

[57] Y. Song, L. Liu, H. Ma. *2012 IEEE Wireless Communications and Networking Conference (WCNC)*, 2012, 2151–2156.

[58] Anand P., Chung G., Li L, Esra E. Hypercells. *Team:Spores. Behavioural Matter v. 2 Architectural Association Design Research Lab* (2013).

[59] S. L. Stephenson and H. Stempen, *Myxomycetes: A Handbook of Slime Molds*, Timber Press, 2000.

[60] M. N. Stojanovic, Y. E. Mitchell, and D. Stefanovic, Deoxyribozyme-based logic gates. *JACS* 124 (2002), 3555–56.

[61] Tendal O. and van der Land, J. Xenophyophora. In: Costello, M.J. et al. (Ed.) (2001). European register of marine species: a check-list of the marine species in Europe and a bibliography of guides to their identification. *Collection Patrimoines Naturels*, 50: pp. 78-79

[62] C. Teuscher and A. Adamatzky A. (Eds.) *Unconventional Computing 2005: From Cellular Automata to Wetware*, Luniver Press, 2005.

[63] S. Tsuda, M. Aono, and Y.P. Gunji, Robust and emergent Physarum-computing, *BioSystems* 73 (2004), 45–55.

[64] K. Yoshikawa, I. M. Motoike, T. Ichino, T. Yamaguchi, Y. Igarashi, J. Gorecki and J. N. Gorecka, Basic information processing operations with pulses of excitation in a reaction-diffusion system, *Int J Unconventional Computing* 5 (2009), 3–37.

[65] R. van de Weygaert and W. Schaap W. The Cosmic Web: Geometric Analysis. In: *Lecture Notes Summer School "Data Analysis in Cosmology" (Valencia)*, eds. V. Martinez, E. Saar, E. Martinez-Gonzalez, M. Pons-Borderia, Springer-Verlag. arXiv:0708.1441 [astro-ph]

[66] A.R. Willms and S.X. Yang. Real-time robot path planning via a distance-propagating dynamic system with obstacle clearance. *IEEE Transactions on Systems, Man, and Cybernetics, Part B: Cybernetics*, 38 (2008) 3, 884–893.

[67] W. Zeng, W. Zong, C. Xiong Performance Optimization for Wireless Network of Ultra Wideband *2012 Fourth International Conference on Computational and Information Sciences (ICCIS)*, 2012, 1100–1103.

Acta Futura 6 (2013) 69-79
DOI: 10.2420/AF06.2013.69

Acta Futura

Soft Robots in Space: A Perspective for Soft Robotics

Huai-Ti Lin,
Department of Biology, Tufts University, 200 Boston Av. Rm. 2613, Medford, MA 02155. USA
Janelia Farm, Howard Hughes Medical Institute, 19700 Helix Drive, Ashburn, VA 20147. USA
Gary G. Leisk,
Department of Mechanical Engineering, Tufts University, 200 College Ave., Medford, MA 02155. USA
Barry A. Trimmer*
Department of Biology, Tufts University, 200 Boston Av. Rm. 2613, Medford, MA 02155. USA

Abstract. Deploying robots in space has been difficult due to safety concerns and the need to operate in confined weightless environments that are complex and 3-dimensional. Some of these concerns can be addressed by deploying soft robots that can change shape, attach to surfaces and climb robustly independent of gravity. These capabilities are already found in soft animals such as caterpillars that move by controlling body deformation instead of actuated joints. To understand some control issues associated with this lack of articulation, we created a soft robot platform as a reduced physical model of a caterpillar. This paper describes and discusses a collection of design concepts that influenced the fabrication and operation of these soft robots to illustrate some advantages and constraints of deploying soft robots in space.

1 Introduction

One of the continuing challenges in robotic engineering is the design of robots that can adapt to unpredictable complex environments or work in close association with humans. This is a particularly difficult issue in many space applications. Robots that are designed to work well in a factory on earth are generally difficult to adapt to the confined weightless environment of an orbiting vehicle. Such robots must also be designed to safely interact with human operators because the potential costs of even small injuries or damage to equipment is unacceptable. For inspiration, we may turn to biology.

In order to achieve adaptability and robustness many existing robot architectures are inspired by animals and seek to replicate the extraordinary movement patterns (i.e. Honda's Asimo) [9, 24] and neural reflexes (i.e. Boston Dynamics' Big Dog) [23] of bipeds and quadrupeds. These approaches have been impressive in producing stable locomotion but they currently require very high power output and sophisticated controls using sensor feedback. They are also potentially dangerous, operating with powerful actuators and relatively stiff materials.

An alternative bio-inspiration is the idea of mechanical adaptation to the environment via soft mechanics. This approach is much less common in robotics because such high deformation systems are thought to require even more complex feed-back. However, recent animal studies suggest that high compliance can be exploited

*Corresponding author e-mail: barry.trimmer@tufts.edu

to produce self-adapting structures that decrease demands on neural sensing. For example, soft-bodied animals can conform to a complex 3-dimensional substrate without knowing its exact geometry [1, 5, 12, 15, 33].

We propose three major attributes that make soft robots useful for space applications. Soft robots are:

1. **Intrinsically safe (rather than "control safe").** Soft materials dissipate forces and minimize the risk of damage or injury through sudden impacts. The full advantage of this property is only realized with structures that are entirely soft; soft coatings on hard robots can improve safety but at the cost of increased weight, bulk and reduced motion precision.

2. **Morphable (size-changing and versatile).** Due to the cost of space travel, a payload faces both weight and volume limitations. Soft robots allow many different ways to fold and may even use inflation for deployment. This flexibility allows users to pack and store these devices at many locations. The ability to change shape also makes these robots very versatile. For access to narrow apertures the robot can be long and thin but for sticking to smooth surfaces the robot might spread out and flatten itself.

3. **Gravity independent (able to move in any orientation).** Because soft robots have a much lower mass density than traditional machines they can be constructed to operate in any orientation or in low gravity situations. This feature has been demonstrated in recent studies where it has been shown that a soft bodied animal can use the same strategy to crawl underwater, upside down, or to climb vertically [32]. This capability would be an obvious advantage for robots operating in space.

To make soft robots functional, there are also three key components of the design and fabrication that must be addressed:

1. **A truly soft body.** Highly deformable machines are difficult to control using traditional approaches. The complex material properties themselves become an important design consideration.

2. **Soft actuators.** The development of soft actuators continues to be a key requirement for the production of autonomous soft machines. Because current active materials vary tremendously in their properties it is important to characterize their responses in detail to guide feature selection and final integration.

3. **Secure attachment devices.** Any robot moving in a space environment must interact safely with different surfaces and be able to control its attachments. Our studies of soft animals give some useful insights into how this can be done very simply.

In this article we will describe how recent findings from research on a soft animal have led to a better understanding of the benefits and challenges of soft robots. Following a brief overview of the animal studies we will concentrate on the design and characterization of three key components (body materials, actuators, grippers) used in our biomimetic soft robots. The robots we describe were not developed specifically for space environments but their development helps to illustrate some of the key design and control areas for soft machines operating in space.

2 Caterpillar locomotion as a case study

Through evolution over millions of years, animals have developed an extraordinary range of materials to support their bodies and to move in different environments. By studying these systems we expect to learn some of the successful strategies that give animals robust and adaptable locomotion. One obvious example is that nervous systems have coevolved with the complex materials and tissues of the body. The nervous system and physical plant are so closely integrated that neither has a function independent of the other. It is possible that future robots will need to be designed in a similar manner with a distributed ""neuromechanical" control system.

One very tractable system that has been exploited to study these phenomena is the caterpillar, *Manduca sexta*, which is the larval stage of a large moth (Fig. 1). Some of the unique technical advantages of these animals have already been discussed [31]. However, they also possess characteristics that are of particular interest in space-based applications.

Firstly, we have shown that crawling caterpillars have minimum or no dynamics (they are quasi-static), the body is generally in tension, and the movement of each segment is preceded by an internal tensile loading [16, 26]. The lack of dynamics reduces the dependency on accurate temporal control and the body remains soft and flexible. Having robots that can pull

 DOI: 10.2420/AF06.2013.69

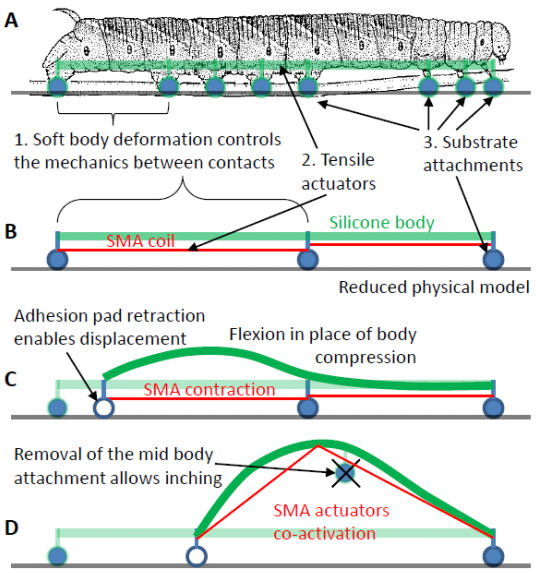

FIGURE 1. *Physical modeling of caterpillar locomotion. (A) A crawling caterpillar can be reduced to three elements: soft body axial deformation, tensile actuators, and substrate attachments. (B) The reduced model is implemented using silicone rubber for the body and shape memory alloy (SMA) coils as the actuators. Controllable attachments are implemented as either retractable adhesion pads or unidirectional gripping flaps. (C, D) Flexion is the primary functional deformation in this soft robot design system. Embedded SMA contractions drive the flexion.*

themselves through very narrow spaces and bend around intricate equipment is well-suited to space applications.

Secondly, the caterpillar does not have circumferential muscles [28] and its hydrostatic skeleton is not under tight pressure regulation during locomotion. Caterpillars with altered body volume and pressure (via saline injection or hemolymph extraction) can still move efficiently. This implies that caterpillar-inspired soft robots do not have to rely on pressurization which could be problematic in space application. Finally, caterpillar legs are equipped with a fail-safe passive gripping mechanism [17]. This system is based on two rows of miniature grappling hooks (crochets) embedded in a soft cuticular membrane. Clearly, the ability to grip and release without significant energy expenditure could be of enormous importance for a robot operating in a weightless environment.

The rest of this article concentrates on what we learned from designing a caterpillar-like robot. In particular we describe some of the critical nonlinear properties of the body materials and actuators and illustrate how key elements of *Manduca's* body design can be used to create highly mobile devices.

3 Moving With a Soft Body

3.1 General design considerations

Based on our previous studies on caterpillar locomotion [16, 26, 30], we can reduce a crawling caterpillar into three key functional components: a highly deformable body, muscle-like tensile actuators and a mechanism to control grip (Fig. 1). We will start by presenting some issues with controlling the movement of a soft body.

3.2 Position control?

Traditionally a robot's workspace is defined by the joint kinematics and limited by the joints' ranges of motion. It is often feasible to control such structures as state machines with some feedback compensation. In contrast, it is extremely difficult to describe the kinematics of a soft robot and without any articulation there is no easy way to predict deformations [7, 10]. This is why most models of soft structures are numerical and require computation that cannot be accomplished in real time. Furthermore, feedback about position is enormously challenging with so many possible configurations. Philosophically, a soft robot should not "lock" into a specific configuration and still be considered "soft".

Caterpillars typically pull their bodies forward along a single linear axis with muscles oriented predominantly along the direction of travel. As long as there is sufficient anterior grip, the exact body deformation does not matter for locomotion. Indeed, there is no evidence that the prominent stretch receptor organs play any role in normal crawling [27]. This suggests that position control is not always necessary.

3.3 Nonlinearity is inherent in large deforming bodies

Nonlinearity creates serious computational challenges for traditional control systems. Unfortunately, soft bodies are inherently nonlinear in their stress-strain responses due to large deformation. To illustrate some of these properties in elastomers used to construct our soft robots, we created a standard uni-axial test (Fig. 2A). Homogenous silicone rubber is linearly elastic up to very high strains in a tensile test but will then exhibit pseudo-elastic behavior in the buckling state (Elastomer 1 & 2,

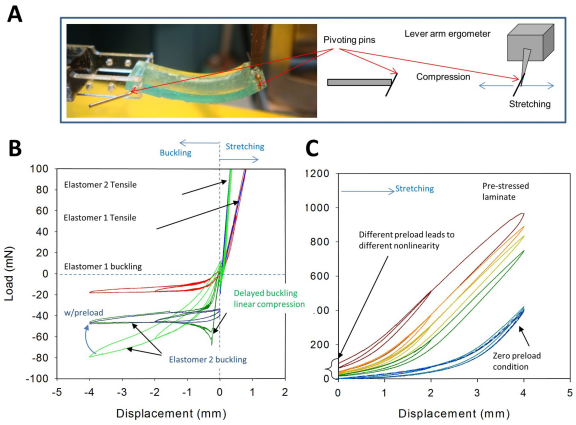

Figure 2. *Nonlinear behaviors from linear materials. (A) Samples of silicone elastomer used in the robot construction were tested in tension and compression. (B) Stretching tests of two elastomers (elastomer 1 and 2) with different stiffness values confirm that they respond linearly in tension. Under compression they buckle, a nonlinear loading condition which depends on the initial conditions (see text for details). Starting the compression test with an initial preload changes the buckling profile completely (in blue). Preventing the buckling leads to a linearly elastic compression profile (dark green). (C) When two different linear elastic materials are cured into a laminate with one side stretched out, the sample naturally buckles at resting state. This residual stress leads to pseudo-elasticity (differing displacements during loading and unloading) and work softening (changing curves with increased displacement).*

Fig. 2B). In the buckling configuration, the compressive force between the two ends is the greatest at the beginning and decreases as buckling progresses. Interestingly, an initial buckling bias preload can alter the loading profile completely (Fig. 2B; dark blue curve). To show that this nonlinearity comes from the loading condition, we prevented one side of the pivoting pin from rotating in Elastomer 2 and performed the same test. This constraint delayed buckling and allowed simple material compression to occur. The resulting loading curve followed a perfect linear trend (Fig. 2B; dark green). Once the loading exceeded a threshold (e.g. ~70mN), the specimen buckled and reproduced the regular curves with preload.

Another inherent nonlinearity in soft material is residual stress. Most biological tissues are developed by lamination and therefore contain residual stress [11]. We can simulate this condition in a silicon rubber specimen by curing one layer of rubber under stress to another unstressed layer. This produces a material with a buckled resting configuration due to the residual stress (Elastomer 3). In extension tests this specimen produces load-stiffening behavior, which depends closely on the amount of preload (Fig. 2C). In essence, any stretching force has to unbuckle the specimen before it can engage in the linear material stretching. The unbuckling process increases the material stiffness gradually as the polymers align themselves to the loading direction. This behavior is highly repeatable and very analogous to the soft cuticle of caterpillars [14]. It is likely that nonlinearity in biological systems is exploited as an intrinsic part of the natural control system.

4 Soft actuators

4.1 Active materials as soft actuators

The biggest challenge in building a practical soft robot of any kind is the lack of suitable actuators. Ideally the actuators should be like muscle, deformable and powered by locally available energy-rich hydrocarbons. Unfortunately all the available synthetic soft actuators have major limitations. The most deformable are chemically reactive gels (which are still far from practical as actuators), and electroactive polymers [4]. Electroactive polymers consist of two major classes, the ionic polymer-metal composites (IPMCs) and dielectronic polymers. It is difficult to interface these polymers with other materials or even with conducting surfaces necessary for their activation. The IPMCs must also be kept wet and the diaeletronic polymers require very high electrical fields. These properties have limited their application even in stable environments let alone the extremes of space.

As an alternative, compliant actuators have been made using pneumatic pistons, hydraulics, McKibbon actuators [34], or inflating elastic compartments [25]. These technologies all have their applications but obviously they require the ability to pressurize and store gas or liquids using rigid materials and off board motors.

In our opinion there are two other existing technologies which hold most promise. Both rely on extreme miniaturization of otherwise hard components to make actuators that do not have a large impact on the bulk material properties of the robot. The first is to deploy linear motors or small spooling motors pulling flexible cables or compliant “tendons”. On a larger scale, this mechanism is a common approach in research robots such as ECCCEROBOT-2 [6] but it has not been attempted in an entirely soft robot which will require motors an order of magnitude smaller.

 DOI: 10.2420/AF06.2013.69

The second approach is to use the crystalline transition properties of shape-memory alloys (SMAs, e.g., Nitinol). Although SMA wires are intrinsically hard, when drawn to a diameter of less than 200 microns and tightly coiled they are macroscopically as soft as fabrics and able to exert strains of 100%. Although the temperature dependency of SMAs is a serious limitation for extravehicular space applications, we have used SMA coils as a development tool to show how extreme non-linear motors can be used to move soft robots

4.2 How does control differ in a soft actuator?

In a classic DC motor, the driving voltage roughly determines the rotational speed and is largely independent of changes in the timing of the input signal. If the motor is driving a load a feedback control circuit can be used to linearize the system. In contrast, the performance of soft actuators such as muscles or SMA coils is critically dependent on stimulus timing, duration and magnitude. It is possible to control SMA actuation to reasonable precision using conventional feedback control in a well-defined rigid body motion (SmartServo RC-1, Toki Corporation, Tokyo Japan). In a soft robot, however, the constantly deforming body makes actuator position control less useful. An alternative approach is to characterize the actuator properties and use them to tailor the robot motor commands.

As an example of this approach we systematically altered SMA (Biometal Helix, BMX100, Toki Corporation, Tokyo Japan) pre-load (3 levels), resisting stiffness (3 levels), and driving power (3 levels) while monitoring the evoked force-length relationships using a uniaxial Universal Testing Machine (Fig. 3A. Instron Inc., model 3366, Norwood, MA). Specifically, we measured the peak force, peak displacement, and initial loading rate. Although the nonlinear responses of SMA are complex, some general trends can be used to design different operating conditions (Fig. 4).

4.3 Force and displacement

While peak force increases monotonically with mechanical resistance (Fig. 4A) and preload, the opposite trend occurs for displacement (Fig.4B). This force-displacement trade-off is not so different from the idea of gearing except that the tradeoff has bias to an optimum. In other words, giving up a unit of displacement does not trade in the same unit of force. One key factor for this bias is appropriate preloading (Fig. 4C),

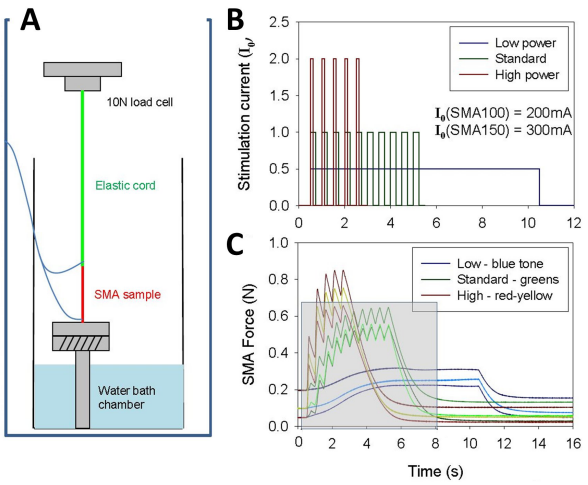

Figure 3. *SMA test data analysis. (A) The SMA samples were held in series with a load cell and an elastic cord for testing. (B) We used low-frequency pulse width modulation signals to stimulate the SMA samples. By controlling the current level and pulse duration, the same amount of energy can be delivered to the SMA at different durations. (C) Force developed by the SMA samples were recorded under different preload and stimulation powers (Low power: **PL**, Standard power: **P0**, High power: **PH**). This is repeated three times and also with different resisting cord spring constants.*

which boosts the force production without losing noticeable displacement. In practice, we need to carefully arrange the SMA actuator installation in the soft robot to ensure appropriate preload and good performance.

4.4 Power and loading speed

Higher stimulating power allows SMA coils to develop larger peak forces quickly (Fig. 4A–C). High power stimuli ensure that all the crystals in the SMA alloy transform into the austenite state at the same time, leading to synchronized force production, analogous to muscle fiber recruitment in animals. That's also why initial loading rate increases with resisting load most dramatically at high power (Fig. 4D). Understanding these speed-power curves allows us to drive different motions with the appropriate speed ranges.

5 Passive Grip, Active Release

A key element for climbing in complex three-dimensional structures is that the substrate must be gripped reliably at multiple points. This grip must pro-

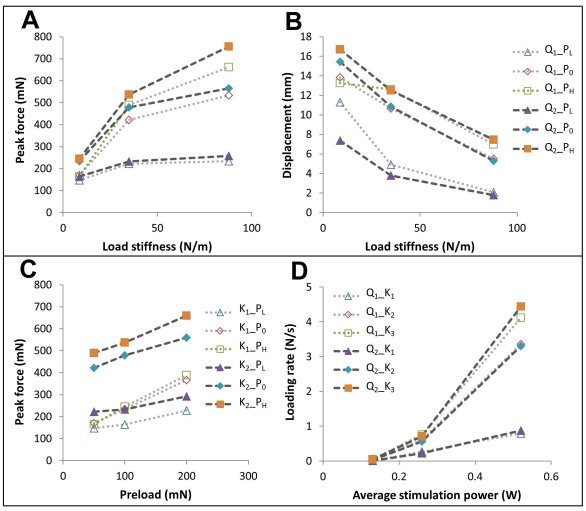

FIGURE 4. *Characterizing shape memory alloy actuators (A) For each preload* Qi *and stimulation power* Pi *(A and B share the same legend), increasing load stiffness induces higher peak forces. Overall, increasing preload also increases the peak forces but this effect is most notable at high stimulation power. (B) The increasing peak force in response to stiffer loads is accompanied by decreasing displacements although the trends are less linear with low preload Q1 and small load stiffness. (C) In general, increasing preload induces higher peak force in a linear fashion. (D) Increasing stimulation power boosts the SMA initial loading rate. The trend depends on the load resistance but not the preload.*

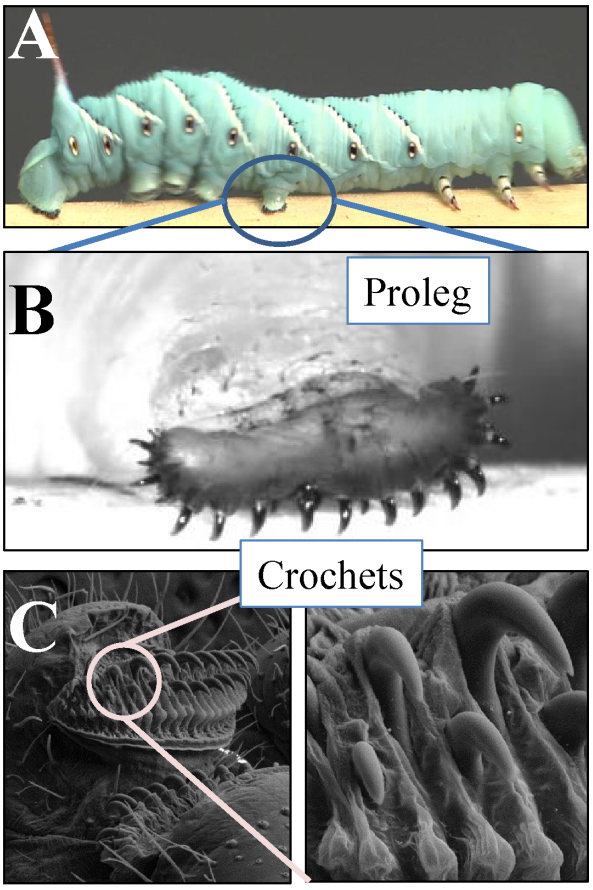

FIGURE 5. *(A) The caterpillar Manduca sexta attaches to the surface with soft limbs called proleg (B) Each proleg has rows of hooks called crochets which are shown in detail in (C).*

vide enough traction to support the weight of the robot or animal (when it is climbing or upside down) and also provide an anchor for propulsive forces. The grip must also releases in a failsafe way at the right timing during forward movements. Caterpillars like *Manduca* have solved this problem by using a passive grappling hook system (crochets) that can be actively released without dragging or producing any resistance to lift (Fig. 5, [16]). These crochets can be deployed passively and as they contact a surface they orient to conform closely to the substrate. With an ideal substrate, these micro hooks grip so well that forcing a caterpillar off the substrate will tear some prolegs off the body (personal observation). The most remarkable part of this gripping system is that the crochets can be rapidly detached through the activation of a single muscle regardless of the substrate roughness or the angle of attachment.

Although hook-based gripping systems work very well on relatively rough surfaces they are not suitable for smooth artificial substrates such as metal or glass.

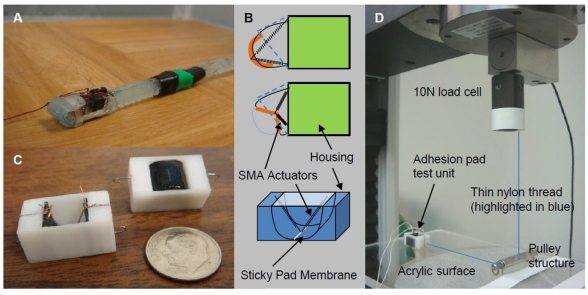

FIGURE 6. *Retractable adhesion pads provide controllable grip. (A) Retractable adhesion pad on GoQBot-III. (B) Schematics of adhesion pad retraction mechanism. (C) Adhesion pad units for testing traction performance. (D) The adhesion pad unit was dragged across an acrylic surface by the load cell via a thin nylon thread over a pulley at a constant speed of 1cm/s.*

DOI: 10.2420/AF06.2013.69

The same general principle of passive grip and active release can be used in a controllable adhesion device. We designed a simple retractable adhesion pad to provide controllable body anchors for the soft robots (Fig. 6). By adding polyorganosiloxanes (POS) to the platinum-cure silicone mixture, we produced a tacky silicone texture. In general, the amount of POS added determines how sticky the end product is [29]. To test the adhesion performance, we dragged a set of experimental adhesion pads across a smooth surface and measured the resisting force (Fig. 6D).

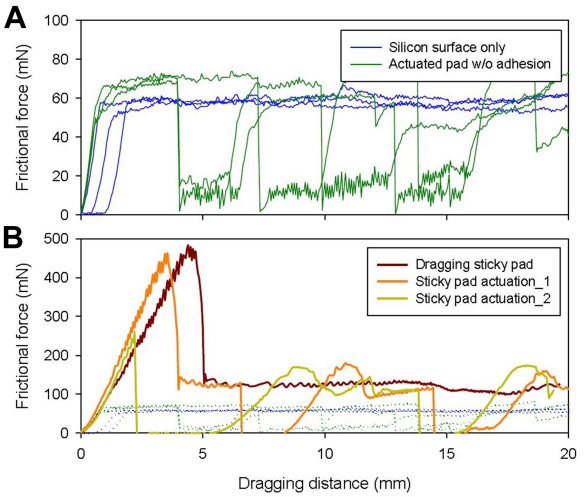

Figure 7. *Retractable adhesion pad test. (A) Without any adhesion material, silicone rubber provides frictional force around 60mN given a normal force of 14.7mN. The retractable pad produces the similar traction and upon actuation, the friction can drop below 20mN. (B) The adhesion pad delivers static traction force close to 500mN before slipping. Once moving, the friction remains twice that of pure silicone rubber provides. Actuation in this state removes the friction almost completely (orange trace). Redeployment of the pad reestablishes the friction. Similarly, adhesion pad can be retracted in the initial phase as well (olive green trace).*

The friction from the silicone surface without adhesion material is about 60mN (Fig. 7A, blue traces). Retraction of the silicone surface drops the friction to around 15mN (Fig. 7A, green traces). These are the performance references without adhesion pads. With an adhesion pad the static traction increases almost 10 fold (Fig. 7B, brown trace). When sliding, the sticky pad still maintains a friction level twice that of plain silicone rubber. Retraction of the adhesion pad decreases the friction to below 15mN (Fig. 7B, orange trace). As the sticky pad is redeployed, the friction level recovers to over 150mN in a sliding condition and is maintained above 100mN consistently. The sticky pad can be retracted early to remove friction during a static loading phase (Fig. 7B, olive green trace) without affecting any later operations. In summary, the retractable adhesion pad can introduce an immediate >100mN traction to a soft robot in motion and provide >400mN anchor in the static condition. Typically our small crawling robots exert forces on the order of 100mN. The adhesion pad therefore can quickly slow down a moving body and lock it in place.

6 Moving soft structures

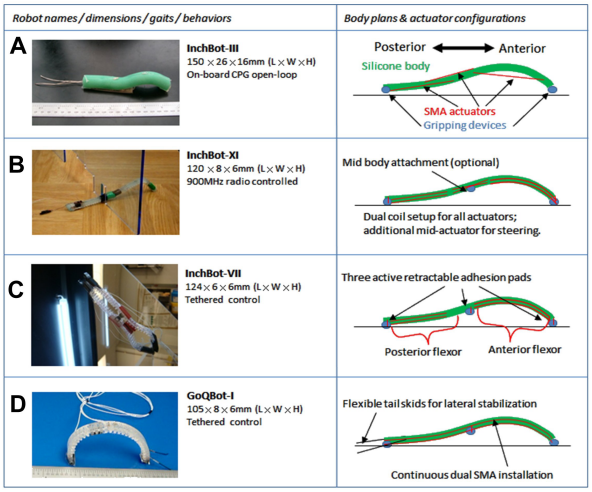

Figure 8. *Soft robot platforms based on caterpillar locomotion. The left panel shows four representative robots and their basic information. The right panel shows the positions of the embedded SMA actuators (red), adhesion pads (blue), and the overall body configurations.*

6.1 A family of soft inching robots

Having all the three components for soft robots is only the first step. Controlling the soft structure to move is yet another challenge. Based on the body plan outlined previously (Fig. 1), we created a family of soft robots to explore different possibilities for locomotion. Some representatives are shown in Figure 8 with key design parameters and schematics conveying the body plan and actuator configurations. We will only pick out some examples for the purpose of this paper.

SMA load tuning has been a big part of motion planning. In the earliest design, displacement was provided by buckling the anterior segments of the robot. An example is InchBot-III (Fig. 8A) which has a 15cm long silicone rubber foam body shaped like a half cylinder. In this anterior inching gait (Fig. 8A) the robot pulls its body forward by flexing the anterior segment while the posterior segment catches up to anchor the body (Fig. 9A). Such body coordination requires that the posterior segment responds faster and yet with smaller amplitude. This was achieved by preloading the posterior segment slightly more and delivering higher power. The activation speed and range of motion therefore can be embedded into the robot itself.

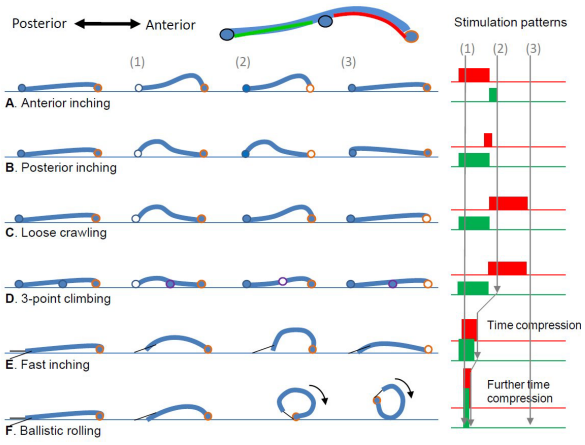

Figure 9. *Gait maps for the soft robots. From top to bottom, these are 6 modes of locomotion for the caterpillar-like robots. From left to right, schematic diagrams illustrate the body configurations in a given gait pattern. Most of the robots have mechanisms for locking down the body (noted by solid circles). Open circles represents attachment devices in the retracted state to allow body displacement. Gaits* ***E*** *and* ***F*** *use a pair of tail skids for lateral stability. The right panel shows the patterns of stimulating pulse trains given to the anterior flexor (red) and posterior (green) flexor respectively. This diagram uses amplitude to show the stimulating power and thes olid block length to show the timing. The exact timing might vary slightly depending on the robot condition.*

InchBot-XI is a radio-controlled soft robot with two retractable adhesion pads and uses two different gaits (Fig. 8B–C) to negotiate through a 1cm hole (Fig. 8B). The entire hole traversal process relies on precise temporal-control of the body curvatures. The introduction of the retractable sticky pads allowed more tolerance in movement timing variation. With three retractable adhesion pads, InchBot-VII propagates a displacement in the anterior-grade manner up an incline of 45 degrees without any noticeable change in kinematics (Fig. 8C). As illustrated in Fig. 9D, the InchBot-VII initiates a crawl cycle by first releasing the posterior adhesion pad and then pulling the posterior segment forward. After replanting the posterior adhesion pad, the mid-adhesion pad releases followed by a forceful contraction in the anterior segment. This transfers the body contraction (buckling) forward. As soon as the mid-adhesion pad reattaches to the substrate, the anterior adhesion pad releases and moves forward. This simple "3-point climbing" gait represents the fundamental mechanism of crawling in caterpillars [32]. Nevertheless, the climbing gait of InchBot-VII climbed from flat-ground to 45 degrees with the same kinematics (minimal slipping and almost identical step length).

6.2 Simple gait transition

Many behaviors can be produced from the same gait pattern by scaling the power and timing slightly. For a soft robot with a loose-crawling gait (Fig. 9C), increasing the actuator power amplifies the body flexion and reduces the phase difference between posterior and anterior flexions. Further temporal compression of the gait pattern improves the body coordination and produces a fast inching gait (Fig. 9E) which is five times faster than the 3-point climbing gait. However, amplified flexion means raising the center of mass much higher. The probability of tipping over increases dramatically as the adhesion pads cannot always resist the lateral tipping moments. Inching caterpillars seem to also experience such trade-offs. Caterpillars typically perform a fast crawl by cycling the waves of muscle contraction more quickly. However, in some cases, they change from crawling to inching, thereby taking the largest possible steps. Our soft robot shows that pacing a crawling gait together with higher stimulation intensity could result in a continuous transition to inching gaits.

Interestingly, further increasing the actuator power tipped the robot forward into a tumble. Such a phenomenon prompted us to consider the possibility of rolling locomotion. Surprisingly, caterpillars indeed do perform such a rolling behavior under special conditions. A group of small caterpillars *Pleuruptya ruralis*, perform a backward ballistic roll when startled [2]. We found several caterpillars from the same family (*Crambidae*) in Costa Rica performing comparable escape behaviors (field observations, H. T. Lin and B. A. Trim-

 DOI: 10.2420/AF06.2013.69

mer). Using this escape behavior as an inspiration and kinematic model, we successfully reproduced ballistic rolling (Fig. 9F) in several versions of GoQBot [13]. On a flat level surface, this mode of locomotion boosts the speed over ten-fold. Development of these soft robot gaits showed that gait transitions can arise from gradual changes in a continuous manner for example by scaling the gait timing and driving power.

7 Summary

The field of soft robotics is still relatively new and there are very few widely accepted design principles for building highly deformable machines. We have taken a bio-inspiration approach by searching for an animal that achieves many of our locomotion goals. The caterpillar is effectively a living prototype for a robot that is capable of climbing in complex three-dimensional structures independent of gravity. By engineering the three key components of caterpillar locomotion (i.e., soft body, soft actuator and attachment mechanism) we demonstrated that it is possible to produce coordinated locomotion.

For space applications in the absence of gravity, neither wheeled systems nor legged robots are likely to be useful (they both require normal down force). To move efficiently under microgravity any mobile robot (not mounted on a structure) will need to fly or crawl. For example, the NASA SPHERES robot uses a collection of small CO_2 thrusters to push itself around in the International Space Station [18]. Soft robots that can climb or crawl provide convenient means to transport equipment or to perform examinations. One can imagine a team of soft robots traveling between space station modules to perform inspections. They can also be deployed outside to check on solar arrays or antenna structures to evaluate if a spacewalk is necessary. As a portable device, a soft robot can fit between structures whenever the astronaut needs a third hand for some specific procedures. When not in use, soft robots can be easily folded up and stored in some odd space which would otherwise be considered a dead space. The morphing capability not only benefits storage, but also provides alternative method of gripping. Perhaps the most notable technology for this role is the controlled jamming of granular materials to produce a universal robotic gripper that automatically forms itself into arbitrary shapes to gently but firmly grasp delicate or complex objects [3].

In terms of implementation, controlling soft structures might not be as far away as we thought. Any complex mechanical system contains information in its structure and materials [22, 21, 19, 8]. It is therefore possible to offload some control to the structural mechanics [20], as many biological systems have demonstrated. We have shown several ways to exploit the nonlinear behaviors that are inherent in soft structures. We are not suggesting that our SMA-powered robotic platform is a deployable space robot at the moment. Due to the large temperature fluctuation in space, SMA actuators would be limited to functions inside the climate-controlled compartments of the spacecraft/space station. However, this work has helped to discover new approaches to controlling soft material structures and highlighted some of the key factors that should be considered for designing and deploying soft robots for space applications.

Acknowledgment

This research was supported by the DARPA ChemBot project (W911SR-08-C-0012) and NSF-IOS Grant 1050908 to BAT. We would like to thank Ethan Golden, Tim Lo and all the other colleagues on the Tufts ChemBot team for their constructive feedback during regular project meetings.

References

[1] D. Accoto, P. Castrataro, and P. Dario. Biomechanical analysis of oligochaeta crawling. *Journal of theoretical biology*, 230(1):49–55, 2004.

[2] J. Brackenbury. Caterpillar kinematics. *Nature*, 390(6659):453–453, 1997.

[3] E. Brown, N. Rodenberg, J. Amend, A. Mozeika, E. Steltz, M. R. Zakin, H. Lipson, and H. M. Jaeger. Universal robotic gripper based on the jamming of granular material. *Proceedings of the National Academy of Sciences*, 107(44):18809–18814, 2010.

[4] F. Carpi, R. Kornbluh, P. Sommer-Larsen, and G. Alici. Electroactive polymer actuators as artificial muscles: are they ready for bioinspired applications? *Bioinspiration & Biomimetics*, 6(4):045006, 2011.

[5] R. Cortez, L. Fauci, N. Cowen, and R. Dillon. Simulation of swimming organisms: Coupling

internal mechanics with external fluid dynamics. *Computing in Science & Engineering*, 6(3):38–45, 2004.

[6] A. Diamond, R. Knight, D. Devereux, and O. Holland. Anthropomimetic robots: Concept, construction and modelling. *Int J Adv Robotic Sy*, 9(209), 2012.

[7] Y. B. Fu and R. W. Ogden. *Nonlinear elasticity: theory and applications*, volume 283. Cambridge University Press, 2001.

[8] F. Hara and R. Pfeifer. On the relation among morphology, material and control in morpho-functional machines. In *Meyer, Berthoz, Floreano, Roitblat, and Wilson (eds.): From Animals to Animats 6. Proceedings of the sixth International Conference on Simulation of Adaptive Behavior*, pages 33–40, 2000.

[9] R. Hirose and T. Takenaka. Development of the humanoid robot asimo. *Honda R&D Technical Review*, 13(1):1–6, 2001.

[10] G. A. Holzapfel, T. C. Gasser, and R. W. Ogden. A new constitutive framework for arterial wall mechanics and a comparative study of material models. *Journal of elasticity and the physical science of solids*, 61(1-3):1–48, 2000.

[11] G. A. Holzapfel and R. W. Ogden. Modelling the layer-specific three-dimensional residual stresses in arteries, with an application to the human aorta. *Journal of The Royal Society Interface*, 7(46):787–799, 2010.

[12] W. M. Kier. The arrangement and function of molluscan muscle. *The Mollusca, form and function*, 11:211–252, 1988.

[13] H. Lin, G. Leisk, and B. A. Trimmer. GoQBot: a caterpillar-inspired soft-bodied rolling robot. *Bioinspiration & biomimetics*, 6(2):026007, 2011.

[14] H. T. Lin, A. L. Dorfmann, and B. A. Trimmer. Soft-cuticle biomechanics: a constitutive model of anisotropy for caterpillar integument. *Journal of theoretical biology*, 256(3):447–457, 2009.

[15] H. T. Lin, D. J. Slate, C. R. Paetsch, A. L. Dorfmann, and B. A. Trimmer. Scaling of caterpillar body properties and its biomechanical implications for the use of a hydrostatic skeleton. *The Journal of experimental biology*, 214(7):1194–1204, 2011.

[16] H. T. Lin and B. A. Trimmer. The substrate as a skeleton: ground reaction forces from a soft-bodied legged animal. *The Journal of Experimental Biology*, 213(7):1133–1142, 2010.

[17] S. Mezoff, N. Papastathis, A. Takesian, and B. A. Trimmer. The biomechanical and neural control of hydrostatic limb movements in *Manduca sexta*. *Journal of experimental biology*, 207(17):3043–3053, 2004.

[18] S. Mohan, A. Saenz-Otero, S. Nolet, D. W. Miller, and S. Sell. SPHERES flight operations testing and execution. *Acta Astronautica*, 65(7):1121–1132, 2009.

[19] R. Pfeifer. On the role of morphology and materials in adaptive behavior. *From animals to animats*, 6:23–32, 2000.

[20] R. Pfeifer and F. Iida. Morphological computation: Connecting body, brain and environment. *Japanese Scientific Monthly*, 58(2):48–54, 2005.

[21] R. Pfeifer, F. Iida, and J. Bongard. New robotics: Design principles for intelligent systems. *Artificial Life*, 11(1-2):99–120, 2005.

[22] R. Pfeifer, M. Lungarella, and F. Iida. Self-organization, embodiment, and biologically inspired robotics. *science*, 318(5853):1088–1093, 2007.

[23] M. Raibert, K. Blankespoor, G. Nelson, and R. Playter. Bigdog, the rough-terrain quadruped robot. In T. I. F. of Automatic Control, editor, *Proceedings of the 17th World Congress*, pages 10823–10825, 2008.

[24] Y. Sakagami, R. Watanabe, C. Aoyama, S. Matsunaga, N. Higaki, and K. Fujimura. The intelligent asimo: System overview and integration. In *IEEE/RSJ International Conference on Intelligent Robots and Systems, 2002*, volume 3, pages 2478–2483. IEEE, 2002.

 DOI: 10.2420/AF06.2013.69

[25] R. F. Shepherd, F. Ilievski, W. Choi, S. A. Morin, A. A. Stokes, A. D. Mazzeo, X. Chen, M. Wang, and G. M. Whitesides. Multigait soft robot. *Proceedings of the National Academy of Sciences*, 108(51):20400–20403, 2011.

[26] M. A. Simon, S. J. Fusillo, K. Colman, and B. A. Trimmer. Motor patterns associated with crawling in a soft-bodied arthropod. *The Journal of Experimental Biology*, 213(13):2303–2309, 2010.

[27] M. A. Simon and B. A. Trimmer. Movement encoding by a stretch receptor in the soft-bodied caterpillar, manduca sexta. *Journal of Experimental Biology*, 212(7):1021–1031, 2009.

[28] R. E. Snodgrass. *The caterpillar and the butterfly*, volume 143:51. Smithsonian Miscellaneous Collections, 1961.

[29] Y. Tadesse, D. Moore, N. Thayer, and S. Priya. Silicone based artificial skin for humanoid facial expressions. In *The 16th International Symposium on: Smart Structures and Materials & Nondestructive Evaluation and Health Monitoring*, pages 728709–728709. International Society for Optics and Photonics, 2009.

[30] B. Trimmer and J. Issberner. Kinematics of soft-bodied, legged locomotion in *Manduca sexta* larvae. *The Biological Bulletin*, 212(2):130–142, 2007.

[31] B. A. Trimmer. New challenges in biorobotics: Incorporating soft tissue into control systems. *Applied Bionics and Biomechanics*, 5(3):119–126, 2008.

[32] L. I. van Griethuijsen and B. A. Trimmer. Kinematics of horizontal and vertical caterpillar crawling. *Journal of Experimental Biology*, 212(10):1455–1462, 2009.

[33] W. A. Woods, S. J. Fusillo, and B. A. Trimmer. Dynamic properties of a locomotory muscle of the tobacco hornworm Manduca sexta during strain cycling and simulated natural crawling. *Journal of Experimental Biology*, 211(6):873–882, 2008.

[34] Z. Zhang and M. Philen. Pressurized artificial muscles. *Journal of Intelligent Material Systems and Structures*, 23(3):255–268, 2012.

Acta Futura 6 (2013) 81-95
DOI: 10.2420/AF06.2013.81

Acta Futura

Bioinspired Air Vehicles for Mars Exploration

Hao Liu *,
Chiba University, Graduate School of Engineering, Chiba 263-8522, Japan
Shanghai Jiao Tong University and Chiba University International Cooperative Research Center (SJTU-CU ICRC), Shanghai 200240, China
Hikaru Aono,
Institute of Space and Astronautical Science / Japan Aerospace Exploration Agency (JAXA), 3-1-1 Yoshinodai, Sagamihara 252-5210, Japan
and Hiroto Tanaka
Shanghai Jiao Tong University and Chiba University International Cooperative Research Center (SJTU-CU ICRC), Chiba University, Chiba 263-8522, Japan

Abstract. In achieving missions for Mars exploration, the concept of exploration technique based on air vehicles has been not established adequately yet and is one of active research topics. Two challenges of very low atmospheric density and rough Mars terrain in the development of such air vehicles indicate that un-conventional low Reynolds number aerodynamics and flight control systems are a must to be explored and established. In this study, we classify the platforms for Mars exploration with a specific focus on the possible designs of air vehicles. We then demonstrate the prototype design of a bioinspired flapping micro air vehicle (fMAV), which is weighted 2.4 - 3.0 g, equipped with a X-type wing and a wingspan of 12 -15 cm. An integrated study of flexible wing aerodynamics and passive dynamic flight stability of the MAV is performed through a combination of flexible wing kinematics and force measurements and computational approaches. Our results show that the clap-and–fling mechanism is indeed realized by the prototype four-winged MAV and the flexible wing deformation even further enhance its effects. Moreover, an extended study on the passive dynamic flight stability of the MAV's forward flight based on a linear theory indicates that the MAV is very likely of dynamical stability even with no active feedback control system. We further discuss about the possible bioinspired designs of robust and high-capability flapping-wing platforms for Mars Exploration.

*Corresponding author e-mail: hliu@faculty.chiba-u.jp

1 Introduction

Mars has answers to many important planetary science questions. Of essential significance is the excellent preservation of the geologic record of early Mars, the period more than 3.5 billion years ago when life began on Earth. Therefore, Mars offers the opportunity to address questions about how and whether life arose elsewhere in the solar system, about processes of planetary evolution on a planet that has undergone notable changes through time, and about the potential coupling between biological and geological history [39, 1].

Successful Mars exploration by either rovers or other possible platforms with robust design is essential to achieve above goals. There are several types of platform proposed and developed for Mars exploration. Rovers, obiters, and combination of them have been well known as well as contributed to Mars exploration in the past decade [9, 29]. While the concept of exploration tech-

nique based on air vehicles has been not established adequately yet and is one of active research topics.

Micro air vehicles (MAVs) are now an active and well-integrated research area, attracting participation from a wide range of talents. With a maximal dimension of 15 cm and nominal flight speeds of around 10 m/s, MAVs are desired to be capable of performing missions such as environmental monitoring, surveillance, and rescue in natural disasters. MAVs normally operate in a Reynolds number regime of 10^4 - 10^5 or lower, in which most natural flyers including insects, bats, and birds, and the prominent feature of MAVs' aerodynamics, in general, is characterized by large-scale vortex flow structure and hence highly unsteady [43]. Furthermore, due to their light-weight and low flight speed and the interactions between moving wings and those vortices, the MAVs' flight characteristics are substantially affected by environmental factors such as wind gust, which may lower the flight stability and hence makes the flight control a very challenging problem. Like natural flyers, the wing structures of MAVs are often flexible and tend to deform during flight. Consequently, the aero/fluid and structural dynamics of these flyers are closely linked to each other, making the entire flight vehicle difficult to analyze [41].

In the past decade, there has been a remarkable increasing in research and development of the MAVs and numerous vehicle concepts, including fixed-wing, rotary-wing, and flapping-wing, have been proposed [31, 35, 36, 46, 40]. As a vehicle becomes a size smaller than 15 cm normally corresponding with a Reynolds number less than 10^5, the fixed wing designs encounter fundamental challenges in low lift-to-drag ratio and unfavorable flight control. There are merits and challenges associated with rotary and flapping wing designs with a smaller size and at lower Reynolds numbers. All the successful flapping-wing MAVs developed till now have flexible and light wings as observed in biological flyers in nature [54], which indicates that wing flexibility is likely to have a significant influence on the resulting aerodynamics as well as the flight stability [41, 40, 55, 30]. Therefore, flapping flexible wing aerodynamics is of great importance not only in uncovering the novel mechanisms in insect and bird flights but also in designing efficient flapping flight vehicles.

In this paper, we first give a review on the platforms designed for Mars exploration, which have been proposed and developed in the past decade involving rovers, obiters, and aero vehicles. In particular, we highlight several concepts and platforms for atmospheric exploration on Mars including fixed-wing, flapping-wing, rotating-wing, and so forth. Then, after giving an overview of the state-of-art of flapping MAVs we describe in detail a recently developed, bio-inspired flapping-wing MAV with a specific focus on a systematic analysis of the flexible wing aerodynamics and passive forward-flight stability. Specific attention is paid on a so-called 'clap and fling' mechanism which is achieved by a crank system, not only because such mechanism is observed in insect flight and thought to enhance the aerodynamic force generation [51], but also because such physical interaction can affect the in-flight deformation of flexible flapping wing and hence aerodynamic performance. Furthermore, we discuss about the insect flight-based possible implication for developing robust and high-capability flapping-wing platforms for Mars exploration.

2 Platforms Designed for Mars Exploration

2.1 Mars Exploration

Recently, a workshop called "Concepts and Approaches for Mars Exploration" has been held in U.S.A. [39, 1] and discussion at the workshop focused on the development of high-pay-off missions potentially beginning with the 2018 launch opportunity, which are responsive to the scientific goals articulated by the National Research Council Planetary Science Decadal Survey [3], to the Mars Exploration Program Analysis Group Goals, and to the US President's challenge of sending humans to the vicinity of Mars in the decade of the 2030s. According to the latest version of the document regarding Science Goals, Objectives, Investigations, and Priorities in Mars exploration [4] four main goals are follows:

1. Determine if life ever arose on Mars – Does life exist, or did it exist, elsewhere in the universe? This is perhaps one of the most compelling questions in science, and Mars is the most promising and accessible place to begin the search;

2. Understand the processes and history of the climate on Mars – Climate and atmospheric studies are key to understanding how the planet may have been suited for life and how major parts of the surface have been shaped, and are directly relevant to our understanding of the past, present, and future climate on Earth. Additionally, characterizing the environment of Mars is also necessary for

 DOI: 10.2420/AF06.2013.81

Figure 1. *Mars exploration programs in NASA and ESA. Top: NASA's Mars Exploration Program [29]. Bottom: ESA's Mars Missions [50].*

the safe implementation of future robotic and human spacecraft missions to the planet;

3. Determine the evolution of the surface and interior of Mars;

4. Prepare for human exploration.

Therefore, successful Mars exploration by either rovers or other possible platforms with robust design is essential to achieve above goals.

2.2 Type of Platform Designed for Mars Exploration

There are several types of platform proposed and developed for Mars exploration. Rovers, obiters, and combination of them have been well known as well as contributed to Mars exploration in the past decade [9, 29]. While the concept of exploration technique based on air vehicles has been not established adequately yet and is one of active research topics. Following are brief summaries of platforms designed for Mars exploration.

Rover:

Ground rovers [9, 29, 50], for example, Curiosity, have significantly contributed to objectives and goals presented in previous section (also see Figure 1). Recently, the European Space Agency (ESA) has presented a plan to search for signs of past and present life on Mars using a rover on 2018 (see Figure 1). Some of limitations of ground rovers are limited searchable areas and speed. To overcome those limitations, a new concept of rover [5] (see Figure 2) and rover-based Mars exploration concepts are proposed and studied.

Orbiter:

Orbiters, for instance, Mars Reconnaissance Orbiter, have contributed to understand the processes and history of the climate on Mars. NASA and ESA has a

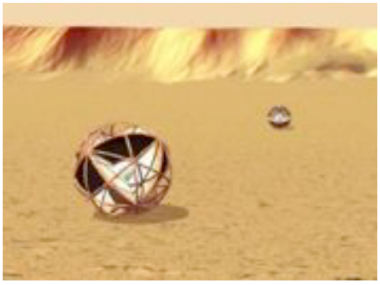

Figure 2. *Mars tumbleweeds rover [5].*

plan to study Martian atmospheric trace gases and their sources and conduct surface environment measurement on 2014 (Mars Atmosphere and Volatile EvolutioN: MAVEN) and 2016 (Exobiology on Mars: ExoMars), respectively (see Figure 1). Generally, the orbiter is capable of sweeping the planet, but suffers from low spatial resolution and drastic diminution of the strength of radar return signal strength with range that falls with the fourth power of the distance.

Aero vehicles:

As mentioned previously, one of main goals in Mars exploration is to search for microclimates and study lower atmosphere climate processes (i.e. atmospheric exploration on Mars). This goal can easily be addressed by in situ atmospheric measurements performed by an aerial vehicle. Moreover, Mars explorations by collaborative platform of rovers and aero vehicles would have far greater capability than either in isolation.

An aircraft flying at an attitude of 2 kilometres has an eight order of magnitude advantage in return signal strength compared to that obtained by an orbiter operating 200 kilometres. The aircraft also would have a two order of magnitude advantage in spatial resolution.

Following challenges are in development of air vehicles for Mars exploration, especially in aerodynamic design point of view:

1. Very low atmospheric density: This causes all-conventional aircraft designs encounter the same limitation. The aircraft must be fast to generate sufficient lift. Also the aircraft will fly under low Reynolds numbers condition.

2. Rough Mars terrain: This would make it virtually impossible for conventional aircraft to successfully land and take off again.

Several concepts and platforms for atmospheric exploration on Mars have been developed and studied including fixed-wing, flapping-wing, rotating-wing, and so forth (see Figure 3). Here we highlight some interesting one as follows:

1) Fixed-wing 1-1) Aerial Regional-scale Environmental Surveyor (ARES) [20, 45, 19, 57, 38, 22, 24]. ARES is an instrumented, rocket-powered, well-tested robotic airplane platform (see Figure 3A-1). It flies between one to two kilometres to collect and transmit previously unobtainable high spatial measurements relevant to the NASA Mars Exploration Program and the exploration of Mars by humans. ARES has been selected to proceed into Phase A as part of the Mars Scout Mission competition in 2002 and receiving a second Category 1 science rating during the Mars Scout competition in 2006. After that the ARES mission concept has continued to mature technologically and scientifically, adjusting to reflect the current exploration goals for assessment of human exploration at Mars and enabling technologies for future missions.

1-2) Cannon Assisted Flying Exploration (CAFE) [13]. CAFE is a concept for Mars atmosphere and surface exploration that was proposed to deploy compressed air cannon on the surface of Mars that launches aerial exploration vehicles (Figure 3A-2).

1-3) Mars Gas Hopper [37, 61, 60, 59]. Mars gashopper is a novel concept for propulsion of a robust Mars flight and surface exploration vehicle that utilizes indigenous CO_2 propellant to enable greatly enhanced mobility (Figure 3A-3).

2) Flapping-wing Flapping wing propulsion is other possible propulsive system. High lift-generating capability under low Reynolds number flight conditions provides an innovative solution to the dilemma of atmospheric flight on Mars [7, 10, 11, 8].

The concept of entomopter [7, 10, 8] and Solid State Aircraft [11, 8] (see Figure 3B) has been proposed as an alternative to the need to fly very fast at Mars. This flyer will follow vortex-based lift enhancements that insects employ on Earth [42]. Such vortex generation and shedding produces higher wing lift coefficients, on the order of 5 compared to maximum lift coefficients of 1 to 1.2 for conventional airfoils. This high lift-generating capability allows insects to fly, hover and maneuver as they do. Wing-flapping drones would need to account for Mars's low air pressure (much more difficult than on Earth) and operate in a very low Reynolds number regime. In addition, there are practical size limitations for vehicles that could be deployed on mis-

 DOI: 10.2420/AF06.2013.81

sions launched from Earth. Because of the low atmospheric density, a wingspan on the order of 1 meter would be in the same flight Reynolds number regime, as are more insects on Earth. The entomopter does not rely on a purely biomimetic paradigm for flight; it goes beyond biomimetics by using a resonantly-tuned circulation controlled pair of autonomically-beating wings, that enable slow flight and landing as well as higher maneuverability than can be achieved with a fixed-wing vehicle [7].

3) Rotating-wing type (see Figure 3C) Rotor craft-based atmosphere exploration also leads to extending the exploration range of surface rovers since the rotorcraft can act as their "eye".

4) Freefalling type [48, 49] Another unique concept is a maple seed-inspired Samara-styled [49] miniature air vehicle that designed to conduct science surveys as it descends. It carries only a science sensor and a communications package to telemeter data back to its deployment module (see Figure 3D).

5) Balloon [53, 17] Balloons offer an excellent vantage point for scientific observations over regional scales at altitudes lower than orbit but higher than the surface. Terrestrial helium superpressure balloons have achieved over two year flight durations and the expectation is that this technology could yield at least multi-month flights at Mars, enabling converge over ground tracks of thousands of kilometres [17]. Recently, a prototype 12-meter diameter Mars superpressure balloon successfully flying in the stratosphere of Earth at 30-kilometer altitude, where the atmospheric density is comparable to that of Mars at altitudes of a few kilometres (see Figure 3E). A superpressure balloon at Mars would float at an altitude of approximately 5 – 6 kilometres.

3 Bioinspired Flapping-Wing Ornithopter

3.1 An Overview on Flapping MAVs

Flapping wing propulsion, as seen in bio-flyers of insects and birds, posses high lift-generating capability under low Reynolds number flight conditions and therefore may provide an innovative solution to the dilemma of atmospheric flight on Mars. Sightorson et al. [44] showed that the flapping wing vehicle is less sensitive to velocity perturbations in all aerodynamic forces and moments than the rotorcraft, except for the forward/backward direction force.

Two key factors in designing MAVs are the wing size and the gross weight. Allowable mass restricts the composition of the actuators, power source, or materials, constraining the wing kinematic, frequency, size, or available aerodynamics forces. Therefore, one of the biggest challenges in building flapping MAVs, in particular for insect-sized or smaller one, is realizing wing kinematics within the severely restricted mass [52]. Here we give an overview on the existing flapping MAVs by their wing sizes and total masses (see Figure 4), as well as the technologies employed.

The upper limit of the wing size is determined not only by aerodynamics but also by available material for the wing. Since flapping motion causes not only aerodynamic force but also inertial force due to the wing mass, the wing base and frame structures should possess enough strength to tolerate the oscillating load and bending moments. In other words, high stiffness-weight ratio is desired for the material of flapping wings in order to reduce the inertia force and resultant bending moment.

In the past decade, most flapping MAVs have been developed with a wingspan ranging from 100 to 10^{-2} m and a mass of 100 kg to 10^{-2} kg, [11, 34, 12]. Electric motors and conventional gear-crank mechanisms are often used to create wing motions. For relatively bigger MAVs [21, 47] the payload can afford some avionics such as vision systems or autonomous control systems; and by processing the captured images with a ground station, autonomous obstacle avoidance can be realized. In these electric ornithopters, the active wing motion is often 1-DOF (degree of freedom) flapping unlike birds or insects demonstrating not only flapping motion but also feathering and lead-lag motions. Their flight maneuver is realized with a rudder or elevators of the tail wing like conventional fixed-wing aircrafts, or a tail rotor like helicopters. A few exceptional ornithopters, however, are able to actively feather the main flapping wings and achieve maneuvering flight without ladders or elevators [2], in which multi servo actuators are employed for additional DOF of wing or body motions.

Recently a tiny fly-like MAV [27] with a wingspan of 30 mm, a weight of 80-milligram and a flapping frequency of 120 Hz is developed, which is equipped with high-power-density piezoelectric flight muscles and built by means of a manufacturing methodology capable of rapidly prototyping articulated, flexure-based sub-millimeter mechanisms. With a modular approach to flight control that relies on limited information about the robot's dynamics, the MAV can achieve a tethered but unconstrained stable hovering and basic controlled flight maneuvers.

DOI: 10.2420/AF06.2013.81

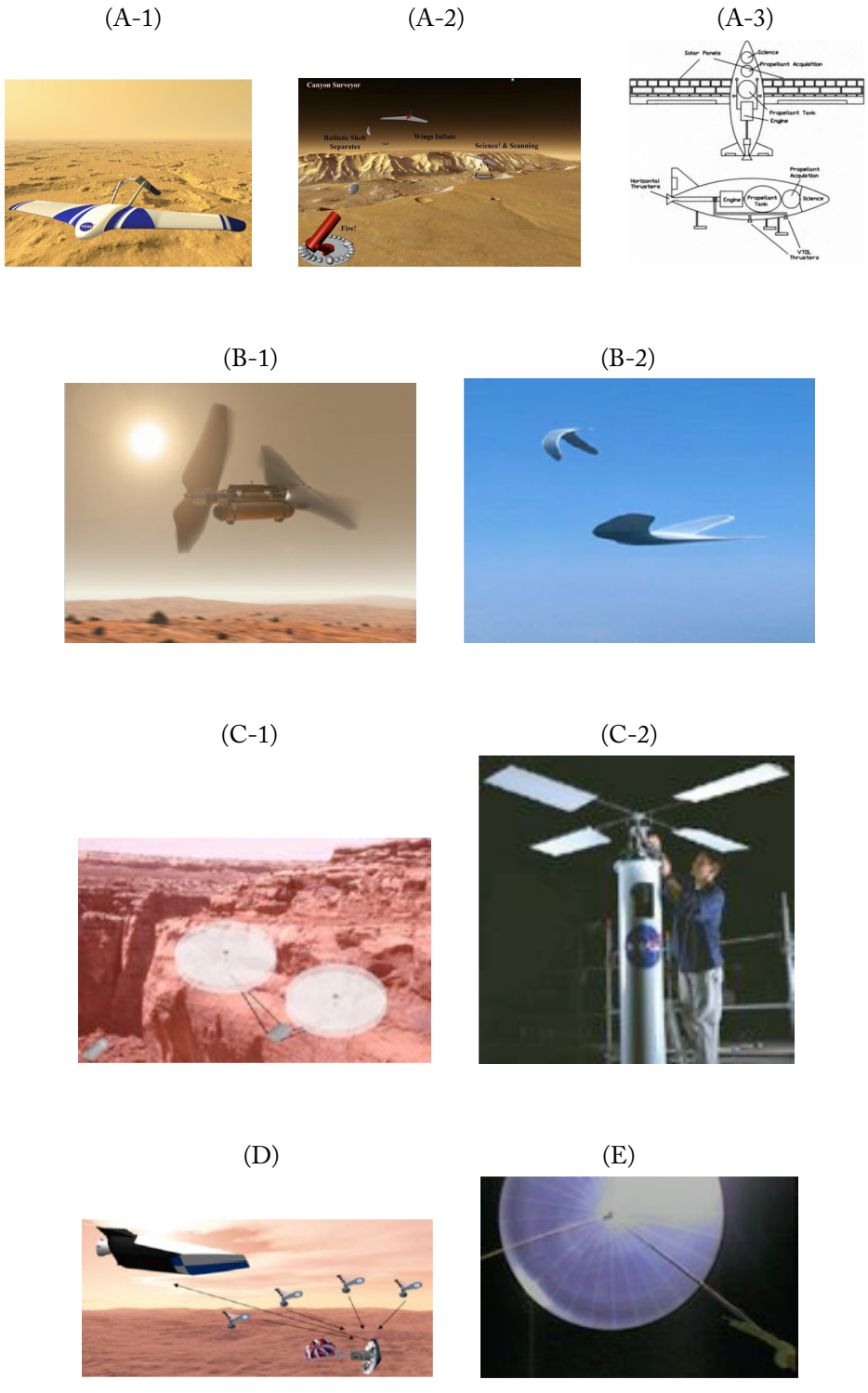

Figure 3. *Concepts for Mars Exploration with Aerial Vehicles. (A-1) ARES [19, 38, 57, 45], (A-2) CAFE [22], (A-3) Mars gashopper airplane concept [24, 61, 60, 59], (B-1) Entomopter [7, 10, 8], (B-2) Wing-flapping drone [11, 8], (C-1) Mars hovercraft [56, 18, 58], (C-2) Mars VTOL UAC rotor [23], (D) Aerocoasting [48], (E) Mars balloon [53]*

DOI: 10.2420/AF06.2013.81

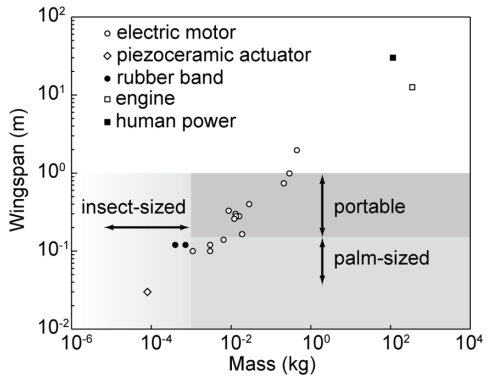

FIGURE 4. *Clarification of flaping wing aerial robots in terms of mass and wingspan.*

All of the successful flapping-wing MAVs developed up [21, 47] to this point have flexible and light wings such as those observed in natural biological flyers [54], which indicates that wing flexibility is likely to have a significant influence on the resulting aerodynamics, as well as the flight stability [55, 30, 33, 40]. In a sense, flapping flexible-wing aerodynamics is of great importance not only in uncovering the novel mechanisms of insect and bird flight, but also in designing efficient flapping flight vehicles. In the following, we present a systematic study of the aerodynamics and flight stability associated with a recently developed bio-inspired flapping wing MAV [34]. This prototype MAV, has four flexible wings and employs the clap and fling mechanism, which is achieved by a prototype crank system. The clap and fling mechanism is utilized here not only because it is commonly observed in insect flight and thought to be capable of enhancing the aerodynamic force generation [51], but also because such physical interaction can affect the in-flight deformation of flexible flapping wings and hence aerodynamic performance.

3.2 Clap-and-Fling Mechanism in Insect Flight

Clap-and-fling is a lift enhancement mechanism, which was first discovered in insect flight by Weis-Fogh [51]. This relates to the wing-wing interaction phenomenon, which takes place at dorsal stroke reversal (see Figure 5). During the clap phase, the leading edges of the paired wings approach each other and the wing rotation (pronation) about the leading edges occurs until the v-shaped gap between the wings disappears. In the fling phase, the wings rotate about their trailing edges forming a gap in between. Investigations on insects and birds showed that as well as being used continuously during the flight, some species utilize this mechanism for a limited time in order to generate extra lift, especially while carrying loads or during the take-off phase.

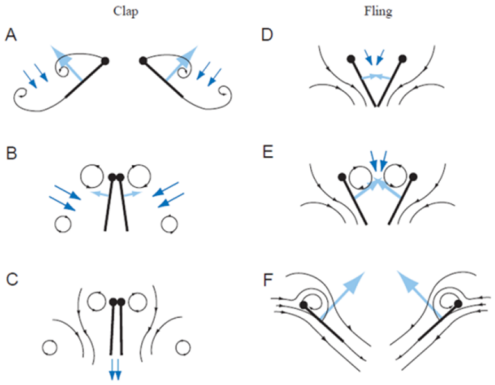

FIGURE 5. *Schematic of the clap-and-fling mechanism.*

3.3 A Bioinspired Flapping-wing MAV

Inspired by the clap-and-fling we developed a prototype flapping-wing micro air vehicle, which as illustrated in Figure 6 is equipped with a X-type wing.

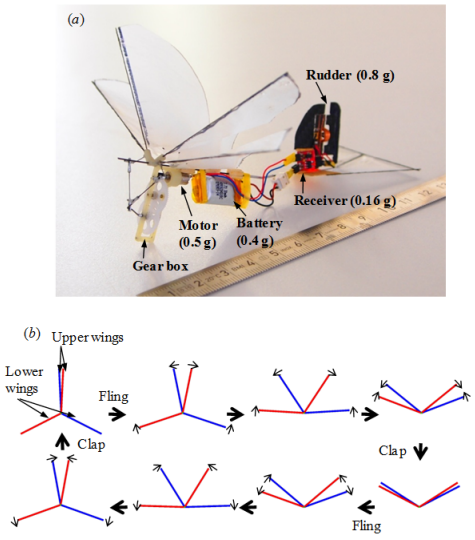

FIGURE 6. *(a) A prototype flapping micro air vehicle (MAV). (b) Schematic of wing kinematics in an X-type wing MAV (viewed from front side of the air vehicle).*

The X-type wing is made of two pairs of wings and achieves three times clap-and-fling at the side and at the top in a wing beat. The wingspan is designed to be around 12 cm with a wing length of 60 mm and a wing chord length of 30 mm at wing base, of a size as observed in hawkmoth and hummingbird. The wing has a semi-elliptic planform, which is made of the polyethylene filmwith a thickness of 0.3 mm and the carbon rod with a diameter of 0.3 mm at leading edge. The mean chord length is calculated to be 23.6 mm. The gearbox is fabricated by cutting the acrylonitrile-butadiene-styrene (ABS) resin so as to ensure a nice match among the motor (MK04S-10, DIDEL), gears and wing hinges. With a speed-reduction ratio of 60/12 teeth of the idler gear, the crank is mounted to link and actuate the two pairs of wings on the 60 teeth final gear. The gearbox system, the crank and the wings are connected by a carbon rod of a diameter of 0.5 mm with the tail, the rudder, the receiver and the remote-controller. The rudder is controlled by a magnetic actuator (Hinge Act, PLANTRACO) so as to move laterally, which is weighted 0.23 g and can provide sufficient control power. The remote-controller with infrared ray offers two channels to control both the motor frequency and the rudder angle. The rechargeable Lithium Polymer battery (FR30SC, FULLRIVER) is utilized as the power source. With all the parts mounted together our flapping MAV weighs less than 3 g in toto and is able to fly with time duration up to 6 minutes, a maximum height over 10 meters and a region of 20 meters by 20 meters. More details can be found in [34].

3.4 Flapping Wing Aerodynamics

To investigate the flexible wing aerodynamics, the high-speed camera (with a frame rate of 1000 per second) filming system is utilized to measure the flexible wing kinematics. Given that the flapping frequency of the MAV normally varies over a range of 20 Hz to 35 Hz, the recorded image sequences are able to provide sufficient temporal resolution for the flexible wing kinematics. The recorded image sequences are downloaded to a computer and the three-dimensional coordinates of these marked points are reconstructed by utilizing the commercial software, DippMotion (Ditect Corp.).

The kinematic model of the MAV's wing is constructed by interpolating the reconstructed coordinates of the markers on the flapping wings. The displacements u(t, x, y) at some point of the wing (x, y) are interpolated by using a function of Fourier series, such as:

$$u(t,x,y) = \sum_{i=0}^{N_x}\sum_{m=0}^{N_y}\sum_{n=0}^{N} (\alpha(l,m,n)x^l y^m \cos(n\omega t) + \beta(l,m,n)x^l y^m \sin(n\omega t)) \quad (1)$$

where terms α and β are derived by the least square method. The wing surface grids are translated by u and the grid is regenerated on the basis of the hyperbolic grid generation scheme.

In order to evaluate the aerodynamic performance of the flexible wing MAV, we use a biology-inspired, dynamic flight simulator [32, 34, 6, 25, 26, 28, 32], which is designed to integrate the modelling of realistic wing-body morphology, realistic flapping-wing and body kinematics, and unsteady aerodynamics in biological flight. A realistic morphological model of the MAV's wing (Figure 6) is constructed by tracing the outline of the wing planform. A uniform thickness is taken but with elliptic smoothing at the leading and trailing edge as well as at the tip. To deal with the complexity of the wing deformation and wing kinematics we use a multi-blocked overset grid method, in which the wing grid is clustered to the wing surface with the minimum grid spacing adjacent to the wing surface controlled by the Reynolds number. The simulation is done as depicted in Figure 6 under the assumption that the left and right wings move and deform symmetrically.

The computational study is performed under the assumption of hovering flight condition. Given the mean chord length c_m as the reference length Lref, the mean wing tip velocity in hovering flight as the reference velocity Uref, which is proportional to $U_{ref} = \omega R$, where R is the wing length and ω is the mean angular velocity of the wing ($\omega = 2\Phi f$, where Φ is the wing beat amplitude and f is the flapping frequency), the Reynolds number in hovering flight can be reformed as

$$Re = \frac{U_{ref} L_{ref}}{\nu} = \frac{2\Phi f R c_m}{\nu} = \frac{\Phi f R^2}{\nu}\left(\frac{4}{AR}\right) \quad (2)$$

where the aspect ratio AR is in a form of $AR = (2R)^2/S$, with a wing area of $S = 2Rc_m$. Note that the Reynolds number here is proportional to the wing beat amplitude, Φ, the flapping frequency, f, a square of the wing length, R^2, but proportional inversely to the aspect ratio of the wing, AR. The reduced frequency that normally characterizing rotational versus translational speeds, is defined in case of hovering flights, such

 DOI: 10.2420/AF06.2013.81

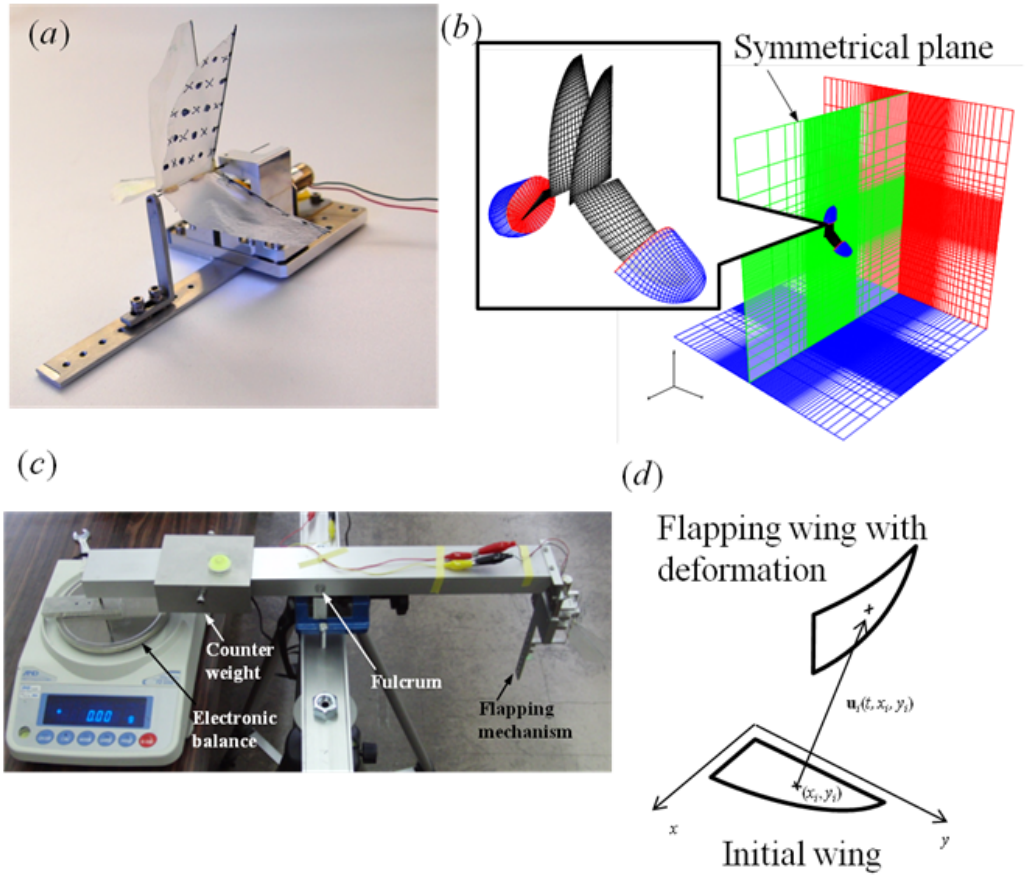

Figure 7. *(a) A mechanical flapping-wing MAV model. (b) A computational fluid dynamic model of MAV wings and a multi-block grid system. (c) Force measurement system. (d) Definition of displacements on wing surface.*

as:

$$k = \frac{\pi f L_{ref}}{U_{ref}} = \frac{\pi c_m}{2\Phi R} = \frac{\pi}{\Phi AR} \qquad (3)$$

Note that the reduced frequency k is proportional inversely to the beat amplitude Φ and the aspect ratio AR of the wing. According to the measured data of the MAV's mechanical model (c_m = 23.6 mm, R = 60 mm, Φ = 1 rad, f = 18.5 s^{-1}, $= 1.5 \times 10^{-5}$ m^2/s), Re and k are calculated to be about 3400 and 0.59, respectively.

The flapping flexible wing aerodynamics is evaluated by both visualized near-and far-field flow structures around the flapping wings and integrated vertical and horizontal forces acting upon the MAV. As shown in Figure 8 the computed results show that a leading edge vortex (LEV) and hence a strong negative pressure region are generated on upper and lower wings during both of the half stroke. As observed in insect flapping flight [25], this LEV likely plays a key role in the lift and/or thrust force-production in the MAV flight. The vortex rings that are formed from the LEV, the tip vortex (TV) and the trailing edge vortex (TEV) are also observed, showing a similar pattern with those of insect flight [26]. Obviously, the strong negative pressure regions are detected between the upper right and left wings, which is induced by the clap and fling mechanism. In addition, the mean aerodynamic force is calculated to be 23.3 mN, which is in reasonable agreement with the measurement of a value of 26.46 mN. The mean force components of Fx and Fz generated by the upper wing are -4.2 mN and 0.2 mN, and, by the lower wing are -3.8 and 2.0 mN, respectively.

Wing deformations due to wing flexibility likely af-

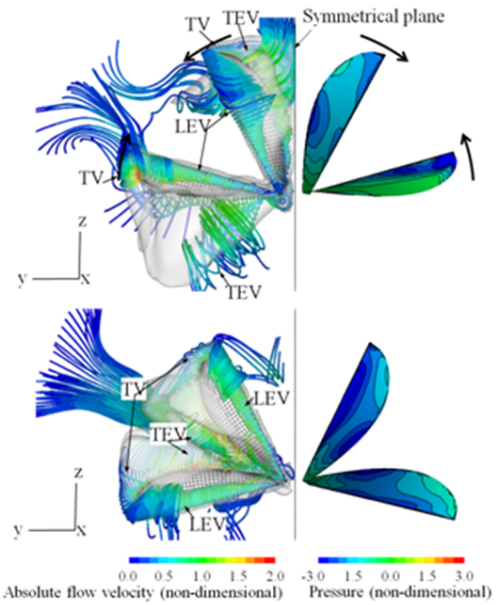

Figure 8. *Instantaneous streamlines, iso-vorticity surface and pressure contours on upper surface of flapping wings at each half stroke.*

fects also the clap-and-fling mechanism. In the present study, we find that with the wing clap the rotational phase of both upper and lower wings at stroke reversal is nearly symmetric, while without the wing clap the rotation of the lower wing obviously exhibits a phase delay at stroke reversal. This implies that the clap and fling of a flexible wing can adjust the feathering angle near the wing tip at stroke reversal so as to avoid some unfavorable phase delay during wing rotation. As a result, the fling-induced additional circulation and the passive deformation-based flexible wing kinematics in total are very likely responsible for augmenting the aerodynamic force production effectively in the present four-winged MAV.

3.5 Passive Dynamic Flight Stability

A Linear Theory:

Aiming at analyzing the passive dynamic flight stability of insect flapping flight, we have recently developed a computational approach by introducing a linear and a nonlinear theory into the biology-inspired, dynamic flight simulator [14, 15, 16]. In this study, the linear theory is employed for the analysis of the passive dynamic stability in MAV's forward flight. With the 'rigid body' assumption that the MAV body does not deform and hence has only 6 degrees of freedom (DoFs) the flapping wing effects on the flight system can be represented by the wingbeat-cycle-average aerodynamic and inertial forces and moments. Furthermore, the MAV's motion is assumed to consist of small disturbances from the equilibrium condition. On the basis of the linearized equations of motion, the longitudinal dynamic flight stability can be considered with 3 DoFs: the forward, the dorso-ventral and the pitching disturbances.

The equations of motion may be then linearized by approximating the body's motion as a series of small disturbance from a steady, symmetric reference flight condition, such that:

$$\delta\dot{u} = H_u\delta u/m + H_w\delta w/m + H_q\delta q/m - g\delta\theta \quad (4)$$

$$\delta\dot{w} = V_u\delta u/m + V_w\delta w/m + V_q\delta q/m \quad (5)$$

$$\delta\dot{q} = M_u\delta u/I_y + M_w\delta w/I_y + M_q\delta q/I_y \quad (6)$$

$$\delta\dot{\theta} = \delta q \quad (7)$$

where $H_u, H_w, H_q, V_u, V_w, V_q, M_u, M_w$, and M_q are the aerodynamic derivatives (H and V are the x- and z-components of the total aerodynamic forces, respectively, and M is the pitching moment); m is the mass of the insect; g is the gravitational acceleration; I_y is the pitching moment of inertia about y axis; '.' represents differentiation with respect to time (t); the symbol δ denotes a small disturbance quantity.

Then the non-dimensional forms of Eqs 4-7 in vector form can be expressed as:

$$\delta\dot{\mathbf{x}} = \mathbf{A}\delta\mathbf{x}(t) \quad (8)$$

, where $\delta\mathbf{x}$ denotes the non-dimensional longitudinal state vector of $\delta u^+, \delta v^+, \delta q^+, \delta\theta^+$. The constant system matrix $\mathbf{A}$ is given by

$$\mathbf{A} = \begin{bmatrix} X_u/m & X_w/m & X_q/m & g \\ Z_u/m & Z_w/m & Z_q/m & 0 \\ M_u/I_x & M_w/I_y & M_q/I_z & 0 \\ 0 & 0 & 1 & 0 \end{bmatrix} \quad (9)$$

, where $X_u, X_w, X_q, Z_u, Z_w, Z_q, M_u, M_w$, and M_q are the aerodynamic derivatives, which are calculated from the previous results of the solutions to the Navier-Stokes equations. Using the technique of eigenvalue and eigenvector analysis, one can estimate the stability of system under a certain disturbance condition by

 DOI: 10.2420/AF06.2013.81

the sign of the real part of the eigenvalue(*). If the real part is positive, the system is dynamically unstable; if the real part is negative, the system is dynamically stable [14, 15, 16].

Forward Flight Stability:

The disturbance from outside that the MAV undergoes is treated as the relative motion of the MAV from a reference flight condition (forward flight). And the three components of the disturbance, namely, the elevation in x-and z-axis and the pitching movement can be transformed to a horizontal velocity u, a vertical velocity w and a pitching angular velocity q about the centre of mass, respectively. In order to estimate the aerodynamic derivatives, we consider three disturbance conditions for the three state variables (u, w, q) separately.

Under the equilibrium condition (the reference flight condition), the MAV is observed to perform a forward flight at a speed of 1 m/s with a body angle of 61 degrees. As shown in Figure 9, the disturbances of horizontal, vertical and pitching angular velocities vary in a range of $[-0.05, 0.05]$. The vertical axis shows the difference between the disturbance and equilibrium. As observed in our previous studies of hawkmoth hovering flight [14, 15, 16], all the three curves show approximately linear variation. Accordingly the aerodynamic derivatives, $H_u^+, H_w^+, H_q^+, V_u^+, V_w^+, V_q^+, M_u^+, M_w^+$, and M_q^+ can be calculated by taking the local tangents of the curves as given in Table 1.

Based on the computed aerodynamic derivatives, the system matrix is obtained, which results in four eigenvalues $\lambda_1, \lambda_2, \lambda_3$ and λ_4 with a pair of complex $\lambda_{1,2}$ as shown in Table 2. These four eigenvalues represent three natural modes: a stable oscillatory motion and two subsidence modes. The state variables can be then obtained which correspond to the three eigenvectors (Table 3); these eigenvectors can be normalized so as to define a pitch-attitude disturbance $\delta\theta^+$ of 1 rad at a zero phase angle.

The eigenvalue of $\lambda_{1,2} = -0.275 \pm 0.436i$ corresponds with the stable oscillatory mode, which results in the time being taken to half the disturbance values of approximately $t_{half} = 2.52$ periods, which indicates that the MAV takes approximately two wing beats to half the initial disturbance values. The fast subsidence mode is also stable with an eigenvalue of $\lambda_3 = -0.1655$, which results in $t_{half} = 4.19$. The slow subsidence mode, however, has a positive eigenvalue of $\lambda_3 = 0.0968$ but quite small, which leads to the time being taken to twice the disturbance values of approximately $t_{half} = 7.16$ periods, which indicates that the MAV can sustain its body attitude up to approximately seven wing beats when getting its the initial disturbance values doubled. In a word, while the initial value of the disturbance is unknown here and hence it is difficult to determine a precise timescale for the disturbance damping, the computed three eigenvalues and eigenvectors together very likely contribute to a dynamically stable one.

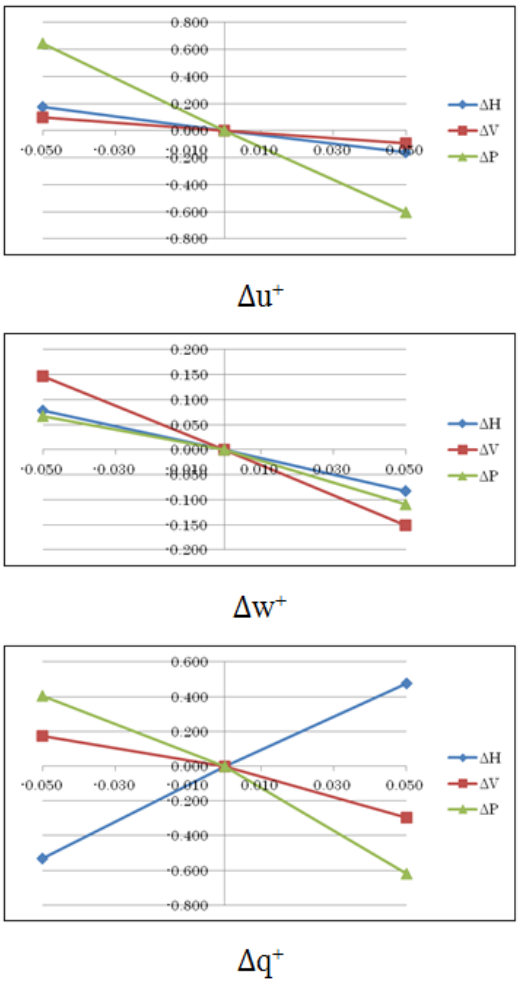

Figure 9. *Horizontal (H) and vertical (V) forces and pitching moments (M) under disturbances of horizontal, vertical and pitching angular velocities.*

H^+_u	V^+_u	M^+_u	H^+_w	V^+_w	M^+_w	H^+_q	V^+_q	M^+_q	m^+	g^+	I^+_{yy}
-3.31	-1.92	-12.49	-1.61	-2.98	-1.76	10.05	-4.70	-10.22	18.32	0.09	37.03

Table 1. *Non-dimensional aerodynamic derivatives.*

$\lambda_{1,2}$	λ_3	λ_4
-0.275±0.436i	-0.1655	0.0968

Table 2. *Eigenvalues of the system matrix*

3.6 Implication for Flapping-wing Vehicles for Mars Exploration

While ground exploration rovers would be main actors in the Mars sample return campaign during the coming decade, in order to conduct more efficient and robust rover-based atmospheric exploration on Mars, development of aerial platforms with flapping / rotating wing-based propulsions are needed. This would further contribute to the safe implementation of future robotic and human spacecraft missions to the plan.

With consideration of two major challenges of very low atmospheric density and rough Mars terrain in development of air vehicles for Mars exploration, we need to explore un-conventional aerodynamics and flight control systems, which should be specified for the flapping /rotating wing ornithopters workable on Mars. Luckily, we can learn and get hints from nature: the low Reynolds number aerodynamic designs of small birds, bats, and insects. Aerodynamics of such natural bioflyers, with the maximum dimension of O(10) centimeters or smaller, and weight of O(10) grams or lighter, intersect with some of the richest problems in aerospace engineering, in which highly unsteady three-dimensional boundary, large-scale vortical flows, unsteady and uncertain flight environment, aeroelasticity associated with anisotropic wing structure, and adaptive control are just a few examples of these problems. Such flyers are significantly more sensitive to wind gust and flight obstacles than larger flyers of passenger aircraft; their agility and spectacular flight performance, owing to their flexible, deformable wing structures as well as outstanding wing, tail, and body coordination, is achieved much better than any state-of-art man-made flight vehicles.

Therefore, a bioinspired flapping-wing platform for Mars exploration, if is used to accomplish a real mission, must have high flight capabilities as: 1) Flights under a wide range of forward velocities including hovering; 2) Flights with high acceleration and angular acceleration; and 3) Flights that are very robust to wind gusts. And such air vehicles need to have the abilities of 1) Large and quick control force/moment; 2) Small variations of aerodynamic force/moment when wind gusts are encountered; and 3) Sensors and actuators with short time-delay and high accuracy.

4 Conclusion

In this paper we have given a review on the platforms designed for Mars exploration involving rovers, obiters, and aero vehicles. Specifically, we have discussed about several concepts and platforms for atmospheric exploration on Mars including fixed-wing, flapping-wing, rotating-wing, and so forth and accordingly would suggest that conducting more efficient and robust atmospheric exploration on Mars does need development of aerial platforms with flapping/rotating wing-based propulsions. Two major challenges of very low atmospheric density and rough Mars terrain in development of air vehicles for Mars exploration indicate that unconventional aerodynamics and flight control systems should be explored and specified for the flapping /rotating wing ornithopters. We may not be able to discover a perfect design from natural flyers of insects, birds and bats but we can definitely get inspiration from such smart bioflyers, which achieve remarkable performance in the similar low Reynolds number regime.

To provide with a prototype concept and platform of bioinspired flapping-wing MAVs, we have demonstrated a recently developed, flapping-wing MAV with a specific focus on a systematic analysis of the flexible wing aerodynamics and passive forward-flight stability. Our aerodynamic analyses have thereby given a comprehensive understanding of the aerodynamic effects based on the clap and fling mechanism on the four-winged flapping mechanism, indicating that the clap and fling mechanism observed in insect and bird flights is indeed utilized by the X-type wing MAV. Furthermore, the simulation-based analyses of the longitudinal passive dynamic stability of the four-winged MAV in for-

 DOI: 10.2420/AF06.2013.81

	Δu^+	Phase angle	Δw^+	Phase angle	Δq^+	Phase angle	$\Delta \theta^+$	Phase angle
Stable oscillatory	0.701	29.5°	0.329	168°	0.516	122°	1.0	0°
Fast subsidence	0.346	0°	2.065	180°	0.165	180°	1.0	0°
Slow subsidence	0.099	180°	0.056	180°	0.097	0°	1.0	0°

Table 3. *Magnitudes and phase angles of each of three eigenvectors*

ward flight, though is conducted by means of a linear theory based on the eigenvalue analysis, shows that this flapping-wing MAV is likely capable to realize a dynamically stable forward flight under various disturbance conditions.

Acknowledgments

The present work was partly supported by a PRESTO/JST (Japan Science and Technology Agency) and the Grant-in-Aid for Scientific Research of No. 18656056, No. 18100002 and No. 24120007.

References

[1] Mars concepts 2012. `http://www.lpi.usra.edu/meetings/marsconcepts2012/`.

[2] Smartbird. `http://www.festo.com/cms/en_corp/11369.htm`.

[3] The national research council of the national academies, vision and voyages for planetary science in the decade 2013-2022. the Planetary Science Decadal Survey, 2011.

[4] Mars exploration program analysis group (mepag): Mars scientific goals, objectives, investigations and priorities, 2012.

[5] J. Antol and G. Hajos. A new paradigm for planetary exploration – the mars tumbleweed rover –. Concepts and Approaches for Mars Exploration, 2012.

[6] H. Aono, F. Liang, and H. Liu. Near- and far-field aerodynamics in insect hovering flight: an integrated computational study. *J. Exp. Biol.*, 211:239–57, 2008.

[7] Y. Bar-Cohen, editor. *Biomimetics: Nature-based Innovation*. CRC Press, Taylor and Francis Group, 2011.

[8] Y. Bar-Cohen, A. Colozza, M. Badescu, S. Sherrit, and X. Bao. Biomimetic flying swarm of entomopters for mars extreme terrain science investigations. Concepts and Approaches for Mars Exploration, 2012.

[9] J. Boyd and G. Bugos. Mars explorations: Contributions of nasa ames research center. AIAA-2012-5313, 2012.

[10] A. Colozza et al. Planetary exploration using biomimetic – an entomopter for flight on mars, phase ii. Project NAS5-98051, 2002.

[11] A. Colozza et al. Solid state aircraft concept overview. In *NASA/DoD Conference on Evolvable Hardware*, 2004.

[12] G. de Croon, M. Groen, C. D. Wagter, B. Remes, R. Ruijsink, and B. van Oudheusden. Design, aerodynamics and autonomy of the delfly. *Bioinspiration and Biomimetics*, 7, 2012.

[13] J. Denhar, D. Justin, L. Petrilli, and S. Webb. Maris cannon assisted flying exploration (cafe). Concepts and Approaches for Mars Exploration, 2012.

[14] N. Gao, H. Aono, and H. Liu. A numerical analysis of dynamic flight stability of hawkmoth hovering. *Journal of Biomechanical Science and Engineering*, 4(1):105–116, 2009.

[15] N. Gao, H. Aono, and H. Liu. Perturbation analysis of 6dof flight dynamics and passive dynamic stability of hovering fruitfly drosophila melanogaster. *Journal of Theoretical Biology*, 2010.

[16] N. Gao and H. Liu. A numerical analysis of dynamic flight stability of hawkmoth hovering passive dynamic stability of a hovering fruitfly: a comparison between linear and nonlinear methods. *Journal of Biomechanical Science and Engineering*, 5:591–602, 2010.

[17] J. Hall, M. Pauken, V. Kerzhanvich, G. Walsh, E. Kulczycki, D. Fairbrother, C. Shreves, and T. Lachenmeier. Mars balloon flight test results. AIAA 2009-2809.

[18] E. Hanna, K. Aaron, and G. Blando. Mars hovercraft, concepts and approaches for mars exploration, 2012.

[19] H.S. Wright et al. Ares mission overview-capabilities and requirements of the robotic aerial platform. AIAA-2003-6577, 2003.

[20] J.S. Levine et al. Science from a mars airplane: The aerial regional-scale environmental survey (ares) of mars. AIAA-2003-6576, 2003.

[21] M. Keennon, K. Klingebiel, H. Won, and A. Andriukov. AIAA-2012-0588, 2012.

[22] C. Kuhl. Mars aerial regional-scale environmental survey (ares) coordinate systems definitions and transformations. NASA/TM-2009-215701.

[23] L. Lemke, J. Heldmann, L. Young, A. Gonzales, V. Gulick, R. Foch, M. Marinova, and J. Gundlach. Vertical takeoff and landing uavs for exploration of recurring hydrological events. Concepts and Approaches for Mars Exploration, 2012.

[24] J. Levine, M. Croom, H. Wright, B. Killough, and W. Edwards. The aerial regional-scale environmental surveyor (ares): New mars science to reduce human risk and prepare for the human exploration. Concepts and Approaches for Mars Exploration, 2012.

[25] H. Liu. Integrated modelling of insect flight: from morphology, kinematics to aerodynamics. *J. Comput. Phys.*, 228:439–59, 2009.

[26] H. Liu and H. Aono. Size effects on insect hovering aerodynamics: an integrated computational study. *Bioinspiration and Biomimetics*, 4, 2009.

[27] K. Ma, P. Chirarattananon, S. Fuller, and R. J. Wood. Controlled flight of a biologically inspired, insect-scale robot. *Science*, 340(6132):603–607.

[28] M. Maeda, N. Gao, N. Nishihashi, and H. Liu. A free-flight simulation of insect flapping flight. *J. Aero Aqua Bio-mech.*, 1:71–79, 2010.

[29] D. McCuistion. Mars exploration program: The path forward – mars – the search for lift -. Presentation in Lunar and Planetary Institute Workshop, 2012.

[30] A. Mountcastle and T. Daniel. Aerodynamic and functional consequences of wing compliance. *Exp. Fluids*, 46:873–82, 2009.

[31] T. Mueller, editor. *Fixed and flapping wing aerodynamics for micro air vehicle applications*. 2001.

[32] T. Nakata and H. Liu. A fluid-structure interaction model of insect flight with flexible wings. *Journal of Computational Physics*, 2011.

[33] T. Nakata and H. Liu. Aerodynamic performance of a hovering hawkmoth with flexible wings: a computational approach. *Proceedings of the Royal Society B: Biological Sciences*, 279(1729):722–731, 2012.

[34] T. Nanaka, H. Liu, Y. Tanaka, N. Nishihashi, X. Wang, and A. Sato. Flexible wings aerodynamics of a bio-inspired flapping micro air vehicle. *Bioinspiration and Biomimetics*, 6, 2011.

[35] D. Pines and F. Bohorquez. Challenges facing future micro-air-vehicle development. *J. Aircr.*, 43:290—305, 2006.

[36] M. Platzer, K. Jones, J. Young, and J. Lai. Flapping wing aerodynamics: progress and challenges. *AIAA J.*, 46:2136–49, 2008.

[37] R. Zubrin et al. Mars gashopper, final report on nasa contract nas3-00074. NASA JPL, 2000.

[38] R.D. Braun et al. Design of the ares mars airplane and mission architecture. *JSR*, 43(5):1026–1034, 2006.

 DOI: 10.2420/AF06.2013.81

[39] S. Mackwell et al. Concepts and approaches for mars exploration-report of a workshop. In *Universities Space Research Association Lunar and Planetary Institute*, 2012.

[40] H. L. H. (section editor). Micro air vehicles. Encyclopedia of Aerospace Engineering edited by Blockrey R and Shyy W (Chichester, UK: John Wiley and Sons), 2010.

[41] W. Shyy, H. Aono, S. Chimakurthi, P. Trizila, C.-K. Kang, C. Cesnik, and H. Liu. Recent progress in flapping wing aerodynamics and aeroelasticity. *Prog. Aerosp. Sci.*, 46:284–327, 2010.

[42] W. Shyy, H. Aono, C. Kang, and H. Liu. *An Introduction to Flapping Wing Aerodynamics*. Cambridge University Press, 2013.

[43] W. Shyy, Y. Liang, J. Tang, D. Viieru, and H. Liu. *Aerodynamics of low Reynolds number flyers*. New York, NY: Cambridge University Press, 2007.

[44] D. Sigthorsson, M. Oppenheimer, and D. Doman. AIAA 2012-0028, 2012.

[45] S.P. Stanford et al. Area and beyond: Autonomous aerial platforms provide a unique measurement capability for earth and planetary science. AIAA-2003-6610.

[46] B. Stanford, P. Ifju, R. Albertani, and W. Shyy. Fixed membrane wings for micro air vehicles: experimental characterization, numerical modeling, and tailoring. *Prog. Aerosp. Sci.*, 44:258–94, 2008.

[47] I. Steadman. `http://www.wired.co.uk/news/archive/2013-04/3/robot-dragonfly`.

[48] M. Thomblom, J. Lukas, and R. Lugo. Systematic and widespread exploration with aerocoasting and reconnaissance of the martian sub-atmosphere (swarms). Concepts and Approaches for Mars Exploration, 2012.

[49] E. Ulrich, D. Pines, and J. Humbert. From falling to flying: the path to powered flight of a robotic samara nano air vehicle. *Bioinspiration and Biomimetics*, 5(045009), 2010.

[50] J. Vago and M. Coradini. Exomars: Mars exploration programme. Presentation in Lunar and Planetary Institute Workshop, 2012.

[51] T. Weis-Fogh. Quick estimates of flight fitness in hovering animals, including novel mechanisms for lift production. *J. Exp. Biol.*, 59:169–230, 1973.

[52] J. Whitney and R. Wood. Conceptual design of flapping-wing micro air vehicles. *Bioinspiration and Biomimetics*, 7, 2012.

[53] A. Wolf, L. Beegle, C. Raymond, J. Plaut, B. Pollard, Y. Gim, X. Wu, and J. Hall. Mars balloon science. 4294, Concepts and Approaches for Mars Exploration, 2012.

[54] R. Wootton. Support and deformability in insect wings. *J. Zool.*, 193:447–68, 1981.

[55] J. Young, S. Walker, R. Bomphrey, G. Taylor, and A. Thomas. Details of insect wing design and deformation enhance aerodynamic function and flight efficiency. *Science*, 325:1549–52, 2009.

[56] L. Young, E. Aiken, V. Gulick, R. Mancinelli, and G. Briggs. Rotorcraft as mars scouts. In *IEEE Aerospace Conference*, 2002.

[57] L. Young, G. Pisanich, C. Ippolito, and R. Alena. Aerial vehicle surveys of other planetary atmospheres and surfaces: Imaging, remote-sensing, and autonomy technology requirements. In *SPIE Electronic Imaging Conference*, 2005.

[58] L. A. Young, E. Aiken, P. Lee, and G. Briggs. Mars rotorcraft: possibilities, limitations, and implications for human/robotic exploration. In *Aerospace Conference, 2005 IEEE*, pages 300–318. IEEE, 2005.

[59] R. Zubrin. The mars gashopper. Concepts and Approaches for Mars Exploration, 2012.

[60] R. Zubrin, D. Harber, E. Bostwick, and J. Kilgore. Advanced gashopper mobility techonology. Final report on Contract NNC07QA50P, NASA JPL, 2007.

[61] R. Zubrin, D. Snyder, D. Harber, K. Johnson, J. Kilgore, and N. Jameson. Mars gashopper airplane. Final report on Contract NNL05AB04, delivered to NASA LaRC, 2005.